FACULTY OF BIOSCIENCE ENGINEERING

SYNTHESIS OF PSILOCYBIN ANALOGUES AND OTHER 5-HT RECEPTOR AGONISTS FOR STIMULATION OF NEUROTRANSMISSION

Anne-Julie Longueville
Student number: 01909938

Promotor: Prof. dr. ir. Christian Stevens

Tutor: ir. Andreas Simoens

Master's Dissertation submitted to Ghent University in partial fulfilment of the requirements for the degree of Master of Science in Bioscience Engineering: Chemistry and Bioprocess Technology
Academic year: 2023-2024

UNIVERSITEIT GENT

Copyright

The author declares the use of generative artificial intelligence, specifically the [OpenAI GPT-4.0 model]. This technology acted solely as a tool to correct writing style and grammar, thus improving the overall quality of the written work. However, the author emphasizes that the content of this work is original and also takes full responsibility for this.

Ghent, June 2024

The promotor,

Prof. dr. ir. Christian Stevens

The author,

Anne-Julie Longueville

Acknowledgements

The journey at the Faculty of Bioscience Engineering at campus Coupure is coming to its end. It has been a remarkable experience, where I was able to uncover my through interests and passions, providing clear insights in what direction I wish to pursue. In this final year, I was able to apply a large part of the knowledge acquired in the previous years. This extended beyond the scientific knowledge, namely the assumed responsibility and the experience of working in a lab environment was very meaningful.

First and foremost, I would like to thank Professor Christian Stevens. Both myself and your other thesis students were very well mentored and guided through this year. During the monthly meetings, we got the opportunity to discuss problems and questions that had arose. Moreover, outside of these meetings, you were always reachable when we needed additional support.

Secondly, I would like to thank my tutor Andreas Simoens. You guided me through the year while providing plentiful of personal freedom. I was able to develop independence and formulate my own ideas. Whenever I needed assistance, I received the necessary guidance and advice.

I would also like to extend my gratitude to Marthe VandeVelde. She was always approachable whenever I had questions or was in need of advice or refreshing ideas, or I simply wished a pleasant conversation.

Finally, I would like to thank my fellow thesis students. We shared many memorable moments together and formed a close group. A special thanks to Fien and Lise, with whom I enjoyed the pleasure of sharing many lunch and coffee breaks together.

Anne-Julie Longueville
June, 2024

Table of contents

1. Literature review 1

1.1 Introduction 1

1.2 Major depressive disorder (MDD) 1

1.3 Psilocybin 2

1.3.1 Traditional use and history of psilocybin 3

1.3.2 Psilocybin in the human body 5

1.3.3 Clinical trials results 5

1.4 Psychedelics in general 7

1.4.1 Pharmacodynamics 9

1.5 Methods for antidepressant discovery and design 14

1.6 Synthesis of psilocybin (analogues) 17

1.7 Concluding remarks 20

2. Results and discussion 22

2.1 First pathway 22

2.1.1 Starting from 5-Bromo-7-indazole 24

2.1.2 Starting from 5-Bromo-1H-indazole 29

2.2 Introducing the borrowing hydrogen strategy 33

2.2.1 Synthesis 5-bromo-3-(N,N-dimethylaminoethyl)pyrrolo[2,3-b]pyridine by applying the borrowing hydrogen strategy 34

2.2.2 Phosphonylation of 5-bromo-3-(N,N-dimethylaminoethyl)pyrrolo[2,3-b]pyridine 36

2.2.3 Reversing the reaction sequence 37

2.3 Synthesis of 5-bromo-N,N-dimethyltryptamine followed by a Suzuki coupling 38

2.3.1 Fisher Indole reaction for synthesis of 5-bromo-DMT 38

2.3.2 Suzuki coupling with 5-bromo-DMT 40

2.4 β-carbolines, another group of tryptamine-like compounds 44

2.4.1 Synthesis of tetrahydro-β-carbolines 47

2.4.2 Dehydrogenation of tetrahydro-β-carbolines to the β-carbolines 49

3. Conclusion and future perspectives 51

3.1 Summary and conclusion 51

3. 2 Future perspectives 51

4. Material and methods 53

1. Automatic Flash Column chromatography 53

2. Dry Solvents 53

3. Liquid chromatography coupled with Mass Spectrometry 53
4. Mass Spectrometry 54
5. Nuclear Magnetic Resonance Spectrometry (NMR) 54
6. Infrared Spectroscopy (IR) 54
7. Thin layer Chromatography (TLC) 54
8. Hydrogen generator 54
5. Safety 55
6. Experimental section 58
7. Bibliography 62

Abstract

Psilocybin, which is one the compounds present in *Psilocybe* mushrooms, gained interest for the treatment of various psychiatric disorders, especially for the treatment of major depressive disorder. Psilocybin in its natural form, as found in *Psilocybe* mushrooms is limited in its therapeutic use, since it still faces different challenges, especially its hallucinogenic effects. This limitation can be mitigated by synthesizing non-hallucinogenic analogues, making them promising antidepressants with a rapid onset and a sustained remission.

In this dissertation, various analogues of psilocybin have been aimed to synthesize, with the purpose of retaining the antidepressant effect but omitting the psychotropic effects. Therefore, different synthetic routes have been explored to develop these kind of analogues, in order to alter their interaction with human enzymes and receptors (mainly the 5-HT receptors) by modifying the indole core. Additionally, the synthesis of β-carbolines was also initiated. These are structures that also show potential as therapeutics for psychoactive disorders such as Alzheimer, again through interaction with 5-HT receptors.

Over the course of this year, psilocybin analogues were synthesized, although primarily as intermediates due to several challenges encountered in the synthetic routes. Synthesizing Psilocybin analogues represents a significant step towards the development of antidepressants with a rapid onset and sustained remission, eliminating the hallucinogenic effects associated with the natural psilocybin. Furthermore, three different tetrahydro-β-carbolines were also synthesized. While psilocybin analogues are promising for treating major depressive disorder, β-carbolines could benefit disorders such as Alzheimer. The synthesized intermediates should be subjected to further research in order to develop the aimed analogues and be subjected to biological testing to evaluate their true potential.

List of Figures

Figure 1.1.....1

Figure 1.2 Representation of the classical psychedelics.....8

Figure 1.3 Representation of the different targets of psychedelics.....11

Figure 1.4 Location of the claustrum (A), whole-brain anatomical connectivity of the claustrum (B), and a summary of the functions related to claustrum connections (C).....13

Figure 1.5 Overview of some 5-HT_{2A} receptor agonists evaluated by Cao et al. (2022).....15

Figure 1.6: 5-HT_{2A} receptor with hydrophobic binding pocket and side extended cavity.....16

Figure 1.7 Agonist behaviour of biased ligands 16

Figure 1.8 Hofmann reaction scheme.....17

Figure 1.9 Synthesis of psilocybin according to Shirota et al. (2003).....18

Figure 1.10 Synthesis of psilocin by Sherwood et al. (2022).....18

Figure 1.11 Synthesis of psilocin using transition metals.....19

Figure 1.12 Psilocin synthesis by Bartolucci et al. (2016).....19

Figure 1.13 Chemoenzymatic approach.....20

Figure 2.1 Reaction scheme starting from 5-Bromo-7-azaindole.....23

Figure 2.2 Reaction scheme starting from 5-Bromo-1H-indazole.....23

Figure 2.3 Mannich type of reaction.....24

Figure 2.4 Acid catalysed formation of iminium ion.....24

Figure 2.5 reaction mechanism for the synthesis of 3-(N,N-dimethylaminomethyl)-5-bromo-7-azaindole.....24

Figure 2.6 Mannich reaction on 5-Bromo-7-indazole.....25

Figure 2.7 Mannich reaction on N-1 position with formation of 1-(N,N-dimethylaminomethyl)-5-bromo-1H-pyrrolo[2,3-b]pyridine 25

Figure 2.8 Chemical structure of N,N-dimethyltryptamine and N,N-dimethylisotryptamine..27

Figure 2.9 N-alkylation of various indoles.....27

Figure 2.10 Initial reaction for the synthesis of 5-bromo-3-(2-nitroethyl)-1H-pyrrolo[2,3-b]pyridine.....27

Figure 2.11 Reaction mechanism for the synthesis of 5-bromo-3-(2-nitroethyl)-1H-pyrrolo[2,3-b]pyridine.....28

Figure 2.12 Actual course of reaction with the formation of 18 as intermediate.....29

Figure 2.13 Mannich reaction on 5-Bromo-1H-indazole.....29

Figure 2.14 Mannich reaction with nucleophilic attack of N at position 1……..30

Figure 2.15 Alkylation using Vilsmeier reagent……30

Figure 2.16 Reaction mechanism using Vilsmeier reagent with nucleophilic attack of C-3 position……31

Figure 2.17 Actual course of reaction with the Vilsmeier reagent……32

Figure 2.18 Reductive amination of 5-bromo-1-formylindazole……..33

Figure 2.19 Reducing the first pathway to 2 reaction steps……33

Figure 2.20 Mechanism of the borrowing hydrogen strategy using an alcohol and transition metal catalyst……34

Figure 2.21 Synthesis of 5-Bromo-3-(N,N-dimethylaminoethyl)pyrrolo[2,3-b]pyridine……35

Figure 2.22 Formation of dimer side product ……35

Figure 2.23 Synthesis of diethyl (3-(2-(dimethylamino)ethyl)-1H-pyrrolo[2,3-b]pyridin-5-yl)phosphonate by a Hirao coupling……..36

Figure 2.24 Hirao coupling reaction mechanism……..37

Figure 2.25 Reversed reaction sequence……..37

Figure 2.26 Phosphonylation of 5-bromo-7-azaindole following a Hirao coupling mechanism……..38

Figure 2.27 Alkylation of diethyl (1H-pyrrolo[2,3-b]pyridin-5-yl)phosphonate……..38

Figure 2.28: Synthesis of 5-bromo-DMT……..38

Figure 2.29 Synthesis of 5-bromo-DMT following a Fischer Indole reaction mechanism……39

Figure 2.30 Catalytic cycle of the Suzuki coupling with boronic acids……40

Figure 2.31 Overview of the different boronic acids……41

Figure 2.32 Synthesis of N,N-dimethyl-2-(5-phenyl-1H-indol-3-yl)ethan-1-amine via Suzuki coupling reaction……41

Figure 2.33 Overview of the different Suzuki coupling with different reaction conditions, tested on different boronic acids……..42

Figure 2.34 Oxidized compounds……43

Figure 2.35 Reduction of oxidized compounds using activated zinc dust……44

Figure 2.36 Carboline alkaloid skeleton……44

Figure 2.37 Pictet-Spengler reaction……..45

Figure 2.38 Representation of the 5 clusters of β-carbolines……..46

Figure 2.39 Synthesis of β-carbolines with Pictet Spengler reduction using nitriles, followed by an aromatization step……..46

Figure 2.40 Synthesis of β-carbolines with Pictet Spengler reduction using aldehydes, followed by an aromatization step……47

Figure 2.41 Synthesis of the THBC of Eudistomin U……..47

Figure 2.42 Synthesis of 7-fluoro-1-(1H-indol-3-yl)-2,3,4,9-tetrahydro-1H-pyrido[3,4-b]indole (cluster 1)……48

Figure 2.43 Synthesis of 1-(6-bromopyrazolo[1,5-a]pyrimidin-3-yl)-2,3,4,9-tetrahydro-1H-pyrido[3,4-b]indole (cluster 3)……48

Figure 2.44 Synthesis of methyl 3-(2,3,4,9-tetrahydro-1H-pyrido[3,4-b]indol-1-yl)-1H-indole-6-carboxylate (cluster 4)……48

Figure 2.45 Synthesis of 1-(1H-indol-3-yl)-6-methoxy-2,3,4,9-tetrahydro-1H-pyrido[3,4-b]indole (cluster 5)……49

Figure 2.46 Aromatization of 1-(1H-indol-3-yl)-6-methoxy-2,3,4,9-tetrahydro-1H-pyrido[3,4-b]indole ……50

1. Literature review

1.1 Introduction

Psilocybin (O-phosphoryl-4-hydroxy-N,N-dimethyltryptamine) is a tryptamine alkaloid which can be found in certain mushrooms, mainly in the genus *Psilocybe.* However, synthetically produced psilocybin is also widely available these days.
It is naturally produced by certain mushrooms such as *Psilocybe, Panaeolus* and others (Strauss et al., 2022), in which they represent a content of 0.2% to 1% of the dry weight (Tylš et al., 2014). These substances can be called psychedelics or hallucinogens, however in this master dissertation, the objective is to synthesize psilocybin analogues with no hallucinogenic activity. Market values from $1.9 to $253 billion are estimated for psilocybin, because of its treatment potential as a non-addictive antidepressant. Currently, the chemical synthesis is performed on a smaller scale than the harvesting from mushrooms and sclerotia on the nutraceutical public market. This is mainly because of the ease of the production of these mushrooms and due to the possible synergism with other hallucinogenic compounds produced in these organisms (Strauss et al., 2022).

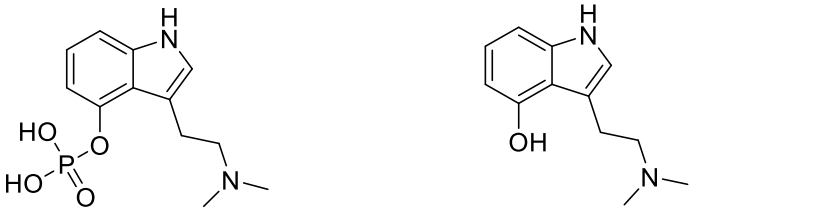

Psilocybin **1**
(O-phosphoryl-4-hydroxy-N,N-dimethyltryptamine)

Psilocin **2**
(N,N-dimethyltryptamine)

Figure 1.1

The Swiss scientist Adolphe Hofmann was the first to isolate the psychedelics psilocybin and psilocin, and gave them their current names. After the isolation, but also synthesis of these molecules by Hofmann, the first 'golden era' in the research of psilocybin occurred. This slowed down after 1971, partially due to Nixon's declaration of the war on drugs. In the period of 1972 to 2010, the researched declined, and the publications per year decreased significantly. After 2011, interest in these compounds increased once again, due to different psychedelic advocates such as the Multidisciplinary Association for Psychedelic Studies (MAPS). In 2020, 140 publications on psilocybin appeared, and in 2021, this even reached 204. This is shaping up to be the second wave on psychedelic research, far exceeding the efforts made in the first research wave during the 1960s (Agrawal et al., 2023).

Modern studies for psilocybin mainly focus on the possibility of psilocybin to treat major depressive disorder. However, other studies on disorders such as obsessive-compulsive disorder, cocaine use disorder, anorexia nervosa, and more have also been conducted using a psilocybin treatment (Strauss et al., 2022).

1.2 Major depressive disorder (MDD)

Major depressive disorder is a widely occurring cause of disability. Currently available treatments take weeks or months before they show any symptom reduction. Additionally to

this, the treatment adherence seems to be problematic for several patients, resistance against the treatments of this depressive illness occurs frequently. 40 To 60% of the patients that were diagnosed once, relapse and its rate also accelerates after every episode. It is thus clear that the discovery of novel treatments, which work more rapidly and produce a sustained remission is an urgent need (Gukasyan et al., 2022).

Several studies already suggested the use of a psilocybin treatment, where antidepressant effects were visible within the short time of a week after administration. Even for treatment resistant patients, the response rate seems to be positive (Gukasyan et al., 2022).

The disease affects 1 in 6 adults, where the amount of women affected is twice the amount of men. It is the second leading contributor to chronic diseases, and it is associated with increasing risks in developing other conditions such as diabetes, heart diseases and strokes. Patients with MDD have almost a 20-fold more likelihood to die by suicide compared to the general population.
The disease has a genetic contribution which is estimated to be 35%, and environmental factors during childhood are strongly associated with the chance of developing MDD during adulthood.
All aspects of the disease in terms of neurobiology are not completely understood yet. What is known, is the fact that MDD is associated with small hippocampal volumes and a change in the activation or the connectivity of the neural networks. The hypothalamic-pituitary-adrenal (HPA) axis, a neurobiological system that mediates the stress response, is altered next to the automatic nervous system and the immune system. This HPA axis forms the most researched biological system in MDD. Cortisol levels are raised in patients with MDD and impaired cognitive function frequently occurs, more common and more pronounced in patients with severe depression and elder patients (Otte et al., 2016).

MDD treatments consist of both psychotherapy and psychopharmacology. 30% Of the patients does not remit from the disease, even after several treatments (Otte et al., 2016). New pharmacological approaches using ketamine and psychedelics find themself under scientific research with promising results, forming the main objective of this master dissertation.

1.3 Psilocybin

Psilocybin is a secondary metabolite occurring in different mushrooms and fungal species. These mushrooms are frequently referred to as magic mushrooms. They have been used for a long time by humanity for spiritual purposes, given its hallucinogenic properties. They mediate interactions between the producing fungi and other organisms. A possible explanation for its evolution is the defence mechanism against fungivores and resource competitors. It can also increase the dispersal of spores by the animals coming near these mushrooms. Another proposed explanation states that psilocybin is synthesized as a store/disposal product for the excess nitrogen, which could otherwise exert a toxic effect on the mushroom itself. Studying the natural mechanisms of psilocybin should not be neglected, since it might help in exploring the different applications for humans. Psilocybin producers are typical fungi that find themselves in dung, late-wood decay niches. They can be found in all sorts of climates, with the highest concentrations in neotropics (Meyer and Slot, 2023).
Typically, the concentration of metabolites such as psilocybin is highest in the fruiting bodies. It is a logical assumption to suspect that animals are targeted by psiloids (the collective name for psilocybin, its precursors and derivates), given their structural similarity to serotonin and

its ability to bind to all kind of receptors as will be described below. These effects can be beneficial for the fungi in different ways. Since they affect physiological processes in animals, there is no doubt that this interferes with the interaction of the mushrooms and the animals (Meyer and Slot, 2023).

Psilocybin and its derivative psilocin are tryptamine molecules, consisting of an indole ring with attached amine side chains. In their pure forms, these compounds can be found as white powders. Bulky phosphate groups of psilocybin render this molecule more water soluble than psilocin, representing the more lipid soluble compound (Strauss et al., 2022). In general, the psychoactive effect of tryptamines is mainly due to the indole alkylamine moiety of the molecules. Alkylations of the side chain nitrogen, substitutions of the indole ring and the side chain carbon are all factors impacting the psychoactive effect of tryptamine derivatives (Ashgar et al., 2022).

Many behavioural assays exist to evaluate the therapeutic potential of possible antidepressants. A commonly used test next to the head twitch response that will mentioned further below, is the forced swim test, where the animal's despair is assessed. A decrease in immobility shows a potential antidepressive effect. Previous tests with psilocybin have shown this decrease in immobility time.

The brain derived neurotrophic factor (BDNF), which are proteins where increased expression modifies gene expression and causes signalling cascades, and decreased BDNF levels increase depressive like behaviour, is upregulated in the medial prefrontal cortex and hippocampus, promote the synaptic plasticity and reduce the immobility, which could mean that these BDNF form biological markers for antidepressive therapeutic potential (Sandoval, 2023). However, this test mainly evaluates the stress coping response of rodents and not necessarily their depression like behaviour (Yin et al., 2023). Which makes using them as markers of antidepressive behaviour possibly not the best option.

1.3.1 Traditional use and history of psilocybin

The first evidence of the use of psilocybin returns to a codex in the years 1500, belonging to the Mixtec culture in Mesoamerica. Even to this day, the use of *Psilocybe* species is continued by different Mexican ethnic groups such as the Chatins, Maztecs etc. Most of these hallucinogenic species were reported to be used by groups in central and southern Mexico, where they are part of an ancient sacred tradition. Current rituals and ceremonies in both Catholic and Mesoamerican context, use *Psilocybe* species for the treatment of spiritual and physical illnesses. Because of the hallucinations associated with the consumption of these species, people have a trance like experience where the soul is able to dissociate from the body. These treatments are conducted by doctors or shamans, typically at night at quiet places, where no food, drinks or other medicines and drugs are allowed to be taken in advance, and travelling is discouraged up to a week after the treatment. Indigenous groups also use the *Psilocybe* mushrooms for the treatment of anxiety, rheuma and sometimes it is used as an analgesic to relieve pain (van Court et al., 2022).

Aztec Indians from South America used to refer to them as 'teonanacatl', which means 'God's flesh'. Secondary metabolites such as psilocybin have proven their potency as novel therapeutics through the years, where they have served as prototypes or lead compounds that can be synthesized chemically with or without certain modifications to increase their potency,

stability, or superiorize drug-like properties. Most of the secondary metabolites from plants, fungi and/or bacteria have known their use in anti-infective and anti-cancer treatments, but recently these are more and more being used in the treatment of disorders of the central nervous system (CNS) such as depression (Nichols et al., 2020).

For psilocybin, it all starts with Benardino de Sahagun, a Spanish Franciscan that engaged in ethnographic research in Mexico. He wrote *the General History of the Things of New Spain*, where in his most famous manuscript (the *Florentine Codex*) he refers multiple times to 'teonanacatl' or 'Gods Flesh', namely the sacred mushrooms in Mesoamerica. For a very long time, the existence of these mushrooms was very controversial and even denied, such that debate existed until 1936. After this, a botanist named Richard Evans at Harvard university identified specimens of three species of these sacred mushrooms where they were identified as *Psilocybe caerulescens, Panacolus campanula,* and *Stropharua cubensis*. World war II interrupted further research. Until in 1952, amateur mycologist R. Gordon Wasson travelled to Mexico on the search for these mushrooms. These trips resulted in the publication of an article in *Life Magazine*, where psychoactive mushrooms were introduced to the wide public (Nichols et al., 2020). The French mycologist Roger Heim was able to cultivate the mushrooms himself and sent samples to Albert Hofmann for further analysis. He subjected extracts of these mushrooms to paper chromatography to separate the different compounds, where he identified the active compound and named it psilocybin. Additionally to psilocybin, he also identified a compound, which was the dephosphorylated psilocybin and named it psilocin (Nichols et al., 2020). The identification of the active compounds in these magic mushrooms were encouraged by the recurring crises in the coffee prices since the 50's (de Teresa, 2022).

In 1970, under the orders of US president Richard Nixon, psilocybin and other hallucinogens have been placed in Schedule I category of the United States Controlled Substances Act of 1970. These substances are implicated with involvement and influence on anti-war protests and cultural movements in the 60's, forming an explanation for this decision. To the current day, these substances remain in this Schedule I status, meaning that the substance has no accepted medical or therapeutic use (Heilman, 2023).

Since 1971, psilocybin mushrooms have been included in the list of illicit substances in Mexico. But their use is tolerated when their consumption is related to medico-religious ceremonies. People travel to the city of Huautla de Jimenez for experiencing the psychoactive effect of these mushrooms. This city played a very important role in the history of psychedelica and in their use across other cultures by the 'counterculture' movement (de Teresa, 2022).

In 1986, there was the establishment of the Multidisciplinary association for Psychedelic Studies (MAPS), a non-profit psychedelic pharmaceutical company, by the founder Rick Doblin. It was established with the goal to facilitate the research of the use 3,4-methylenedioxy methamphetamine (MDMA) as a therapeutic, being an apparent move against the Drug Enforcement Administration (DEA) wanting to criminalize MDMA. A study of the use of MDMA in treating pain, anxiety and depression in cancer patients was conducted by Charles Grob, a member of this organization. Thanks to the completion of this study, the Food and Drug Administration of the US (FDA) accepted the use of psychedelics in human clinical research with the same standards as other potential prescription drugs. Even though Grob's initial focus was on MDMA, he focused on psilocybin in the treatment of cancer patients because he thought that this research would be less controversial than his MDMA research. For the research of lysergic acid diethylamide (LSD) assisted psychotherapy, the MAPS extended its

research to Switzerland, since it there received the permission to conduct research that it did not receive from the FDA. Eventually in 2008, the Swiss study was accepted by the FDA and finally, the last one of the classic psychedelics was accepted for research (before research with MDMA, psilocybin, N,N-Dimethyltryptamine (DMT), tryptamine, ketamine and mescaline had already been approved) (Heilman, 2023).

1.3.2 Psilocybin in the human body

Psilocybin is usually administered in doses of 15, 25 or 30 mg (Holze et al., 2023). 90 To 97% of the psilocybin is dephosphorylated to psilocin in our metabolism, which appears in the blood plasma after oral administration. They both affect the serotonergic pathway, a system that regulates functions such as pain, cognitive function, vascular tone, motor activity etc. (Dodd et al., 2022). This dephosphorylation takes place in the acidic environment of the stomach or by alkaline phosphatase and a non-specific esterase present in the intestine and kidney. This compound is now lipid soluble and able to cross the blood brain barrier. Psilocin is subsequently distributed to other tissues, with an estimate of the apparent volume of distribution of 298 L, exceeding the volume of the human body, when applying a one compartment model. During its first pass through the liver, a demethylation and oxidation phase 1 metabolism by mono-amine oxidase and aldehyde dehydrogenase on psilocin to form 4-hydroxindole-3-acetic acid (4-HIAA), 4-hydroxy-indole-acetaldehyde and 4-hydroxytryptophol takes place (Dodd et al., 2022). About 4% of psilocin is metabolised in this way. Another possibility, is the oxidation of psilocin to products with an O-quinone or imino-quinone structure by hydroxyindole oxidases (Tylš et al., 2014).

Subsequently, a phase 2 metabolism takes place, mainly catalysed by endoplasmatic enzymes (UDP-glucuronosyltransferases, or UGT). Psilocin is glucuronidated to psilocin-O-glucuronide. There is an extensive glucuronidation in the small intestine by UGT1A10. When the compounds are absorbed into the circulation, UGT1A9 contributes most to the glucuronidation (Dodd et al., 2022). It is in this form, the psilocin-O-glucuronide, that 80% of the administered psilocybin is excreted (Tylš et al., 2014).

Psilocybin and its metabolic derivatives are found in our blood plasma 20 to 40 minutes after an oral administration and maximum levels are observed after 80 to 105 minutes. Oral ingestion half-life is around 2.5 hours, intravenous administration half-life is approximately to be 1.23 hours. The conjugated form of psilocin represents the biggest part in the blood plasma (80%). Both psilocin and psilocybin can be detected in human urine, they are detected unmodified but mostly conjugated with glucuronic acid. The biggest part is excreted 3 hours after the oral administration and there is a complete elimination from the human body after 24h (Tylš et al., 2014).

1.3.3 Clinical trials results

A phase 1 randomized, double-blind and placebo-controlled study was conducted by Rucker et al. (2022), to assess the safety of psilocybin administration to healthy people. Short and longer term changes in cognitive functions were assessed by a Cambridge Neuropsychological Test automated Battery (CANTAB) panel and an emotional processing scale. Additionally, the safety of psilocybin administration was evaluated using the CANTAB global composite score and by monitoring treatment-emergent adverse events (TEAE) (Rucker et al., 2022). During the study, 89 healthy adults with a mean age of 36.1 years were randomized and dosed with

10 mg of psilocybin, 25 mg of psilocybin or placebo. The participants were being followed up for 12 weeks after the drug administration. In the results of the study, 511 TEAEs were observed with a mean duration of a day. These TEAEs all started and resolved again on the same day. Hence, it could be concluded that the doses of 10 and 25 mg of psilocybin were well tolerated and no detrimental short- or long-term effects on the cognitive functioning and the emotional processing were caused. These findings support the further research and studies on psilocybin related treatments for different psychiatric disorders (Rucker et al., 2022).

In the follow up of phase 1 studies, phase 2 studies are now also being conducted. Another randomized placebo-controlled, 6-week trial in 104 people that received a 25 mg dose of psilocybin was conducted by Raison et al. (2023). This phase 2 study was randomized and multiblinded, comparing a single dose psilocybin with niacin (a placebo controller). The outcome assessments were exerted by blinded centralized raters to gain information on the timing of the onset of action, the lastingness of the beneficial effects and the safety of psilocybin during a period of 6 weeks. The efficacy was examined using the MADRS score, which is 10-item scale that has a scoring range from 0 to 60, where the higher the score, the more depressive the patient. These scores were compared from baseline to day 43. Next to this, changes in the Sheehan Disability Scale (SDS) and the percentage of patients with a sustained depressive system response, were assessed. Next to its efficacy, the safety of psilocybin administration was evaluated in this study. Adverse effects such as elevated blood pressure, headache, nausea and others were examined. The statistical analysis was conducted using a covariance matrix for the continuous outcomes of the mixed effects, sensitivity analysis, logistic regression, odds ratios with 95% confidence intervals, and sequential significance testing to ensure an overall α level of 0.05. Two-sided tests were used to compare the MADRS score from the baseline to day 43 and day 8. The incidence of the adverse effects was examined using counts and percentages, and a Clopper-Pearson interval with 95% confidence intervals. The participants that received psilocybin showed a greater difference in MADRS score from baseline to day 8 as to day 43, compared to the group that received niacin ($P < 0.001$). The treatment with psilocybin had associations with improvements in the reduction of global disease severity, depressive and anxiety symptoms, and quality of life. Looking at the results regarding the safety, the most commonly occurring adverse effect was headache, followed by nausea and visual perceptual effects. Both statistically and clinically, this study showed a significant decrease in depressive symptoms. These improvements were visible within 8 days of the dosing and knew a fast onset of action. Mean differences in the SDS score showed improvements in psychosocial functioning. The adverse effects that were experienced during the dosing were most of a mild nature and only occurred during the acute period of dosing (Raison et al., 2023).

Another double-blind, randomised clinical trial with 52 patients suffering from MDD received a single moderate dose of psilocybin (0.215 mg/kg body weight) or a placebo. By the assessment of MADRS and Beck depression inventory (BDI) score, the severity of the patient's depression was estimated. This BDI is multiple-choice self-report inventory that consists of 21 questions. It is another widely used instrument to assess the severity of depression. Again, the higher the total score, the more the severity of the depression (Beck et al., 1961). The patients receiving psilocybin showed a decrease in the severity of depression symptoms, namely a decrease of 13 points of the MADRS score compared to baseline ($p = 0.0011$) after 14 days. The findings suggest that this dose of psilocybin has significantly reduced the patient's depression symptoms for a minimum period of 2 weeks (von Rotz et al., 2022).

A systematic review and meta-analysis of clinical trials was conducted by Vargas et al. (2020). This review with meta-analysis was performed on the following databases: PubMed, Web of Science, Scopus, and SciELO. The Boolean operator with a specific search strategy was used. Additionally, the reference's list of the relevant articles were also examined to check for more work. In total, 670 articles were evaluated. For the statistical analysis, weighted mean differences (WMD) of the intervention group (receiving psilocybin) and control group (receiving placebo), between the change in pre-and post-treatment mean values, were used. The psychometric scales of the study were the BDI and the State-Trait Anxiety Inventory (STAI). Where BDI is used to assess depression, STAI is used to assess anxiety. STAI is just like BDI, a self-report questionnaire, being able to detect the presence and severity of anxiety symptoms and the general propensity to feel anxious. Furthermore, it is divided into 2 subscales: the STAI-Trait and the STAI-State (Vargas et al., 2020). Through the meta-analysis it could be concluded that for BDI, the intervention group was favoured over the control group ($p = 0.002$). In order to do this, 11 effect sizes were considered. As for BDI, 11 effect sizes were considered for STAI-Trait. The same conclusion as for the BDI could be conducted, namely the favouritism of the intervention group over the control group ($p < 0.001$). For the STAI-State, 9 effect sizes were chosen. The outcome was the same as for the previous two ($p < 0.001$). Hence, this study demonstrates the effectiveness of psilocybin to reduce symptoms of depression and anxiety (Vargas et al., 2020). These promising results emphasize the importance of psilocybin (clinical) research.

Clinical trials both assessing the safety and adverse effects of psilocybin administration and studies regarding its therapeutic potential show that the compound possibly forms an interesting anti-depressant. Even taking into account the publication bias which was performed by Vargas et al. (2020), the compound is still regarded as effective. Now that these clinical studies have been performed, it's important to further conduct mechanistic studies that try to fully clarify the action mechanism of the drug, which is still under quiet some discussion as will be further described below.

1.4 Psychedelics in general

The molecular structure of psychedelics resembles a serotonin molecule, and they are defined by their serotonergic action mechanisms. Apart from the rise of their use in meditative settings, they are also more and more studied in clinical studies testing their potential for treatment of psychiatric disorders. However, both early and more recent research demonstrated that repeated administration of psychedelics can induce cross-toleration, lowering their effectiveness. Classical psychedelics share a common mechanism of action, comprising their partial agonism for the 5-hydroxy-tryptamine 2A (5-HT_{2A}) receptors and their binding to receptors that activate a whole lot of intraneuronal signalling pathways. Different psychedelic drugs can be compared, having the same occupancy of a certain receptor (5-HT_{2A}R), for their difference in efficacy, selectivity or their polypharmacology (Grieco et al., 2022). The administration of a compound named ketanserin prevents the effects associated with psychedelics, since it acts as a 5-HT_{2A} antagonist (van Elk et al., 2022). In this way, ketanserin blocks dose dependently the perceptual disturbance and hallucinations that are induced by psychedelics such as psilocybin (Dodd et al., 2022).

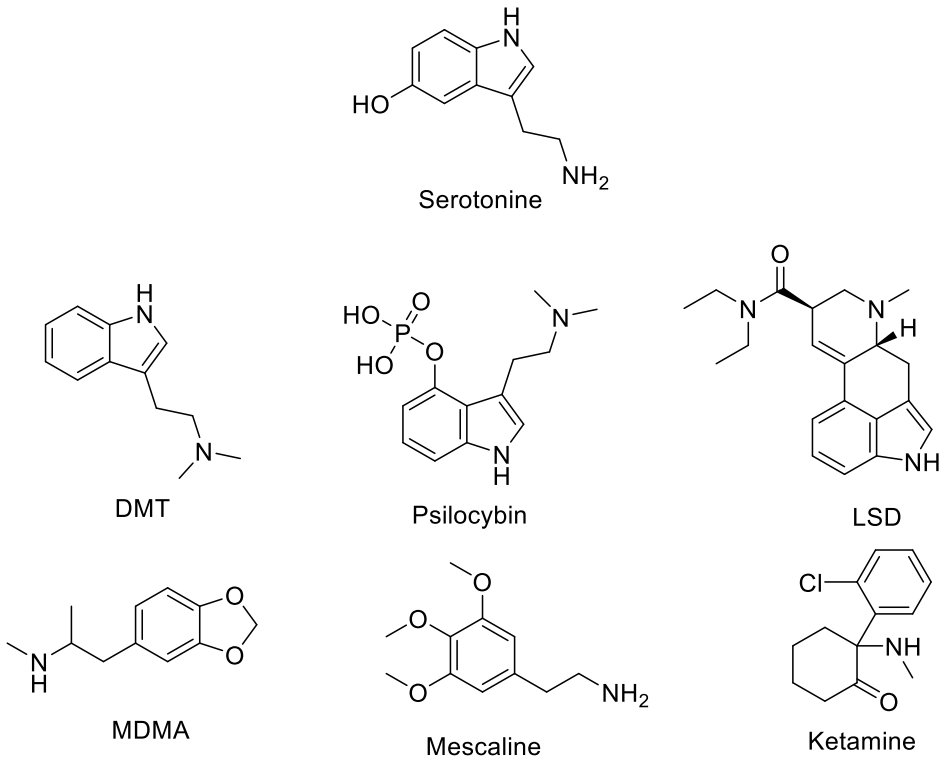

Figure 1.2: *Representation of the classical psychedelics*

Different animal studies, of which the most reliable seems to be the head twitch response, indicated the important role of the 5-HT_{2A} receptor. The head twitch response in rodents forms a reliable way to make a distinction between hallucinogenic and non-hallucinogenic 5-HT_{2A} agonists. This type of response is a side-to-side head movement, that occurs in rodents when the 5-HT_{2A} receptor is activated and therefore indicates hallucinogenic effects (Nakagawasai et al., 2004).

Because of their agonism to this receptor, an increased frequency of cortical layer 5 pyramidal neurons is observed, next to evoking excitatory post-synaptic currents and an increase of their firing rate upon its activation. Activation of these receptors is necessary for tryptamine psychedelic analogues to fulfil their antidepressant effect. Both the hallucinogenic as well as the therapeutic effects are a result of the activation of the same receptor. Psychedelics stimulate the growth of neurons in the medial prefrontal cortex (mPFC), however their produced experiences are very subjective. Changes in neuroplasticity are also associated with psilocin, these neuro-plastogenic effects were proposed to be a part of the non-hallucinogenic part of the therapeutic effect. This together with a 5-HT_{2A} activation of phosphatidylinositol hydrolysis, this receptor agonism activates the tropomyosin receptor kinase B pathway (TrkB) and possibly also other pathways (Dodd et al., 2022). Serotonergic psychedelics promote neuroplasticity by activating rapamycin. It is known that the hallucinogenic effect from psychedelics is due to their agonism of the 5-HT_{2A} receptors, but unclarity remains among the role of this receptor in the mechanisms of long-lasting changes in the neuronal structure and behaviour. Both evidences as conflicting results have been established, which makes drawing conclusions a hard task (Cameron et al., 2023). 5-HT_{2A} receptors are involved in a lot of functions, they play a role in the memory, pain, perception etc. They are present in the pyramidal neurons in layer 5 of the neo-cortex, in the thalamus, and the reticular nucleus. Next

to these, high concentrations are present in higher-order association areas of the brain: the temporo-parietal junction and the medial prefrontal cortex. Possibly explaining the influence of psychedelics on e.g., emotional functions. Looking at the density of these receptors, the highest concentration was found in the visual cortex, forming a possible explanation for the visual hallucinations associated with psychedelics. However, even given the proof of the role of the 5-HT_{2A} receptor, limitations are found in recent research. Even after administration of ketanserin, hedonic behaviour after psilocybin administration was not affected. This blocking of the receptor did induce the abolishment of the head twitch response, but the induced changes in structural plasticity were not changed. These findings all point in the direction of possible additional pharmacological action mechanisms of psychedelics.

1.4.1 Pharmacodynamics

The usual anti-depressants onset time is about 3 to 4 weeks, which is much longer than would be desired in cases where an urgent therapeutic effect is needed for the benefit of the patient. Additionally, to that, there is only an ameliorating effect in one-third of the patients, showing the importance of improved antidepressants with fast-working action. Psychedelic drugs are promising for healing depressions, but their hallucinogenic effects limit their current application. The target molecules therefore would keep their anti-depressive effect but omit the hallucinations. The 5-hydroxy-tryptamine receptor, a G protein coupled receptor, forms the receptor where hallucinogens such as psilocybin bind to. Recent studies from China explained mechanisms through which the hallucinogens exert their anti-depressive effect by structural biology. High resolution density maps of ligand-receptor complexes were obtained, and by comparing the different conformations of different compounds bound to this receptor, 2 binding pockets were found. The orthosteric binding pocket (OBP) and the extended binding pocket (EBP). For hallucinogens, their binding to the two pockets differs, but for the non-hallucinogenic compounds, they bind less strongly to the EBP. Binding to OBP activates a G protein signalling pathway where binding to the EBP activates the β-arrestin pathway. So, hallucinogenic effects could be a consequence of a simultaneous activation of these pathways. Molecules that bypass the OBP and only bind to EBP and therefore target the activation of the β-arrestin pathway may not have these unwanted hallucinogenic effects. Analysis of the head twitch response (which indicates hallucination) in mice, even by high doses of designed compounds that mainly bind to EBP and not to OBP resulted in no head twitch response. Based on the structural features of the target sites of the receptors, analogous molecules may be designed, circumventing the problems related to hallucinations (Yin et al., 2023). The concept of ligand bias of the 5-HT_{2A} receptors has been identified as way of creating biased agonists with potentially greater therapeutic power over the known agonists with a balanced agonism between the G-protein dependent pathways and the β-arrestin pathways. In this way many side effects, such as hallucinations could be further avoided (Cameron et al., 2023). This is further described below.

Psychedelics and in particular psilocybin can react with various receptor subtypes, respectively following this order ranked according to affinity: 5-HT_{2B} > 5-HT_{1A} > 5-HT_{2A} in a rat or bovine cortex. It was shown that psilocin is also bound to other receptors than 5-HT_{2A}, namely: 5-HT_{2B}, 5-HT_{2D}, dopamine D1, 5-HT_{1E}, 5-HT_{1A}, 5-HT_{5A}, 5-HT_{7}, 5-HT_{6}, D3, 5-HT_{2C} and 5-HT_{1B}, ranked from lower to higher affinity (Dodd et al., 2022).

It is also possible that the psychedelics target an intracellular pool of these 5-HT_{2A} receptors instead of the receptors on the membrane surfaces. Since serotonergic psychedelics are

lipophilic compounds, they can pass the cell membrane and some of them such as psilocin even target these intracellular receptors and induce neuronal growth. However, it remains unknown if this targeted volume of receptors is sufficient to obtain neuronal growth or if there are other properties and signalling pathways that lead to the effects induced by these substances (Cameron et al., 2021).

Other interesting compounds, such as the modified 2-bromo-LSD, are partial agonists to the 5-HT_{2A} receptor. They form mild agonists for different 5-HT receptors, but also show agonism to the dopamine D2 and D4 receptors. Since it only partially activates the 5-HT receptors and partially antagonizes in the presence of serotonin, it may explain the lack of hallucinogenic effects. Hence, their might be a threshold below which side effects are not activated. This is another example that may suggest that the hallucinogenic part of psychedelics is not a necessity for their therapeutic potential (Cameron et al., 2023).

Psychedelics induce a cascade of pharmacological processes, of which several had been described in literature. One of these mechanisms is the psychoplastogen model. At the neural level, it was found that psychedelics increase the number of connections between neurons, increasing the synaptic growth and increasing the complexity of the dendrites and the amount of synapses. This increased neuroplasticity is due to post-synaptic effects in layer 5 of the medial prefrontal cortex. This induces a glutamate release and the activation of the α-amino-3-hydroxy-5-methyl-4-isoxazolepropionic acid receptor (AMPAR). Brain derived neurotrophic factor-tropomyosin receptor kinase B (BDNF-TrkB) is released as a result and the mammalian version of rapamycin signalling is triggered, upregulating the expression of genes related to neuroplasticity and the synthesis of protein from synaptic components by the eukaryotic elongation factor 2 (eEF2). Al these effects together amplify the neuroplasticity which can have a therapeutic effect. This forms indirect evidence for the neuroplastic effects since depressive patients show lower levels of brain derived neurotrophic factor (BDNF). Additionally, direct evidence was found in animal studies where it was indicated that prosocial behaviour was increased and stress-induced behaviour was reversed, but it must be mentioned that it is questionable how these neuroplastic effect could be beneficial for humans. In recent studies, it was shown that only high levels of e.g., LSD resulted in increased BDNF levels, whereas this was not the case for lower doses. Following this view of psychedelics, they can be seen as ‘psychoplastogens’, molecules promoting the rapid neural plasticity. It is therefore likely that neural plasticity plays a role in the therapeutic effects of psychedelics, but the evidence is limited because of lack of specificity (van Elk et al., 2022). Psychedelics increase levels of the psychoactive substance oxytocin, a hormone leading to feelings such as empathy and sociability. Acute effects that are experienced can therefore be the result of these increased oxytocin levels.

In addition to binding to receptors, molecules such as serotonin are chemically reactive molecules that can bind in a covalent way to glutamine residues of several proteins, which is called transamidation and is catalysed by transglutaminase 2 (TGM 2). When molecules such as serotonin bind to key proteins, they can influence cytoskeletal rearrangement, transcriptional regulation, mitogenesis and different processes regarding synapse formation and maturation. Since psychedelics resemble serotonin, they serve as substrates for these amidation reactions in place of endogenous enzymes. There is a hypothesis that both the 5-HT_{2A} agonism and the TGM2-amidation reactions work in a conjunction to establish the effects inside cells. Primary amines can directly undergo this amidation by TGM-2, other psychedelics

such as secondary or tertiary amines would have to be demethylated first, which occurs in vivo quite rapidly. Now the question arises whether this TGM-2 activity mediates the therapeutic affects in some way. In a landmark study it was shown there was a decreased histone serotonylation in patients with MDD who were not taking any antidepressants. Further research has to be performed to check whether these histone marks influence depression, anxiety and others (Cameron et al., 2023).

On the genetic level, psychedelics also exert an effect since they affect the transcription by activating a small amount of 5-HT_{2A} receptors. These are called 'trigger neurons', who activate anti-inflammatory mechanisms, giving psychedelics the potential to be used in treatments for other disorders such as Alzheimer and Parkinson. These are diseases where the immune system is chronically over activated, thereby turning psychedelics into potential remedies because of their anti-inflammatory character. This anti-inflammatory behaviour could also be beneficial for the treatment of depression and addiction. Cytokines trigger the inflammatory response in our body. Disturbances of these cytokines are linked to depression and anxiety-related disorders (van Elk et al., 2022).

It is thus clear that psychedelics exert many different effects on the pharmacological level, and it is likely that the combination of all these effects forms the basis for why psychedelics are of interest for all kinds of disorders where depression only represents one of them.

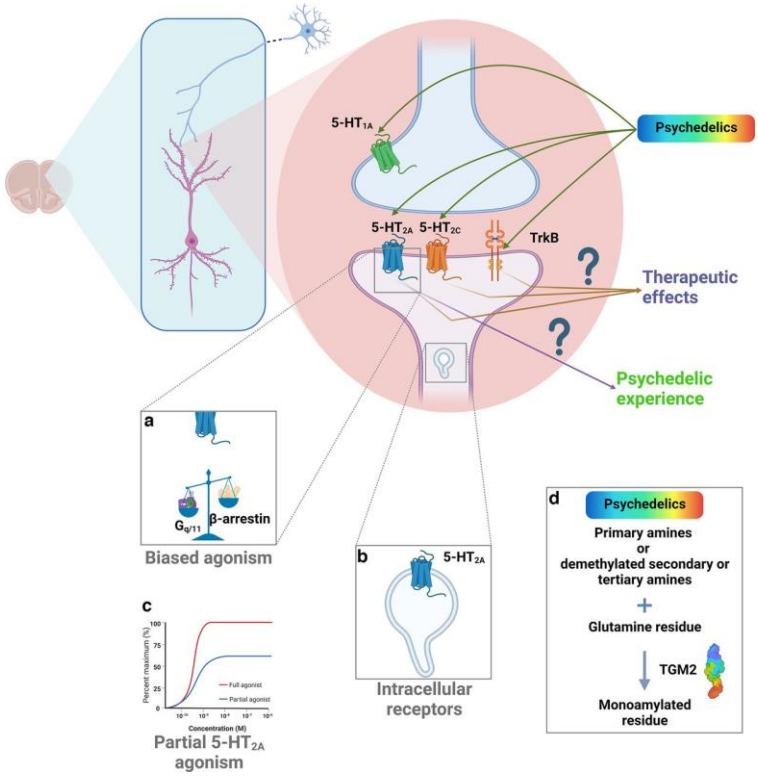

***Figure 1.3**: Representation of the different targets of psychedelics. Mainly in the pyramidal neurons of cortical areas such as the prefrontal cortex (Cameron et al., 2023)*

Looking at neuroscientific explanations, different hypotheses have been proposed, namely: the thalamo-cortical filter theory, the relaxed beliefs under psychedelics model (REBUS) and the claustro-cortical circuit model (CCC). Overall, it appears that there is a detrimental effect of psychedelics on cognitive and attentional processing, where the different theories mentioned above can give possible explanations for this detrimental effect. The first theory,

the thalamo-cortical filter theory mentions the functioning of our brain through feedback loops between cortical regions and the thalamic nuclei. These loops prevent the overload of sensory and interoceptive information. The thalamus has a filtering function since it controls the amount of signals that go to higher-level cortical regions. This filter function is then controlled by the prefrontal cortex, where psychedelics would release the inhibitory control mechanism, meaning that there is a reduction in the inhibitory control of the prefrontal cortex on the thalamus, which then results in an overload of information to higher-level brain regions. These events are associated with different neural mechanisms such as an excessive stimulation of the 5-HT_{2A} receptors. Both PET-studies and recent fMRI studies showed that psychedelics alter the activity and the connection between the prefrontal cortex and the thalamus. In this model, similarities are seen with the psychotic state, which leads to the name of psychotomimetic model for psychedelics, since they provide some sort of psychotic state. It is the intensification of sensory processing that bears similarities to this psychotic state (van Elk et al., 2022).

The second mentioned model, the REBUS model represents an integrative account since it integrates the entropic brain hypothesis with the free energy principle. Since psychedelics act on the 5-HT_{2A} receptors, they promote excessive excitement of deep-layer pyramidal neurons, which encode our precision of belief. In our everyday consciousness there is this hierarchal model that gives predictions on sensory input that enters our senses. When there is a mismatch between this prediction and the input, a prediction error is generated, that in turn will update the generative model. So, psychedelics will fail to suppress these prediction errors, loosen prior predictions, and increase the sensitivity towards these prediction errors. As mentioned before, perceptual effects of psychedelics might appear since there is high density of 5-HT_{2A} receptors in the visual system. The effect of loosening prior predictions can be shown by the 'breathing walls' phenomenon, here our perception of a wall is no longer constrained by the prior perception, being a solid object. This absence of the correct prediction error results in an event named visual trails, referring to the fact that moving objects leave a visual trace (van Elk et al., 2022). When looking at higher doses of psychedelics, higher level regions according to cortical hierarchy are affected. The Default Mode Network plays an important role here, being implicated in task-free processing such as self-referential processing. In fMRI studies it has been shown that there is a decreased activity in this DMN during a psychedelic experience. However, this is contradictory with other studies showing an increased activity in prefrontal areas. Both differences relating to methodologies as the dynamic nature of a psychedelic experience may explain these discrepancies (van Elk et al., 2022). Additionally, this model also integrates the entropic brain hypothesis, where there is an increased connection between brain regions that are normally not very interconnected. So, the phenomenon of the 'entropic brain' refers to the fact that our brain is in a state of increased disorder compared to our normal functioning. This hypothesis helps to explain the synthetic experiences that might be experienced under psychedelics, such as sounds inducing certain colours. Psychedelics may have disruptive effects on attention, thereby keeping in mind that attention can be conceived of the precision of prior expectations that shape our perception. Hence, impaired attentional processing is a result from less precise predictions because of loosened prior predictions. This REBUS model can partly explain the therapeutic effects of psychedelics. A disorder such as depression is characterized by a maladaptive hyperprior, which are beliefs that are resistant to change e.g., overly negative self-images. Other beliefs, actions and emotions are influenced by these hyperpriors. Psychedelics temporarily loosen these maladaptive hyperpriors by

directly acting on how these prior beliefs are coded in our brain. Hence, people can become more open to new beliefs, also outside the psychedelic experience, in the following weeks and months. Again, this model is subjected to criticism on both methodological and conceptual level (van Elk et al., 2022).

Another model, the claustro-cortical circuit (CCC) is mainly based on neuroimaging observations. The claustrum is located between the insula and the putamen, and is highly saturated with 5-HT_{2A} receptors and connected to different cortical and sub-cortical regions. This grey matter is involved in different tasks relating to cognitive control and sensory conflict. Activation of this claustrum results in cortical activation, and the activation of the claustrum itself is mainly driven by the prefrontal cortex, resulting in this so called claustro-cortical circuit. Psychedelics can destabilize canonical brain network states and decouple prefrontal areas from the claustrum. It has been suggested that this coupling and thus coordination between the claustrum and these prefrontal areas is important in cognitive control, whereby psychedelics seem to disrupt this cognitive control. The effects that psychedelics have on the claustrum may form the reason for a decrease in the executive functioning.

Summarizing what is written above, 3 frameworks are proposed for a psychedelic experience: a filtering mechanism, the relaxing of beliefs and the claustrum cortical circuit. Next to neurological effects, psychedelics also exert different psychological mechanism where several effects such as altered states, belief change, social effects and others can be observed (van Elk et al., 2022).

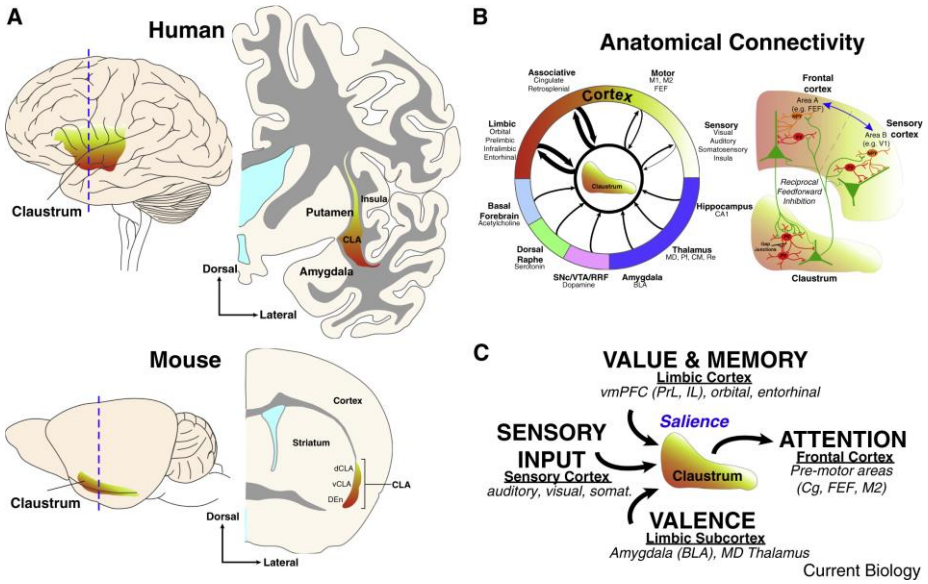

Figure 1.4: *Location of the claustrum (A), whole-brain anatomical connectivity of the claustrum (B), and a summary of the functions related to claustrum connections (C) (Smith et al., 2020)*

1.5 Methods for antidepressant discovery and design

The process of drug discovery can be roughly divided into experimental, knowledge based and computational methods. In the experimental methods, combinatorial methods, and high throughput screening (HTS) are popular. In this combinatorial chemistry a large library of structurally differing molecules is synthesized, leading to a rapid lead generation, diversity, and a cost-effective synthesis method. Thanks to HTS, this large chemical library of compounds can be rapidly pharmacologically screened in vivo. Lead identification is dominated by this technique (Immadisetty et al., 2013).

In the knowledge-based methods, structure-activity relationships (SAR) and the molecular hybridization technique stand central. Biostructural data and different available chemical entities provide the necessary information. These SAR studies are especially relevant in the optimization of a lead component towards their specific target by generating different structural analogues. A chimeric bioactive compound with superior characteristics is generated by the combination of features from different bioactive compounds, in a technique called molecular hybridization. In this way, receptor selectivity may be improved. However, this method is mainly interesting for creating analogues of already existing molecules, rather than generating novel drug scaffolds (Immadisetty et al., 2013).

The third category of methods, the computational methods are expected to take the lead in drug discovery. High-throughput virtual screening (HTVS) forms the in-silico alternative to HTS. Databases containing up to millions of chemical structures can be ranked according to their predicted affinity to a certain receptor or other targets. These HTVS methods can be further subdivided into ligand-based, structure-based and a hybrid method, combining the 2. In the ligand-based methods, the interactions between ligands and proteins are predicted based on structures of already established ligands in a pharmacophore approach, without further information on the structure of the targeted protein. In a pharmacophore approach, the spatial orientation of the ligand required for the biological activity is taken into account. This is interesting when there is no information available on the binding sites because of a lack of an X-ray crystallographic structure of the target. Compared to structure-based HTVS, this is computationally less intensive but on the other hand, there is a reduction in the likelihood of finding novel scaffolds and there is a requirement for the conformation of at least one bioactive ligand. When there is information available on the target proteins, structural based methods are preferred. The technique used in these methods, is ligand docking on the target. In the absence of crystal structures, homology models are used, where the 3D structure of evolutionary related structures are used as a basis for alignment. The different chemical compounds present in a certain library, are docked in the site of interest of targeted proteins and are subsequently being ranked. A force-field measuring the interaction between a ligand and a protein is the most frequently used. Visual inspection is however required since the accuracy is still quite limited. Enrichment of these studies can be improved by the use of ensemble docking, where multiple conformations of the targeted protein is used (Immadisetty et al., 2013).

An example of such a structure-oriented method for the synthesis of non-hallucinogenic antidepressants was performed by Cao et al. (2022). Their design strategy was the identification of structures that target the EBP and mimic the second binding pose of psilocin, without engaging to the deep hydrophobic binding pocket, which is responsible for the

antagonist working action of the 5-HT_{2A} receptor. Risperidone and ritanserin are two 5-HT_{2A} receptor antagonists, that both have a deep binding pose, characterized by a fluorobenzioxazol ring and a 4-fluorophenyl group. Their moiety resembles the second binding pose of psilocin.

Other 5-HT_{2A} receptor antagonists such as atypical antipsychotics have a similar 4-fluorophenyl group, of whom is suspected by Cao et al. (2022) to have the same deep binding pose. Three rigid moieties were identified for a possible binding to the EBP: the moiety from lumateperone (IHCH-7113), the moiety from spiperone (IHCH-7117) and the moiety from pimozide and benperidol (IHCH-7125). The tetracyclic core of lumateperone orients towards the EBP (revealed by analysis of crystalizing lumateperone in the receptor) and has a similar pose as the second binding pose of psilocin. Just as risperidone and ritanserin, the 4-fluorophenyl group from lumateperone is placed in the deep hydrophobic binding pocket. The contact between this group and residues in the proline-isoleucine-phenylalanine motif (PIP) and the 'toggle switch' seems to prevent a rearrangement which would be necessary to activate the receptor and hence forms a possible explanation for the antagonist activity of lumateperone (Cao et al., 2022).

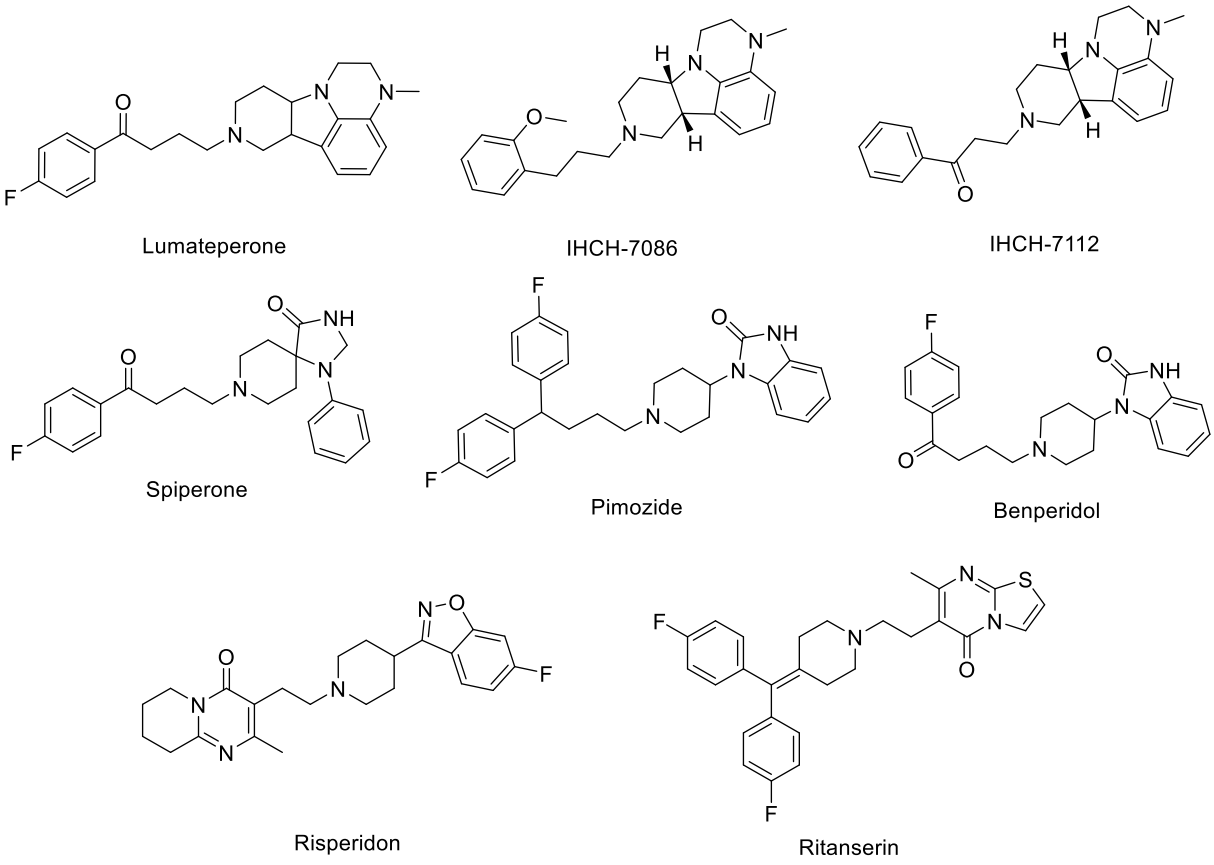

Figure 1.5: *Overview of some 5-HT_{2A} receptor agonists evaluated by Cao et al. (2022)*

IHCH-7112 (lumateperone analogue: shortening of one carbon of linker group and the removal of the fluorine atom) was further modified by the introduction of a 2-methoxy or 2-hydroxy substitution on the terminal phenyl group. In this way, the major interaction with the EBP, determining the β-arrestin-bias, was retained (bias of 3.7 for IHCH-7112), but an increased flexibility limited their binding to a conserved serine in the side extended pocket (SEP). The most potent analogue to IHCH-7112 was e.g.. IHCH-7086 (Cao et al., 2022).

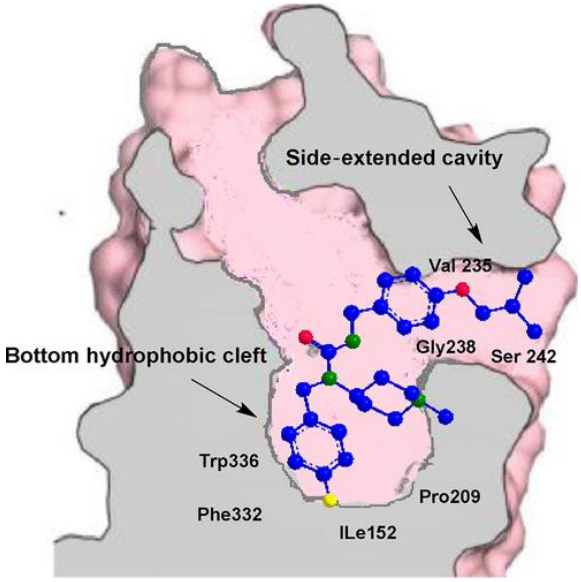

Figure 1.6: *5-HT$_{2A}$ receptor with hydrophobic binding pocket and side extended cavity (SEP) (Albujuq et al., 2023)*

In the case of LSD, it appears that there is no requirement for a hallucinogenic effect to have an anti-depressant like effect. Components such as IHCH-7086 are supposed not to cause hallucinations and therefore they were assessed for their in vivo antidepressant potential. Acute administration of these compounds clearly decreased depression like behaviour in the forced swimming test and the tail suspension test. Even the low efficacy of these 5-HT$_{2A}$ receptor agonists is sufficient to exert an antidepressant effect (Cao et al., 2022).

By the identification of a second binding mode of psilocybin, it was possible to do a structure-based design of β-arrestin-biased ligands such as IHCH-7086. β-arrestin activity is a key factor in anti-depressant like behaviour, but it is insufficient for the introduction of psychoactive actions.

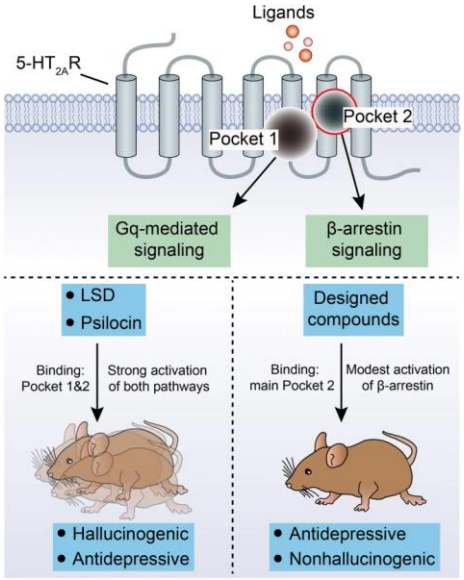

Figure 1.7: *Agonist behaviour of biased ligands (Yin et al., 2023)*

To have a hallucinogenic effect, it seems to be necessary to have a high transduction efficiency of the 5-HT_{2A} agonists for both G-protein-mediated signalling as the β-arrestin activity. The low transduction efficiency of these β-arrestin-biased ligands is sufficient to eliminate the hallucinogenic effect. This is illustrated in Figure 1.7, where a binding to pocket 2 mediates the β-arrestin signalling and binding to pocket 1 mediates G-protein signalling (Cao et al., 2022).

A last method, the hybrid approach, conjugates the ligand- and structure-based approaches. These HTVS are superior to HTS in certain aspects, since they can provide a larger screening library and time and money is saved. But the overall reliability is still lower than HTS given its virtual nature, and the hits found by HTVS still need to be tested in vitro (Immadisetty et al., 2013).

1.6 Synthesis of psilocybin (analogues)

The different synthetic routes used for the synthesis of psilocybin analogues are the same as those for tryptamine synthesis. A substitution of the indole at position 3, the creation of the 5-membered ring starting from a functionalized aromatic and a methodology involving coupling reactions catalysed by different transition metals such as iridium and palladium, form possible synthesis methods.

Hofmann was one of the first to synthesize psilocybin in 1958. In this reaction scheme, an amino-ethyl group was inserted in the 3 position of the indole core. After a few steps, a phosphorylation using O,O-dibenzylphosphorylchloride was performed, followed by a hydrogenation of palladium on carbon (Figure 1.8) (Hofmann et al., 1958).

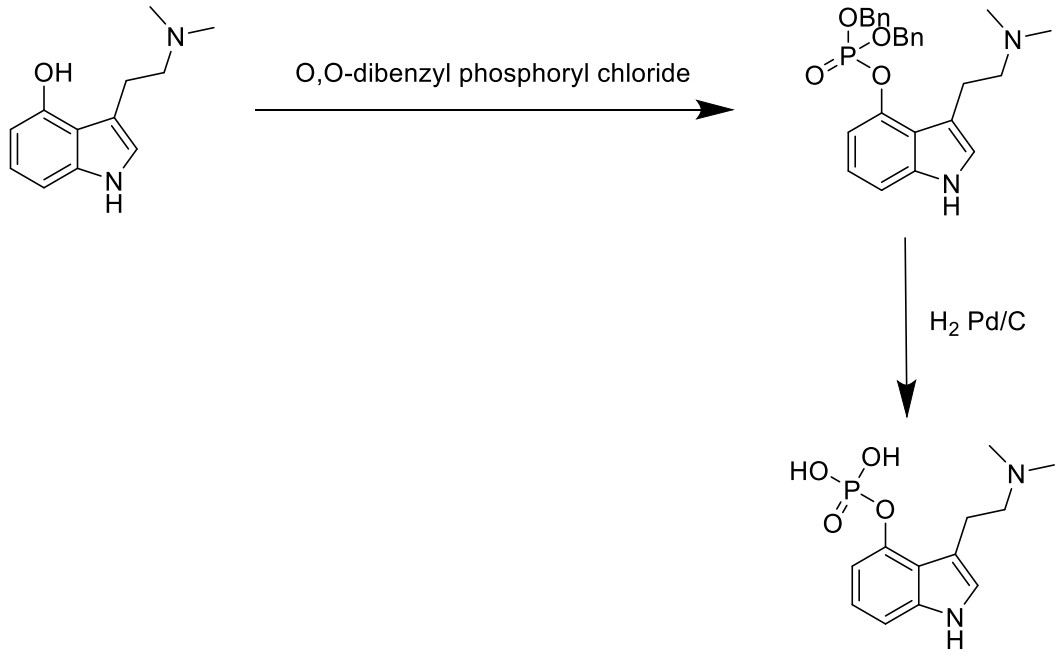

Figure 1.8: *Hofmann reaction scheme*

The years following this synthesis, different improvements in yield and purity were obtained. Different phosphorylation protocols, for example, were used. Nichols et al. (1986) used another phosphorylating agent, tetra-O-benzyl-pyrophosphate, which increased the yield from 20% to 46.9%. However, there appeared to be a hydrolytic cleavage of one O-benzyl

group at room temperature, and in addition the purification of psilocybin appeared to be difficult.

An adaptation of the Speeter-Anthony tryptamine synthetic pathway using Shirota's conditions (Figure 1.9) performed by Sherwood et al. (2022), was able to obtain psilocybin in a high purity (99.9%). Therefore, 4-acetoxyindole was acylated with oxalyl chloride, leading to **3**. This intermediate **3** was then reduced with $LiALH_4$, leading to a mixture of compounds, including a β-hydroxy derivative. Allowing this mixture to reflux, resulted in psilocin **2** (Figure 1.10). This was then phosphorylated using the rearrangement protocol.

Alternative solutions for the use of expensive reagents such as tetra-benzyl-pyrophosphate were developed in a second-generation synthesis, where phosphorus oxychloride was used as a replacement. This resulted in a more atom efficient process (Serreau et al., 2022).

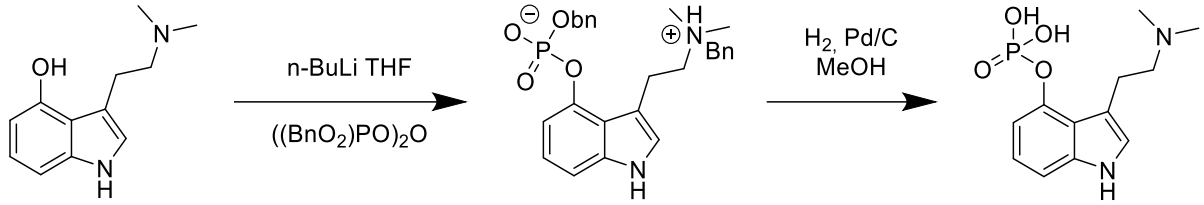

***Figure 1.9**: Synthesis of psilocybin according to Shirota et al. (2003)*

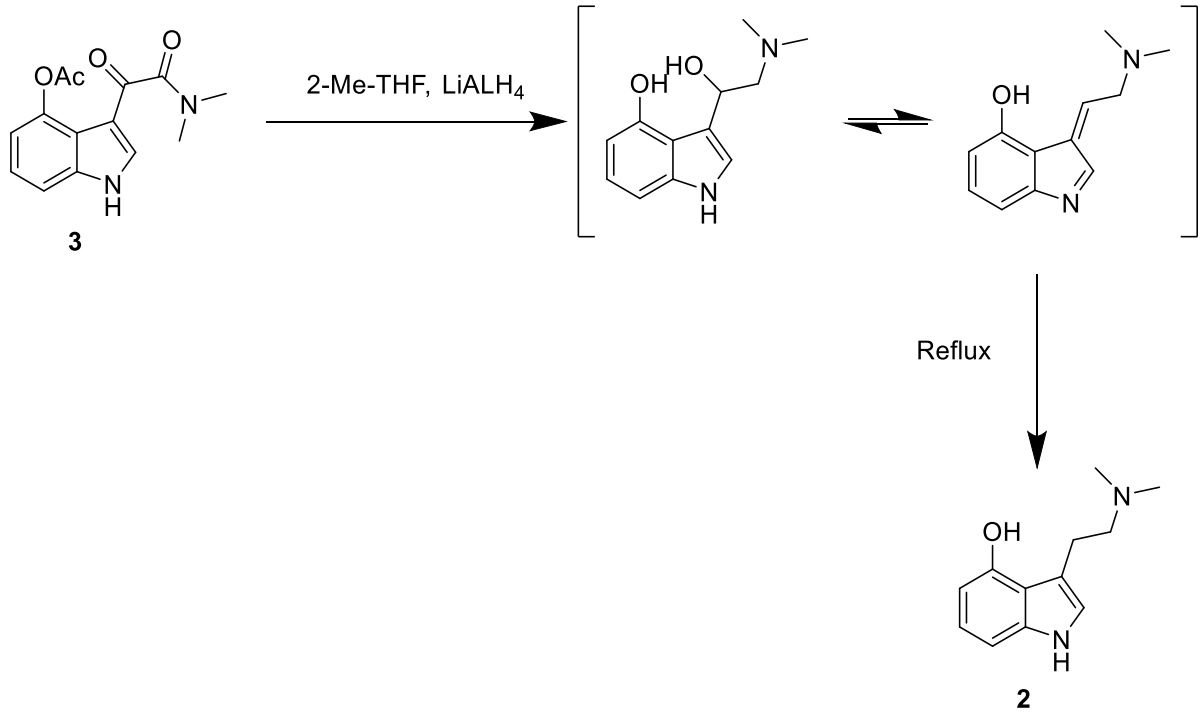

***Figure 1.10:** Synthesis of psilocin by Sherwood et al. (2022)*

Psilocin can also be synthesized by metal-catalysed reactions, giving the opportunity to start the synthesis from a wider range of functional groups. The indole core structure can be obtained via a palladium-catalysed cyclization reaction starting from 4-hydroxy-ortho-iodoaniline **4** and a silylated alkyne that bears the dimethyl aminoethyl chain. The silyl group is then removed using trifluoroacetic acid, and in a third step, the methyl group is removed

using boron tribromide. According to this protocol, a yield of 24% was obtained (Figure 1.11) (Serreau et al., 2022).

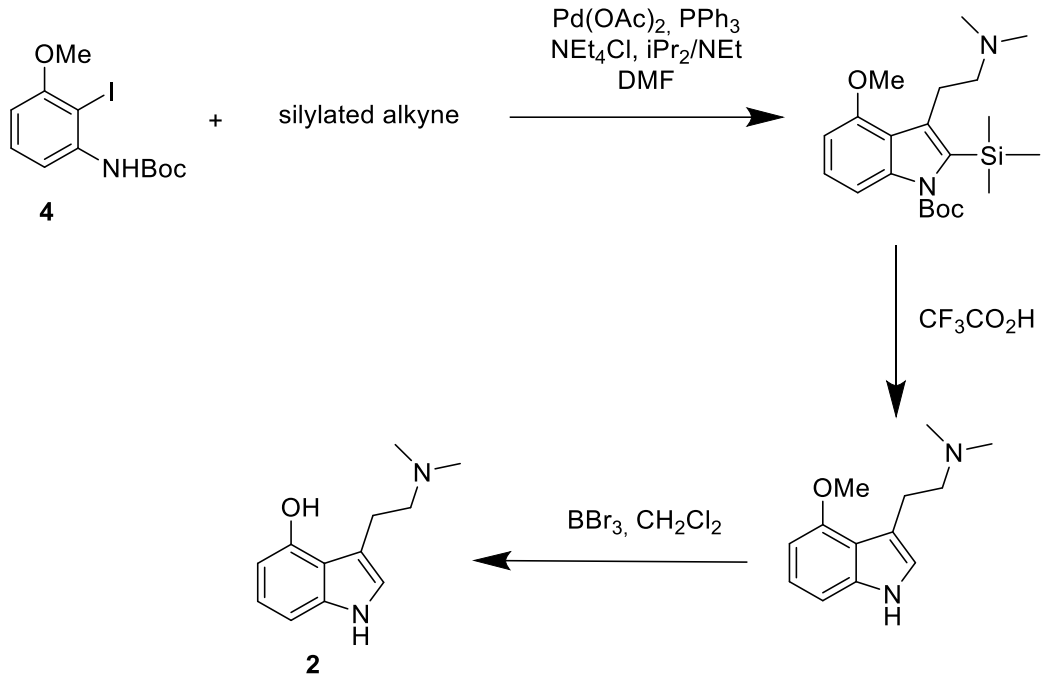

***Figure 1.11**: Synthesis of psilocin using transition metals*

A more recent approach, using the borrowing hydrogen strategy, starts from an indole **5** and introduces the alkyl chain at the 3-position. A selective iridium-catalysed alkylation on the C3 position of the indole using an N-protected ethanolamine has been reported. This transformation was performed at 150 °C for 48 hours and caesium carbonate was used as a base (Figure 1.12) (Bartolucci et al., 2016). However, it must be noted that these reactions with transition metals are interesting for small scale applications but become more difficult at larger scale seen the high cost of these catalysts (Serreau et al., 2022).

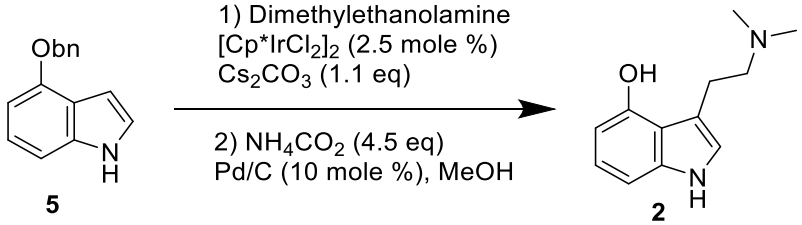

***Figure 1.12:** Psilocin synthesis by Bartolucci et al. (2016)*

Given the known difficulties in the synthetic routes and the increasing use and demand of these molecules given their therapeutic potential, solutions comprising enzymatic routes were sought. Biocatalytic synthesis in vitro and in vivo in microbial hosts were performed by using the kinase gene for psiK (4-hydroxytryptamine kinase) that has been identified in *Psilocybe* mushrooms. Hence, the compounds need to be extracted from the matrices to eliminate cellular dishes. To avoid these issues, a combined synthesis was developed using both a chemical pathway and biosynthesis route. PsiK was first produced by E. coli. After psiK conducted the phosphorylation step, another enzyme, an S-adenosyl-L-methionine (SAM)-dependent N-methyltransferase acts twice and forms psilocybin. In this research performed

by Fricke et al. (2020), the dual characteristic of the enzyme psiK was discovered, namely both its biosynthetic as its protective role, accepting both 4-hydroxytryptamine as psilocin as substrates.

Fricke et al. (2021) developed a chemo-enzymatic synthesis approach, using the Speeter-Anthony tryptamine synthesis with a subsequent enzymatic phosphorylation by psiK. This is convenient since the formation of 4-hydroxylated tryptamines is relatively straightforward, but the subsequent phosphorylation step forms the difficult part from a chemical synthesis point of view. With the help of ATP, the enzyme psiK originating from *Psilocybe cubensis* replaces the chemical phosphorylating step. The commercially available 5-methyl-1H-indol-4-ol **6** is protected with an acetyl group using acetic anhydride and $NaHCO_3$, resulting in 1H-indol-4-ol-acetate **7**. Afterwards, a modified version of the Speeter-Anthony tryptamine synthesis resulted in the amine substituted derivate. The 1H-indol-4-ol acetate **7** reacted with oxalyl chloride and dimethylamine to result in the ketoamide **8**. This was further reduced using aluminium hydride. The resulting amine **9** was incubated with the enzyme and ATP. This hybrid chemoenzymatic synthesis of C4-C5 substituted compounds was performed, and after the in vivo bioassay, its psychedelic like activity was shown to be retained. This encourages further research to check for other substrates that could also be appropriate for this phosphorylation by the enzyme, and to check whether the structure activity relationships of the disubstituted tryptamines are retained (Fricke et al., 2021).

In this way heavy metals and expensive reagents can be avoided, yielding a synthesis route in a greener way with reduced costs (Serreau et al., 2022).

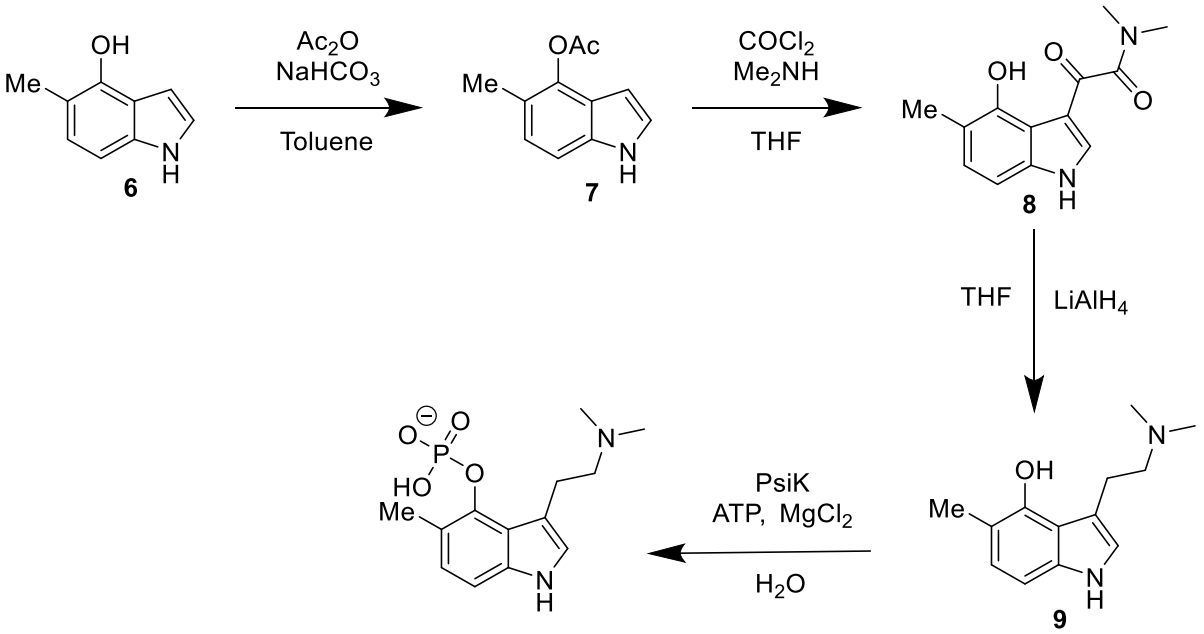

Figure 1.13: *Chemoenzymatic approach (Fricke et al., 2021)*

1.7 Concluding remarks

As indicated by the clinical trials regarding psilocybin use, and its use during history by mankind, the therapeutic potentials of this compound are demonstrated. However, the fact that it comes along with hallucinogenic effects, still forms an unwanted side effect hampering its current use. Current research, trying the understand the mechanism of action of the drug

in combination with docking studies can give lead to compounds resembling psilocybin and its derivatives. In this way, anti-depressants can be discovered without the hallucinogenic effects, and maybe even showing enhanced therapeutic effects.

Different synthesis methods can be used, purely chemical, purely enzymatical or a combination of the 2, where difficulties concerning certain reaction steps can be overcome using enzymes. Additionally, this can add to a greener way of producing drugs, avoiding toxic solvents, catalysts and high energy demands for the harsh reaction conditions sometimes required.

2. Results and discussion

2.1 First pathway

As has been extensively discussed in the literature review, the search for new (fast lane) antidepressants is prominent. In this master dissertation, an attempt at finding and synthesizing such molecules was made. Several molecules analogous to psilocybin were targeted for synthesis, using different kind of pathways. It is the intention to subsequently test these molecules for their antidepressant character and their (non)-hallucinogenic properties. Throughout this master dissertation, different pathways and methods were considered in order to obtain these analogues. Initially psilocybin analogues were aimed at synthesizing with the intention of creating compounds, where the labile phosphate bond is replaced with a more stable P-C bond, making the molecule less susceptible to the human enzymes. During the year, methods were frequently switched around because of several difficulties that arose.

In the first series of attempts, psilocybin analogues with substitutions at different places of the indole core of the molecules, formed the objective of the synthesis routes, namely **16** and **16b**. In this first series of attempts, two different starting products were used: 5-Bromo-7-azaindole **10** and 5-Bromo-1H-indazole **10b**. Therefore, a substitution with a phosphoric acid group on this azaindole and indazole ring will be attempted at position 5. The motivation behind targeting the C-5 position was based on prior testing and evaluation of similar molecules by Vandevelde 2023.

The first series of experiments were performed on 5-bromo-7-azaindole. In a first step, a Mannich reaction was performed in order to substitute the azaindole-core with a diamine group at position 3, leading to **11**. The second step consists out of an oxidation of the diamine group to a nitrogen oxide group (**12**). After this, the nitro ethyl group will be reduced to the amine analogue (**13**) using zinc. Subsequently, the amine group should be transformed into the dimethyl amine analogue (**14**). After this, the bromo atom will be substituted by a diethyl phosphite group (**15**), through a Hiroa coupling. In a last step, the diethyl group will be hydrolysed to form the phosphoric acid analogue (**16**). This first pathway is represented in Figure 2.1.

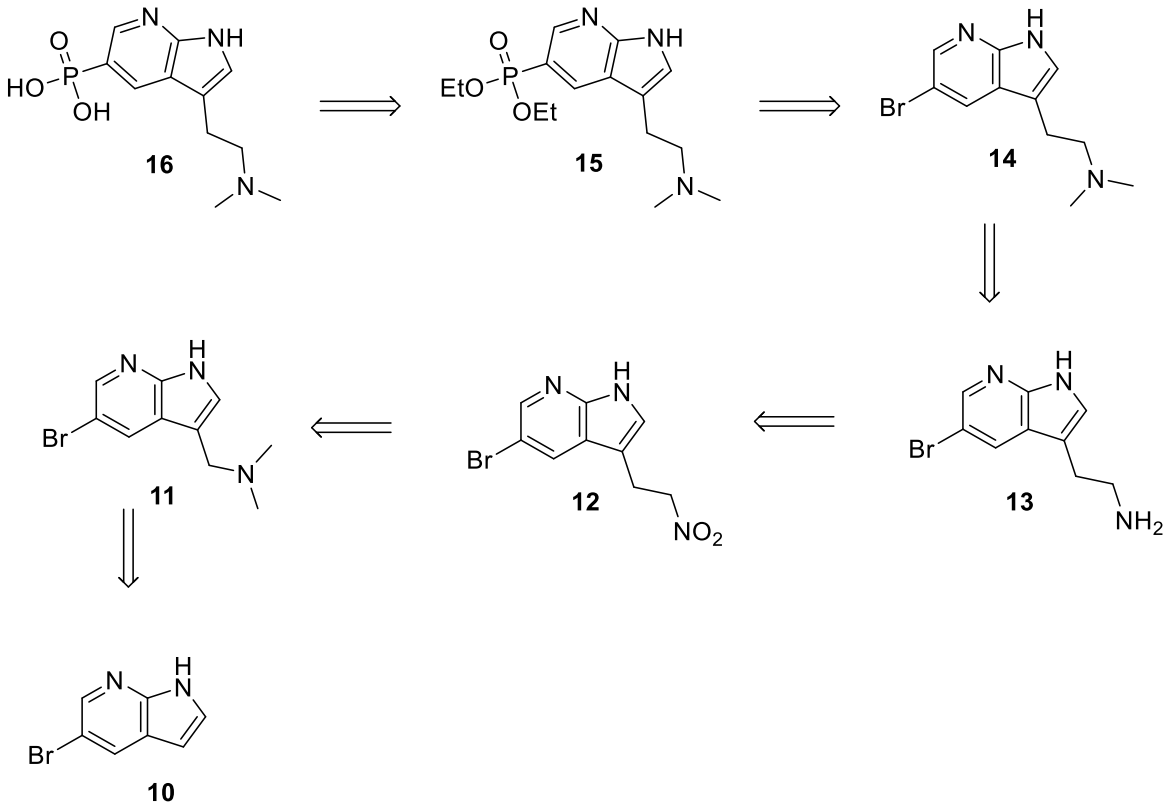

Figure 2.1: *Reaction scheme starting from 5-Bromo-7-azaindole*

This same type of strategy will be used starting from 5-Bromo-1H-indazole (Figure 2.2)

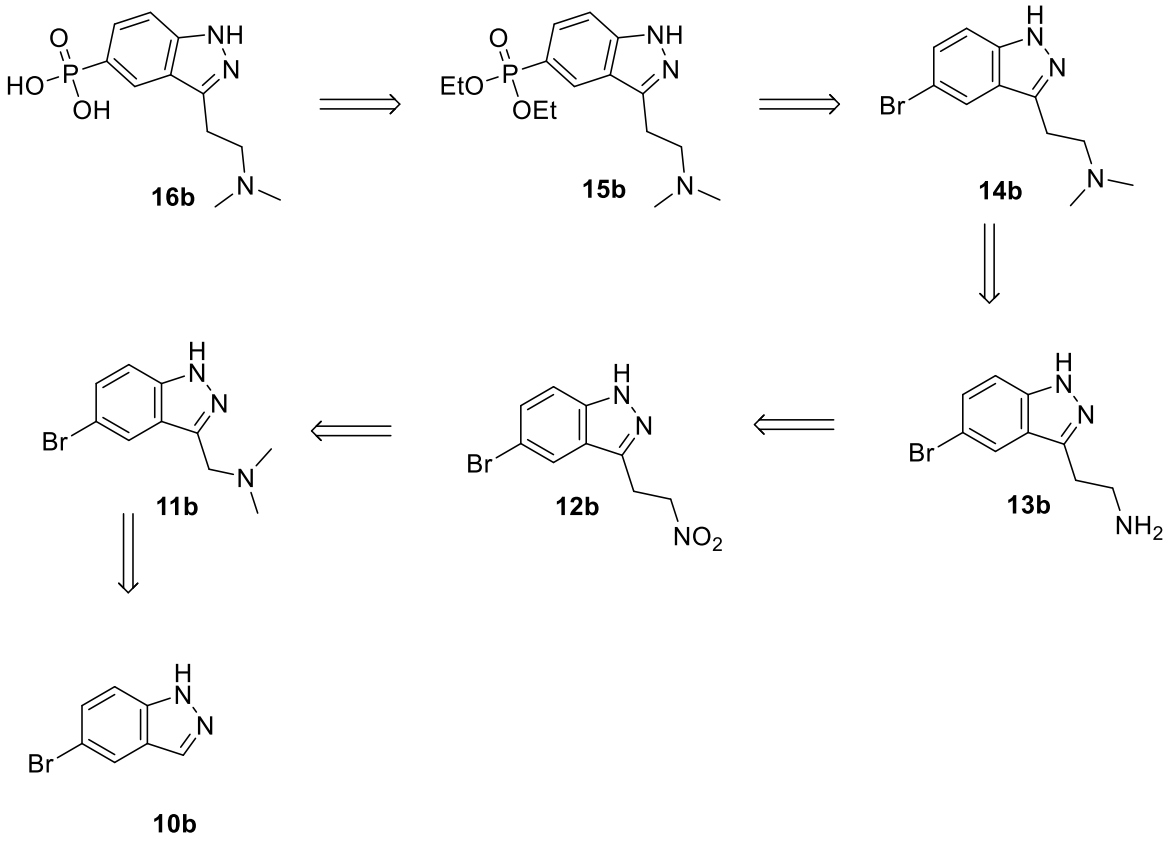

Figure 2.2: *Reaction scheme starting from 5-Bromo-1H-indazole*

2.1.1 Starting from 5-Bromo-7-indazole

2.1.1.1 Mannich reaction for the synthesis 3-(N,N-dimethylaminomethyl)-5-bromo-7-azaindole

In a first step, 5-bromo-7-indazole is subjected to a Mannich reaction. This method is used to synthesize β-amino carbonyl compounds by formation of carbon-carbon bonds. It involves the use of a carbonyl donor, an amine and an acceptor aldehyde (Figure 2.3)(Córdova, 2004). The reaction mechanism for this type of reaction is presented in Figure 2.3 and Figure 2.4. In this case, the reaction is acid catalysed. First, the formaldehyde is activated and the amine performs a nucleophilic addition. Water is eliminated and the iminium ion is formed. Next, the double bond of **10** in the five membered ring will attack the iminium ion, yielding an enamine intermediate. This will, via an imine-enamine tautomerisation, give rise to the imine **11**. Glacial acetic acid will act as the acid catalyst and formaldehyde as the carbonyl donor.

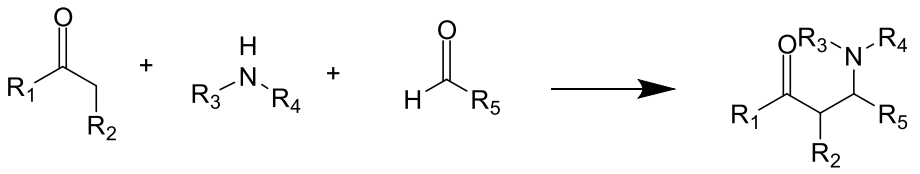

Figure 2.3: *Mannich type of reaction (Córdova, 2004)*

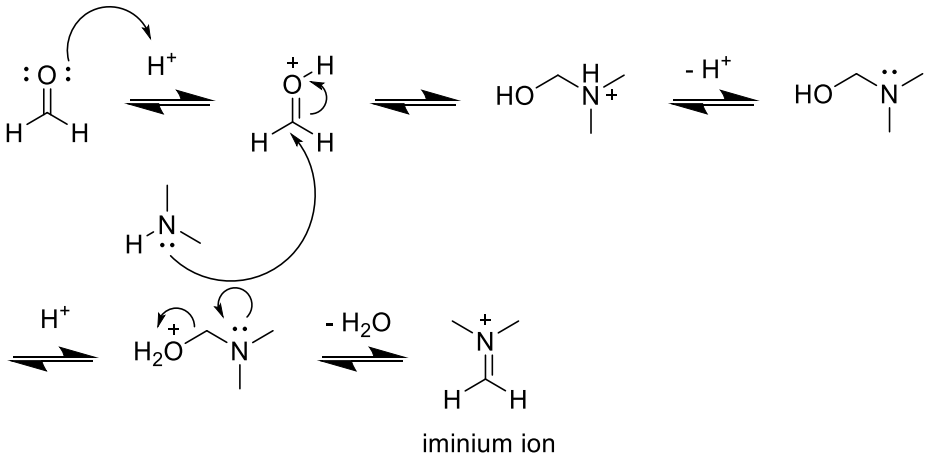

Figure 2.4*: Acid catalysed formation of iminium ion*

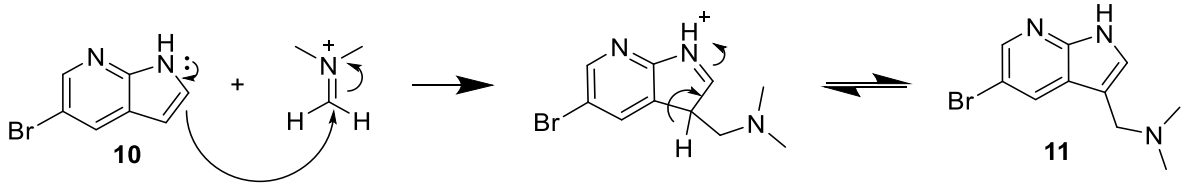

Figure 2.5*: reaction mechanism for the synthesis of 3-(N,N-dimethylaminomethyl)-5-bromo-7-azaindole*

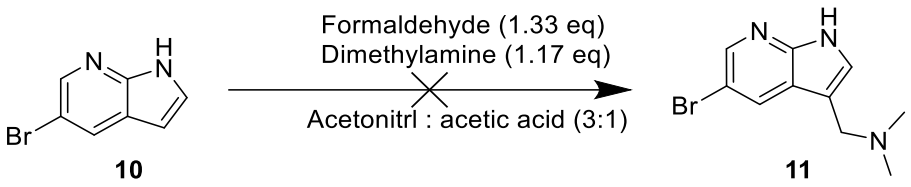

***Figure 2.6**: Mannich reaction on 5-Bromo-7-azaindole*

The reaction conditions for this reaction were followed as described by Alzweiri et al. (2021). Therefore, **10** was dissolved in acetonitrile and glacial acetic acid was added at a temperature of 0 °C in a ratio of 3:1, respectively. Subsequently formaldehyde and dimethylamine were added. The solution was stirred at room temperature for 2 hours. The resulting mixture was basified with sodium hydroxide and extracted twice with ethyl acetate. The organic phase was dried with magnesium sulfate and the solvents evaporated. For the purification, both normal- and reversed-phase liquid chromatography with different solvent mixtures were tested. Regarding the normal-phase chromatography, solvent mixtures were tested on silica plates using TLC. The solvent mixtures tested consisted out of, hexane-ethyl acetate and chloroform-acetone in different ratio's. The best separation of the compounds was achieved with a mixture of chloroform-acetone in a ratio of 90:10.

In first instance, the reaction depicted in Figure 2.6 was thought to be successful, the associated mass was indicated on LC-MS and the spectrum of the ^{1}H-NMR analysis revealed a peak for the two methyl groups and a CH_2 peak. However, there appeared to be a fourth aromatic peak, which was first overlooked and thought to belong to some leftover starting product. But even after purification, this peak remained. Additionally, the peak belonging to the NH of the pyrrole ring also seemed to have disappeared. From this, it was concluded that the Mannich reaction had occurred at the N-1 position rather than the C-3 position of the 7-azaindole core (Figure 2.7).
The mixture was thus purified using normal-phase chromatography with chloroform and acetone as eluents, leading to **17** instead of **11** as a white powder with an isolated yield of 63%.

This observation revealed that this brominated 7-azaindole exhibits a different kind of activity compared to the brominated indole derivatives examined in the dissertation of Vandevelde (2023). In this way, the N-1 alkylated 7-azaindole instead of the 7-azagramine was formed, which does not form the target molecule since an alkylation occurred at the incorrect position of the 7-azaindole ring. Literature was reviewed to look for an explanation for this reaction behaviour.

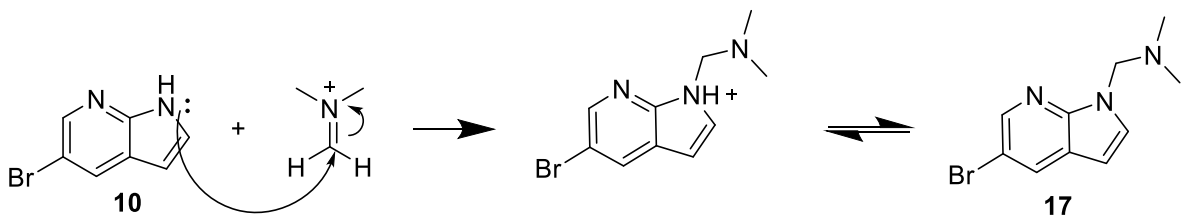

***Figure 2.7**: Mannich reaction on N-1 position with formation of 1-(N,N-dimethylaminomethyl)-5-bromo-1H-pyrrolo[2,3-b]pyridine*

When comparing the reactivity of 7-azindole to indole at the C-3 position, there appears to be a relative inertness of this C-3 position in 7-azaindole. Most probably this is the result of the electron-deficient nature of this pyridine moiety, which causes a reduction in the overall nucleophilicity of the heterocyclic system. Other strategies for a direct acylation at the C-3 position are reported in literature, e.g. by enhancing the nucleophilicity of the 7-azindole moiety. This can be achieved by reacting an 7-azaindolyl Grignard reagent with diethyl oxalate to form the α-keto ester (Popowycz et al., 2007).

The replacement of the carbon atom at position 7 of the indole ring with a nitrogen atom decreases the reactivity at the 3-position. This reactivity is even more reduced in the presence of a Lewis or Bronsted acid. The basic strength of this 7-azaindole, with a pK_a of 4.59, is higher than the one of indoles, with a $pK_a < 1$. Protonation of this nitrogen causes a lowering in the electron availability at the 3-position compared to indoles (Kannaboina et al., 2020).

A characteristic feature of these azaindoles is that because of their fused bicyclic system, there is a directly opposite displacement of the π-electrons in each ring. This creates a π-electron deficient pyridine ring and a π-electron excessive pyrrole ring. An electrophilic reaction such as a Mannich and Vilsmeier reaction is more difficult to perform on this C-3 position compared to indoles. Additionally, substitutions on the N-1 position can have considerable effects on the reactivity of this C-3 position. They change the electron density and the ability of the protonation of the nitrogen in the pyridine moiety (Yakhontov et al., 1968).

However, the same type of Mannich reaction on 5-bromo-7-azaindole was performed by Brnardic (1998), and proved to be successful at the C-3 position when performed at elevated temperatures (60 °C). This increase in temperature seems to enhance the reactivity of the C-3 position.

Even though the targeted 7-azagramine was not formed, an N1-alkylazaindole was formed instead. These compounds also seem to have interesting antidepressant activities and show promising interactions with 5-HT receptors (Dunlap et al., 2020). They are receiving increased attention in medicinal chemistry, given both their hydrogen-bond donor and acceptor properties, resulting in a broad spectrum of activities (Kannaboina et al., 2020).

Other research in literature reports on the effects of these compounds. Psychedelic compounds such as the N,N-dimethyltryptamines (DMT) have showed a clinical efficacy for the treatment of depression; this molecule therefore forms an important starting point for medicinal chemistry. Analogues of DMT have also been evaluated in this dissertation, as will be described in section 2.3. Next to several difficulties in synthesizing DMT derivatives in a rapid way, these DMT's are also known to be potential hallucinogens. This is where the N,N-dimethylaminoisotryptamine (isoDMT) come into play, as it shows a reduced hallucinogenic potential and allows an easier and faster N-alkylation. They also appear to have a comparable affinity for the serotonin receptors (Dunlap et al., 2020). Research conducted by Glennon et al. (1984) compared the 5-HT receptor affinity for a series of isoDMT and DMT. This study revealed that the isoDMT appeared to possess a greater affinity than the DMT. The neuronal growth seems to be promoted, even in the absence of the N-H bonds. Additionally,

because of the loss of a hydrogen bond donor (lack of NH), the polar surface area is decreased which appears to improve the central nervous system multiparameter optimization (CNS MPO) score (Dunlap et al., 2020). This CNS MPO, which is based on 6 physicochemical properties, forms one of several approaches that medicinal chemists use in their decision making for the design of novel drug candidates (Wager et al., 2016).

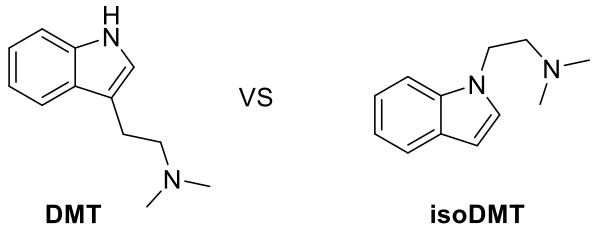

Figure 2.8: *Chemical structure of N,N-dimethyltryptamine and N,N-dimethylisotryptamine*

Thus, even though these molecules first appeared to be unwanted side products, they may form even more interesting compounds, creating new opportunities for further research. Methods leading to the synthesis of these isoDMT's often result in higher yields. Therefore, the use of crystallization as purification instead of column chromatography could lead to higher isolated yields. It also appeared that substitutions on the indole ring did not impact reaction performance, nor did substitutions for related heterocycles (Dunlap et al., 2020). As depicted in Figure 2.9, using 2-chloro-N,N-dimethylethan-1-amine as the alkylating agent resulted in yields in the range of 41% to 95%, depending on the substitutions, as reported by Dunlap et al. (2020). They suggest that the reaction proceeds through a S_N2-mechanism with negligible participation of neighbouring groups.

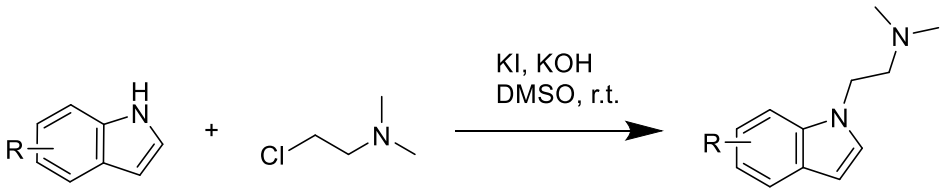

Figure 2.9*: N-alkylation of various indoles*

2.1.1.2 Synthesis of 5-bromo-3-(2-nitroethyl)-1H-pyrrolo[2,3-b]pyridine

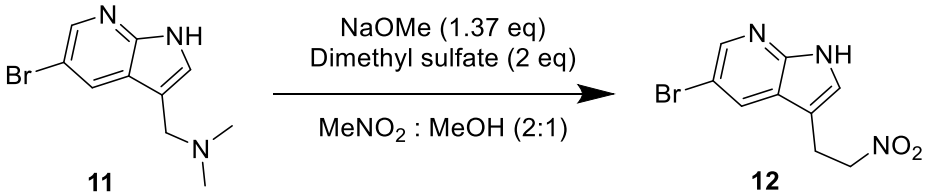

Figure 2.10: *Initial reaction for the synthesis of 5-bromo-3-(2-nitroethyl)-1H-pyrrolo[2,3-b]pyridine*

In a subsequent step, **11** would be reacted with sodium methoxide and dimethyl sulfate to form the nitro analogue **12** (Figure 2.10). This reaction would be performed in a nitromethane/methanol mixture and stirred at room temperature for 24 hours. However, because the formation of **11** failed, the reaction procedures were performed on **17**.

Since during the course of these reactions, it was still assumed that **11** was formed instead of **17**, the associated mass of **12** was sought during the follow up of the reaction using LC-MS. Due to the match in mass associated with **12** and **18**, the reaction was initially thought to be successful. Consequently, an appropriate extraction and purification method was sought for the assumed product, **12**. The compound was attempted to be extracted, using dichloromethane, followed by washing it with ammonium hydroxide (5%), hydrogen chloride (1M), and brine. However, the compound remained in the aqueous phase. A solution of 3M instead of 1M hydrogen chloride was used and the reaction mixture was acidified until a pH of 3 was obtained. Instead of acidifying the mixture, it was opted to basify the mixture with potassium hydroxide. This still resulted in an unsuccessful extraction. Because of the difficulties during this extraction, another method was evaluated. The reaction was repeated, and the mixture was filtered off. Toluene was then added, and this was evaporated. The product was dissolved in saturated potassium hydrogen carbonate, and extracted with ethyl acetate. This was once more washed with brine. The organic phase was dried with magnesium sulfate, and the solvents evaporated. Because of the presence of several impurities, the reaction mixture was subjected to a TLC analysis. Different solvent mixtures were tested, but hexane/ethyl acetate (50:50), chloroform/acetone (80:20) and (90:10) did not result in a proper separation. Therefore, the decision was made to attempt purification with reversed-phase chromatography using acetonitrile and water as eluents, employing a rising gradient of acetonitrile. However, during a final analysis with ^{1}H-NMR, ^{13}C-NMR and 2D spectra, it was discovered that not **19** was formed, but rather an intermediate with the same associated mass on the LC-MS spectrum. It is assumed that the reaction stopped at the formation of **18** (Figure 2.12), resulting in an isolated yield of 35% of **18**.

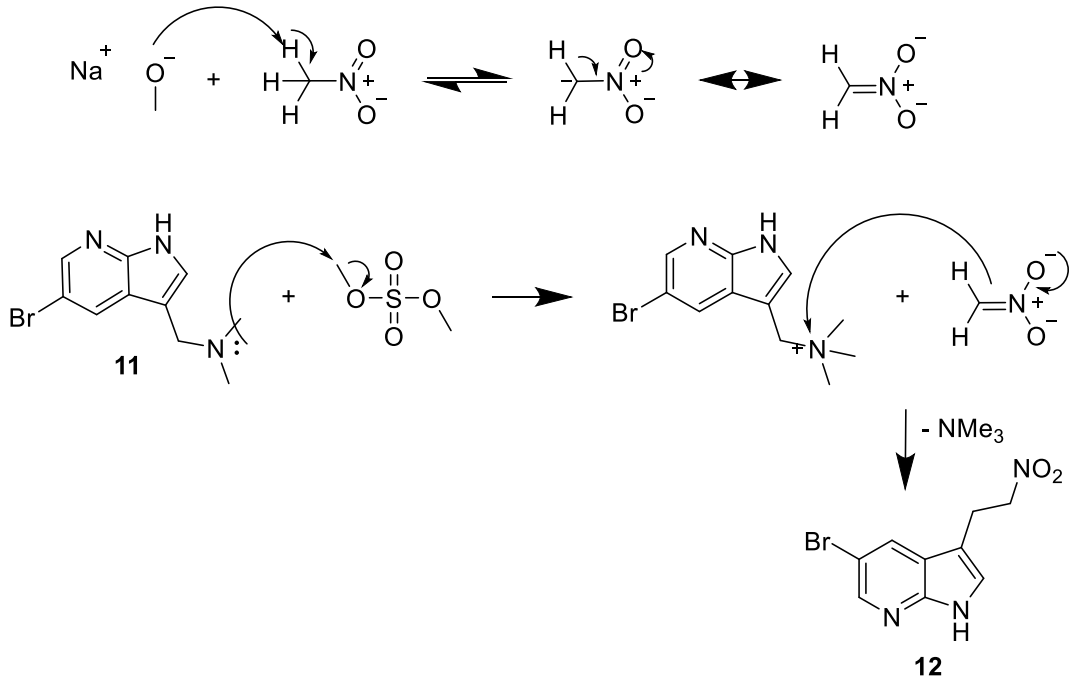

***Figure 2.11**: Reaction mechanism for the synthesis of 5-bromo-3-(2-nitroethyl)-1H-pyrrolo[2,3-b]pyridine*

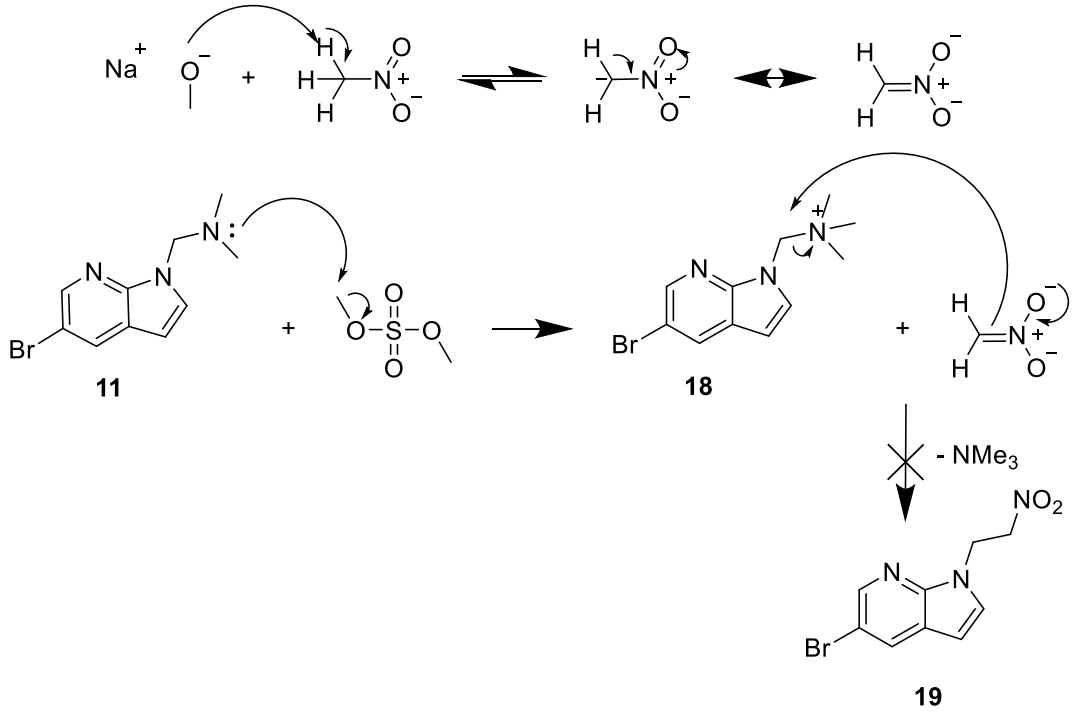

*Figure 2.12: Actual course of reaction with the formation **18** as intermediate*

2.1.2 Starting from 5-bromo-1H-indazole

2.1.2.1 Synthesis of *5-bromo-3-(N,N-dimethylaminomethyl)indazole* with a Mannich reaction

Simultaneously, the same pathway was initiated, but starting from 5-bromo-1H-indazole, starting with a Mannich reaction. Therefore, **10b** was dissolved in acetonitrile and glacial acetic acid at 0 °C in a ratio of 3:1. Subsequently, formaldehyde and dimethylamine were added, and the solution was stirred at room temperature for multiple hours. The reaction progress was followed up on LC-MS. However, analysis with ^{1}H-NMR indicated the absence of **11b**.

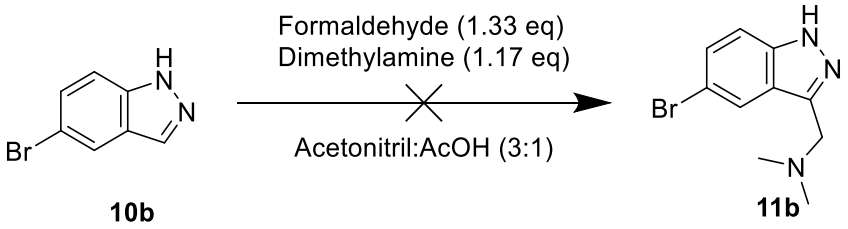

***Figure 2.13:** Mannich reaction on 5-Bromo-1H-indazole*

Similar to the brominated 7-azaindole, the C-3 position of the indole did not conduct the nucleophilic attack on the iminium ion. The nitrogen at position 1 did, resulting in the formation of **20** (Figure 2.14).

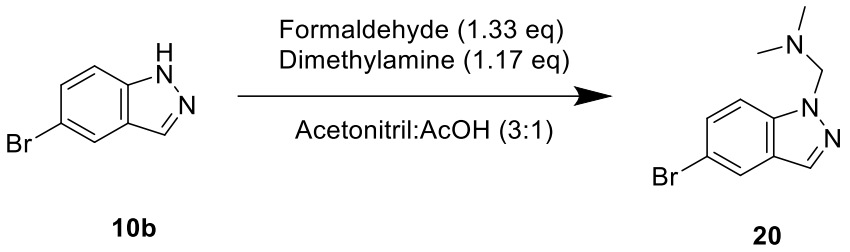

Figure 2.14: *Mannich reaction with nucleophilic attack of N at position 1*

2.1.2.1 Synthesis of *5-bromo-3-(N,N-dimethylaminomethyl)indazole* via 5-bromo-3-formylindazole and a reductive amination

Another type of reaction, using a Vilsmeier reagent, was also evaluated to determine if this could lead to the synthesis of the target molecule **11b**. To achieve this, the aldehyde derivative first needed to be synthesized using a Vilsmeier reagent to yield **21** (Figure 2.15), which could then further undergo a reductive amination leading to **11b**.

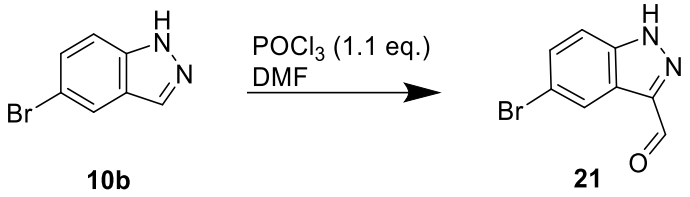

Figure 2.15: *Alkylation using Vilsmeier reagent*

A reaction with a Vilsmeier reagent, often includes N,N-dimethylformamide (DMF) and $POCl_3$, where a Vilsmeier reagent is first formed. This should then react with **10b** through an electrophilic substitution and addition reaction. The reaction mechanism is depicted below in Figure 2.16.

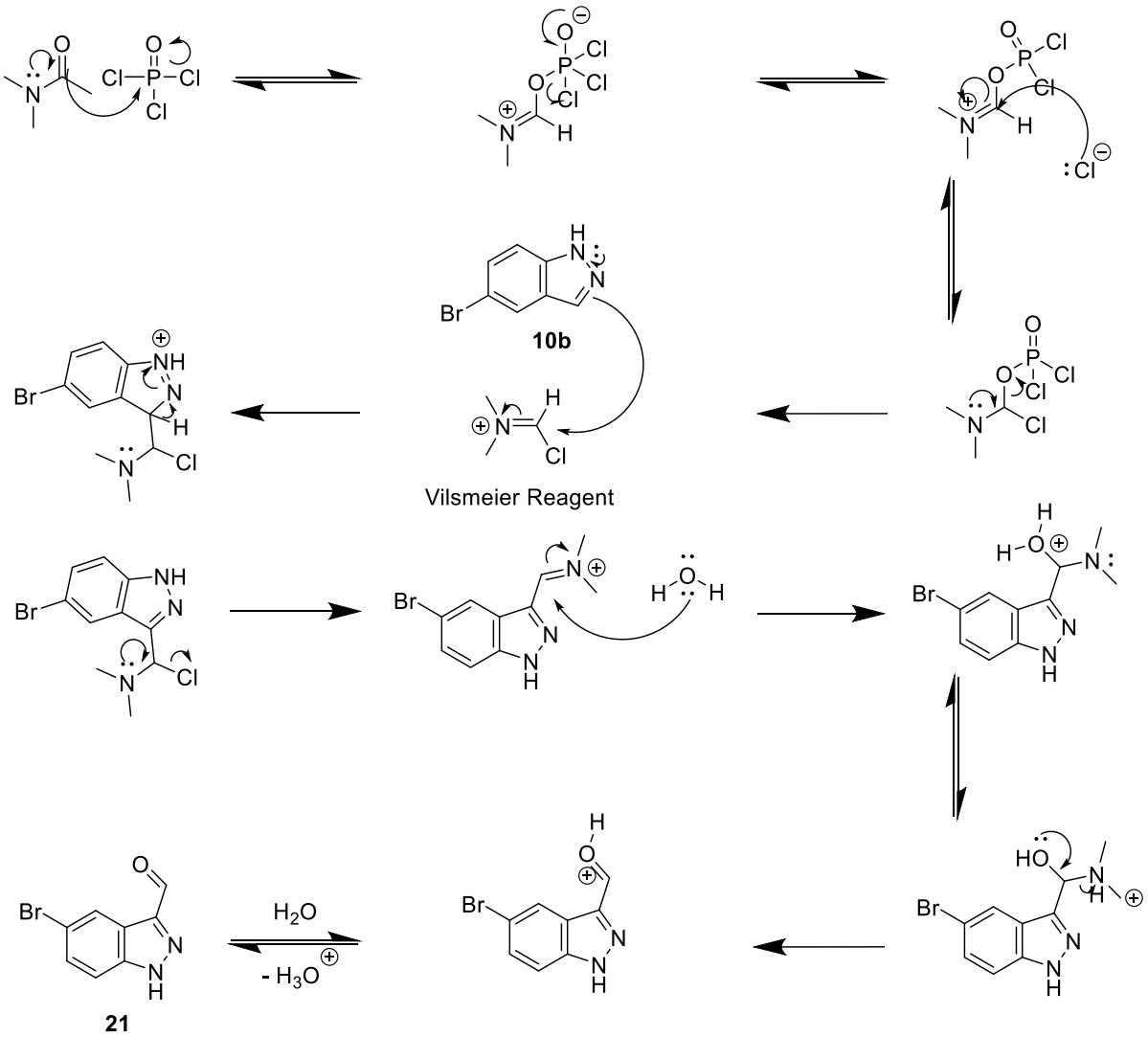

***Figure 2.16**: Reaction mechanism using Vilsmeier reagent with nucleophilic attack of C-3 position (Valiulin, (2020))*

The Vilsmeier reagent was made by adding dropwise the $POCl_3$ in DMF, whilst stirring for 15 minutes between 0 °C and 5 °C. Compound **10b** was dissolved in DMF and added to the Vilsmeier reagent. This mixture was allowed to stir overnight. Analysis with LC-MS indicated the mass associated with **21**, but an ^{1}H-NMR analysis revealed that it was the nitrogen at position 1 that reacted with the Vilsmeier reagent (Figure 2.17).

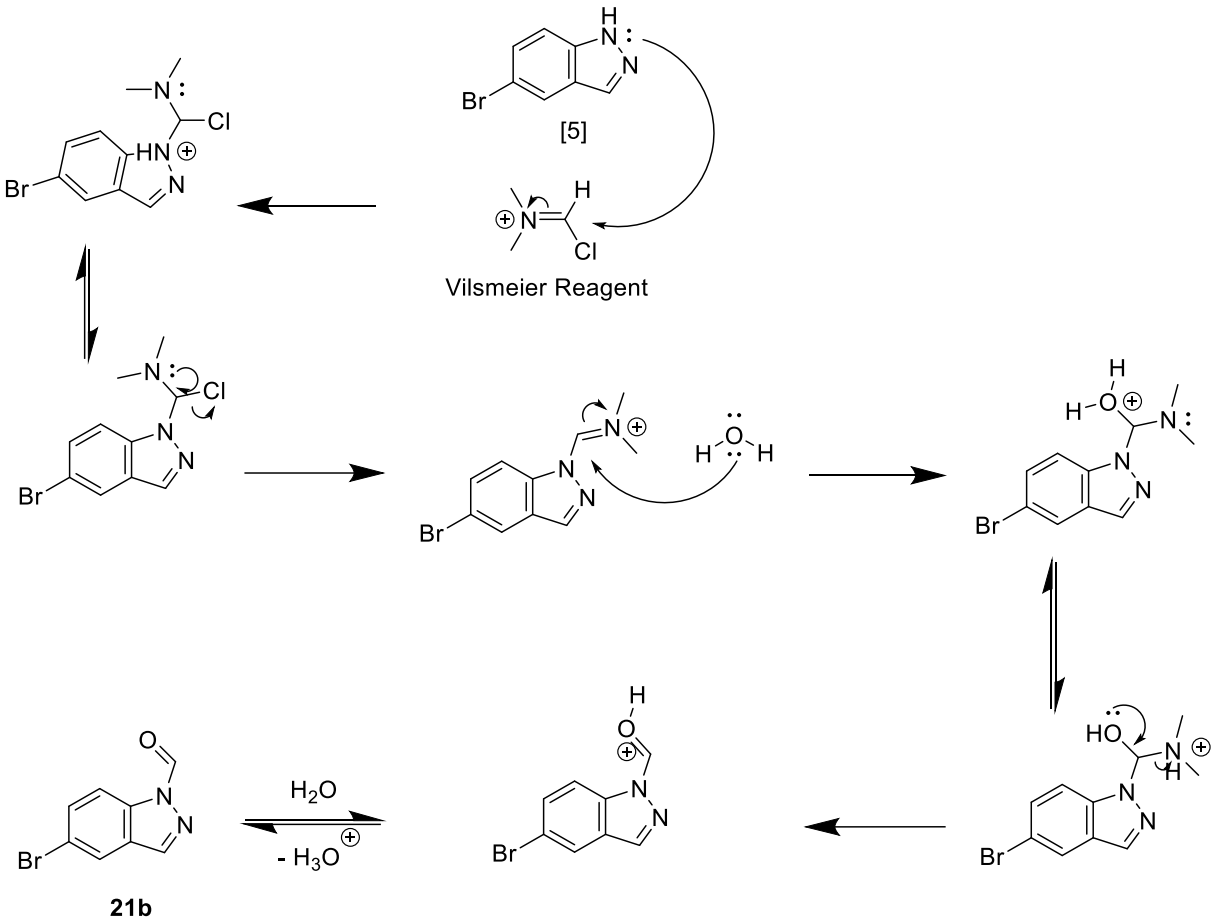

Figure 2.17: *Actual course of reaction with the Vilsmeier reagent*

The mixture was poured over crushed ice, and sodium hydroxide was added. A white/yellowish precipitate arose. This precipitate was filtered off and recrystalized with hot ethanol. An isolated yield of 31% was obtained for **21b**.

In the subsequent step, **21b** should undergo a reductive amination using a Lewis acid catalyst, where DMF acts as the dimethylamino source, reductant and solvent. This leads towards a greener character of the reaction, as DMF serves multiple purposes. Currently, the majority of reductive aminations is performed by the use of heterogenous boron hydrides or homogenous catalytic hydrogenation. The use of boron hydrides often generates a lot of waste and has multiple other shortcomings, such as its toxic nature. In organometallic hydrogenation, noble metal catalysts and complex ligands are often required, which also tends to result in a low chemoselectivity (Yang et al., 2018).

The reaction where carbonyl compounds are reduced with ammonium formate is called the Leuckart-Wallach reaction. However, in this reaction a temperature of 240 °C and an autoclave are required. A reductive amination with only DMF and H_2O would still require harsh conditions (250 °C and an autoclave). The use of the Lewis acid is critical, since it accelerates the hydrolysis of DMF to produce the dimethylamine and the formic acid, thereby making the reaction conditions milder. It also promotes the imine formation by increasing the electrophilic reactivity of the carbonyl compounds, which then undergo a condensation with the dimethylamine (Yang et al., 2018).

The reaction conditions for the reductive amination were followed as described by Yang et al. (2018). The obtained crystals **21b** from the previous reaction were dissolved in DMF. The most promising catalyst according to Yang et al. (2018), the Lewis acid zinc acetate dihydrate-catalyst ($Zn(OAc)_2 \cdot 2H_2O$), was added in a concentration of 10 mole%, along with 5.5 equivalents of water. The reaction mixture was stirred at 150 °C for 24 hours (Figure 2.18). The reaction progress was followed up on LC-MS. After 24 hours, a conversion of 100% was obtained, but according to LC-MS there was no formation of **20**. The reaction mixture was however diluted with brine and subsequently extracted with ethyl acetate. The organic phase was dried, and the solvents were evaporated. This resulted in a red coloured oil that was dissolved in an ethyl acetate-methanol (9:1) mixture and filtered over a silica plug. Analysis by ^{1}H-NMR revealed the absence of **20.**

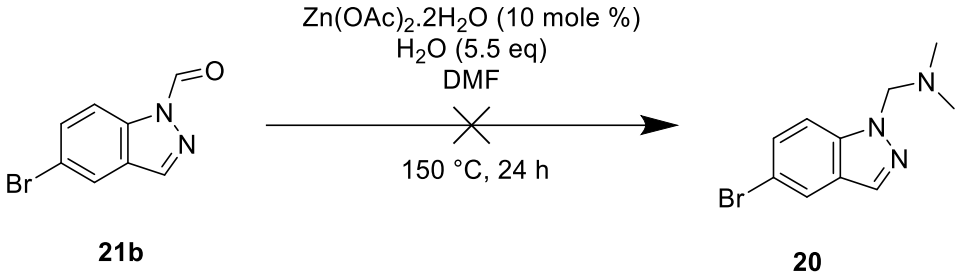

Figure 2.18: *Reductive amination of 5-bromo-1-formylindazole*

Both the Mannich reaction as the reaction with a Vilsmeier reagent did not result in the formation of **11b,** but led to the formation of **20** and **21b**, respectively. Although they were not the targeted molecules, as described in the previous section, these compounds may even have better therapeutic potential and certainly form an interesting basis for future research.

Because of other ongoing research at the SynBioc Research group, attention was shifted to another method. This method aimed at replacing the four first reaction steps of the initial pathway (Figure 2.1) to a single step (Figure 2.19), potentially leading to the substitution of the ring at the initial targeted C-3 position.

2.2 Introducing the borrowing hydrogen strategy

The first pathway presented in section 2.1 is here replaced by a two-step pathway in which an amine alkylating step is followed by a phosphonylation step (Figure 2.19). In this pathway, the first step is able to replace the first four reaction steps of the first pathway.

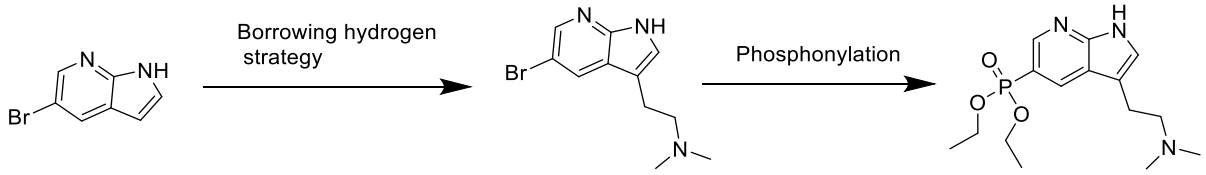

Figure 2.19: *Reducing the first pathway to 2 reaction steps*

2.2.1 Synthesis 5-bromo-3-(N,N-dimethylaminoethyl)pyrrolo[2,3-b]pyridine by applying the borrowing hydrogen strategy

A new reaction, using the borrowing hydrogen strategy could reduce the four first reaction steps of the first pathway to a single step. The reaction mechanism of this protocol is depicted in Figure 2.20. It can be used for the replacement of the Friedl-Crafts alkylation of indoles. A poorly reactive alcohol is dehydrogenated, and the created hydrogen equivalents will afterwards be consumed again for the hydrogenation of the imine. In these types of reactions, a set of hydrogenations is linked to an intermediate reaction involving a generated intermediate. In this strategy, an alcohol (or amine) is converted to a carbonyl (or imine) through a transition-metal catalysed dehydrogenation. This can be further condensed with an amine, which can then be reduced by the [MH_2] species that was generated in the initial dehydrogenation step (Figure 2.20). In this way the catalyst is regenerated to its active form, and it forms a catalytic cycle. This approach enables commodity alcohols to be used as alkylating agents, thereby avoiding multistep approaches and the formation of stochiometric side products (Reed et al., 2021).

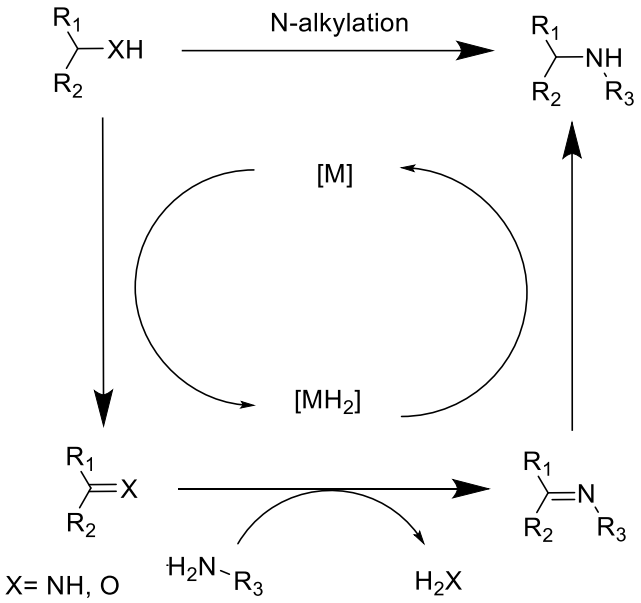

Figure 2.20: *Mechanism of the borrowing hydrogen strategy using an alcohol and transition metal catalyst (Reed et al., 2021)*

Different transition metal catalysts were examined by Bartolucci et al. (2015), but for the alkylation of indoles an Iridium-catalyst, namely the pentamethylcyclopentadienyliridium(III) chloride, dimer [$Cp^*IrCl_2]_2$, proved to be the most effective.

N-acetyl ethanolamine functions here both as an amino ethylene alkylating agent and as a source of hydrogen, which eliminates the need for the use of an external reductant.

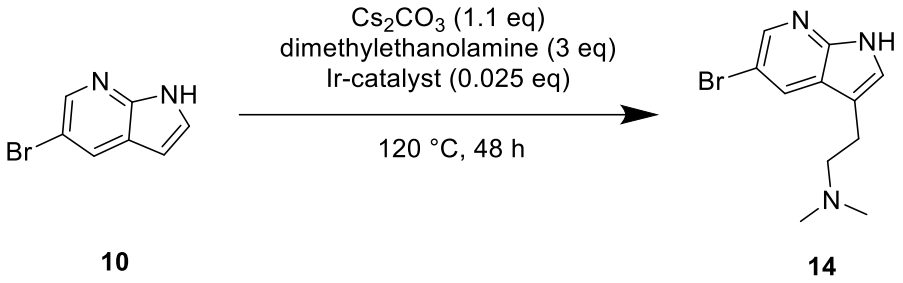

Figure 2.21: Synthesis of 5-Bromo-3-(N,N-dimethylaminoethyl)pyrrolo[2,3-b]pyridine

A GC-MS vial was flame dried with a Bunsen burner to remove as much water as possible. Afterwards, **10** was added to the vial, along with caesium carbonate, the catalyst (pentamethylcyclopenta-dienyliridium(II) chloride dimer), and dimethylethanolamine, which also serves as the solvent in this reaction. The vial was sealed and flushed with nitrogen. The mixture was stirred at 120 °C for 48 hours, and on regular time intervals, samples were taken and analysed on LC-MS to follow up on the reaction progress (Figure 2.21). The temperature was chosen at 120 °C (lower than described by Bartolucci et al.), trying to reduce the formation of the dimer side product **22** (Figure 2.22). Formation of this dimer was already visible within 30 minutes. This dimer was formed through the addition of **10** to a transient azafulvene (Figure 2.22) (Bartolucci et al., 2015)

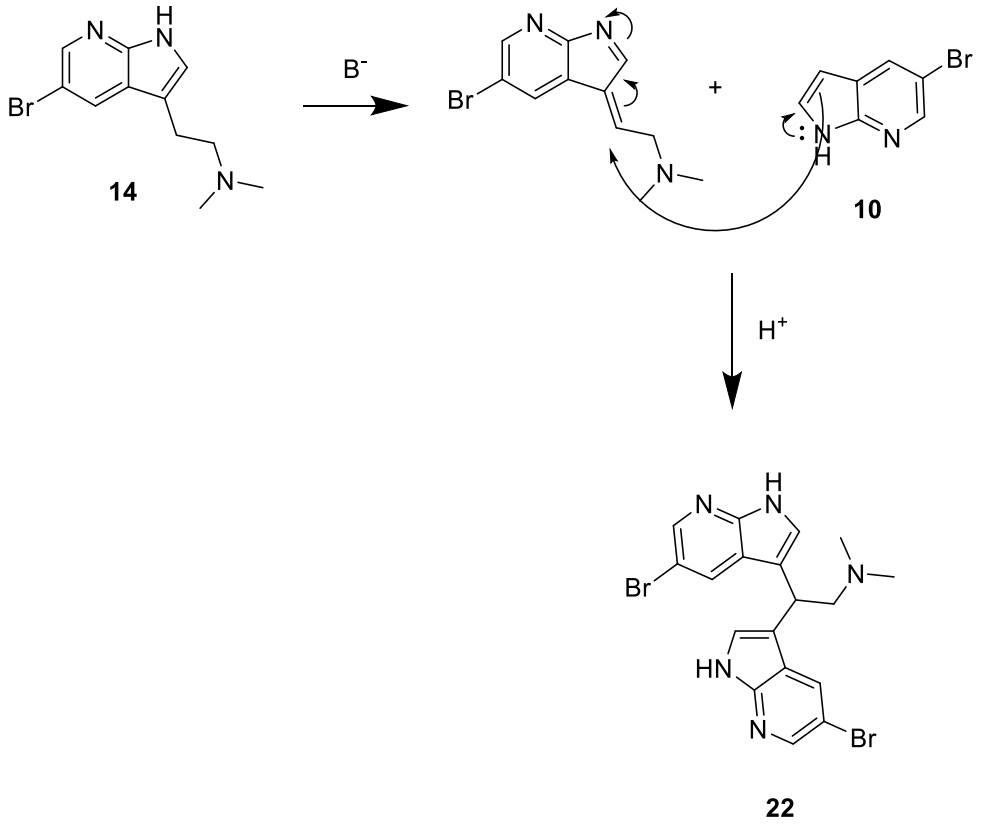

Figure 2.22: *Formation of dimer side product*

After 48 hours, the reaction mixture was allowed to cool to room temperature and the mixture was dissolved in an ethyl acetate-methanol mixture in a ratio 9:1, respectively. This residue was filtered through a silica plug. Afterwards, this silica plug was rinsed with methanol to re-

move the residual product on the plug. The main fraction of the reaction product **14** was collected in the first fraction that came off the silica plug along with the dimer. Several solvent mixtures were tested with TLC to search appropriate eluents for a normal-phase liquid chromatography. Cyclohexane/ethyl acetate in a ratio of (10/90), cyclohexane/ethyl acetate in a ratio of (30/70), ethyl acetate/methanol (95/5), and ethyl acetate/methanol (90/10) were tested but did not result in a successful separation. A reversed-phase chromatography using water and methanol as eluents resulted in a successful separation. An isolated yield of 85% was obtained, where **14** was visible as a brown, beige precipitate.

The borrowing hydrogen strategy forms therefore a successful method for substituting the molecule at the C-3 position of the 7-azaindole derivative.

2.2.2 Phosphonylation of 5-bromo-3-(N,N-dimethylaminoethyl)pyrrolo[2,3-b]pyridine

In a subsequent step, **14** was attempted to be phosphonylated (Figure 2.23). This mechanism involves a palladium catalysed coupling mechanism, known as the Hirao coupling (Figure 2.24).

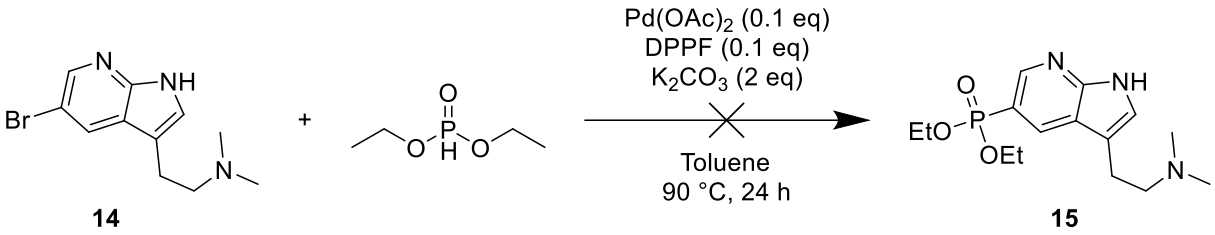

Figure 2.23: *Synthesis of diethyl (3-(2-(dimethylamino)ethyl)-1H-pyrrolo[2,3-b]pyridin-5-yl)phosphonate by a Hirao coupling*

During a Hirao coupling reaction, dialkyl phosphites and aryl halides are coupled in the presence of a palladium catalyst and a base, providing the aryl phosphonates, and several mono- and bidentate P-ligands. Instead of the sensitive and rather expensive $Pd(PPh_3)_4$, palladium precursors such as $Pd(OAc)_2$ can be used. In this case, the active catalyst is formed in situ, and a reduction of Pd(II) to Pd(0) takes place. This reaction follows a catalytic cycle where three classic steps are followed. First, an oxidative addition of the aryl halide to the Pd(0) occurs, resulting in the formation of an intermediate complex. Then, a ligand exchange takes place where the X-anion is replaced in the Pd-complex. Finally, a reductive elimination generates the desired product and regenerates the active catalyst. It must be noted that both electron donating as electron withdrawing groups substituted on the aromatic ring decrease the reactivity of the substrate, which will result in the requirement of more harsh reaction conditions (Henyecz and Keglevich, 2019). In this specific coupling, aryl bromides were used, where X represents a bromide atom.

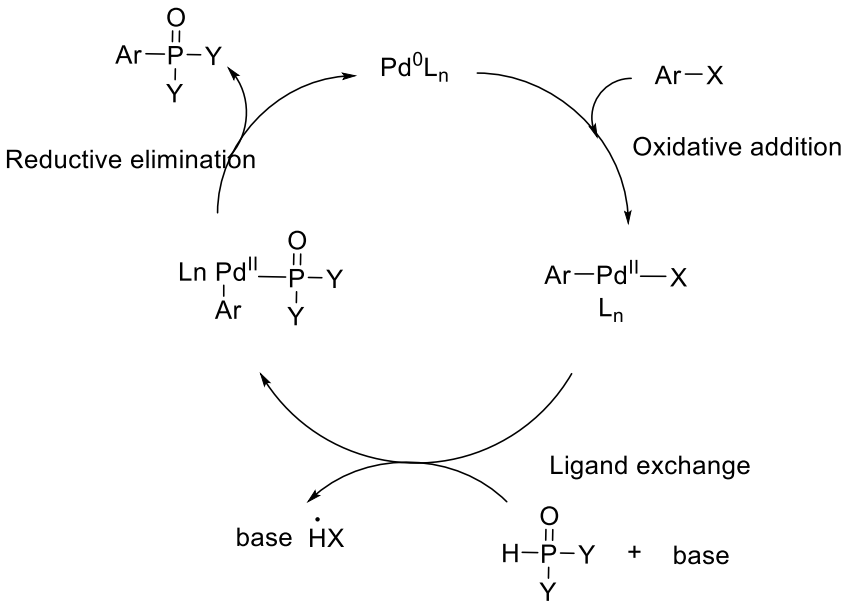

Figure 2.24: *Hirao coupling reaction mechanism (Henyecz and Keglevich, 2019)*

Compound **14,** along with the palladium catalyst, the ligand (DPPF) and the base (potassium carbonate), were added to a flask. The flask was sealed and flushed with nitrogen. The bottle containing the diethyl phosphite was first flushed with nitrogen, and afterwards the diethyl phosphite was added (Figure 2.23). The flask was once more flushed with nitrogen, reducing the oxygen content to a minimum. The reaction was followed up on LC-MS. However, even after 24 hours, there was still 0% conversion, as observed on LC-MS and ^{1}H-NMR.

2.2.3 Reversing the reaction sequence

Due to the failure of this reaction sequence (Figure 2.19), it was decided to reverse the order of the reaction. First a phosphonylation step was attempted, followed by an alkylation using the borrowing hydrogen strategy (Figure 2.25).

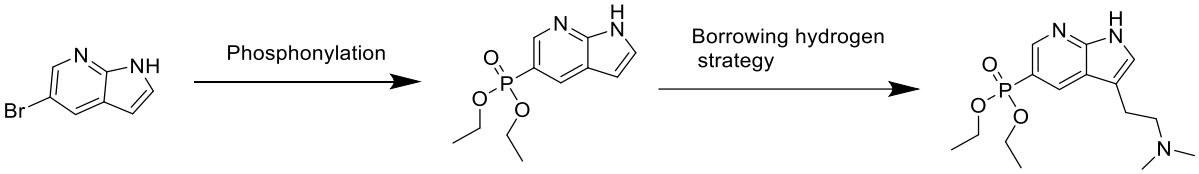

Figure 2.25*: Reversed reaction sequence*

2.2.3.1 Phosphonylation of 5-bromo-7-azainole

For the phosphonylation, similar reaction conditions were used as described in section 2.2.2 (Figure 2.26). After 16 hours, the reaction was stopped, and the solvents were evaporated. The residue was dissolved in ethyl acetate and filtered through a silica plug. This fraction was collected, and methanol was subsequently used to rinse the plug. This fraction was collected separately. Compound **23** appeared to be present in both fractions, along with a lot of diethyl phosphite, as shown by LC-MS and ^{1}H-NMR. However, the first fraction appeared to be the purest. This first fraction was subjected to reversed-phase liquid chromatography, using acetonitrile and water as eluents. The pure product was isolated as brown/yellow oil, with a yield of 63%. The purity of this residue was confirmed by LC-MS and ^{1}H-NMR.

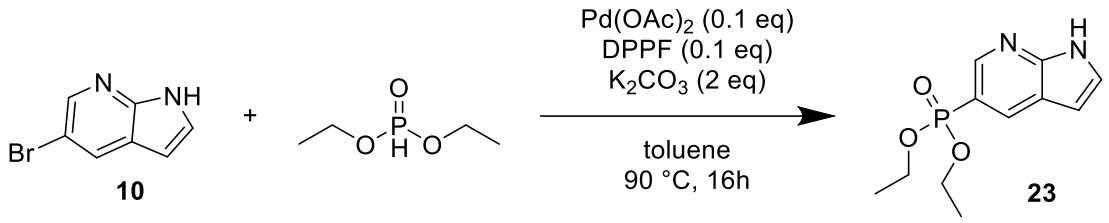

Figure 2.26: *Phosphonylation of 5-bromo-7-azaindole following a Hirao coupling mechanism*

2.2.3.2 Alkylation of diethyl (1H-pyrrolo[2,3-b]pyridin-5-yl)phosphonate using the borrowing hydrogen strategy

In a subsequent step, **23** was subjected to the alkylation conditions, using the same reaction mechanism and conditions as described in section 2.2.1 (Figure 2.27). At a temperature of 120 °C, there was still no sign of compound **15** on either LC-MS or ^{1}H-NMR. The temperature was raised to 150 °C, but still without success.

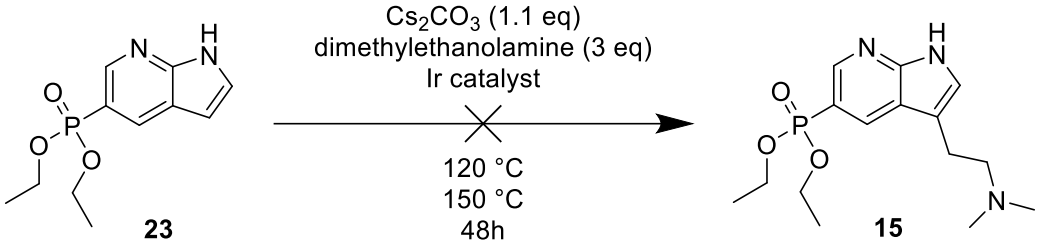

Figure 2.27*: Alkylation of diethyl (1H-pyrrolo[2,3-b]pyridin-5-yl)phosphonate*

Because of the several difficulties that were encountered during the previous experiments, it was decided to change strategy and switch the targeted synthesis molecules.

2.3 Synthesis of 5-bromo-N,N-dimethyltryptamine followed by a Suzuki coupling

In a new strategy, different alkylations were attempted on 5-bromo-N,N-dimethyltryptamine (5-bromo-DMT), shifting from a 7-azaindole ring to an indole ring. In a first step, the 5-bromo-DMT is synthesized, which will then be subjected to a Suzuki coupling using different boronic acids.

2.3.1 Fisher Indole reaction for synthesis of 5-bromo-DMT

The synthesis of **24** is conducted by a Fischer Indole reaction (Figure 2.28).

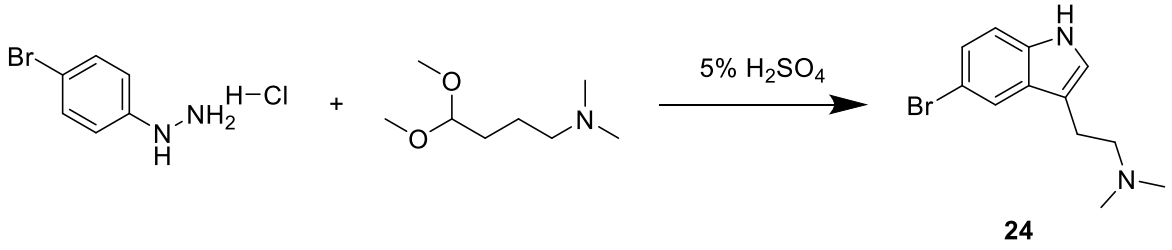

Figure 2.28*: Synthesis of 5-bromo-DMT*

In this Fischer indolization, the following steps are involved: first, a hydrolysis of the dimethylamino acetal to the hydrazone occurs. Then, an isomerization takes place, yielding the ene-hydrazine. This undergoes a sigmatropic rearrangement, followed by a ring closure resulting in the indole (Chen et al., 1994). These reaction mechanisms are depicted in Figure 2.29.

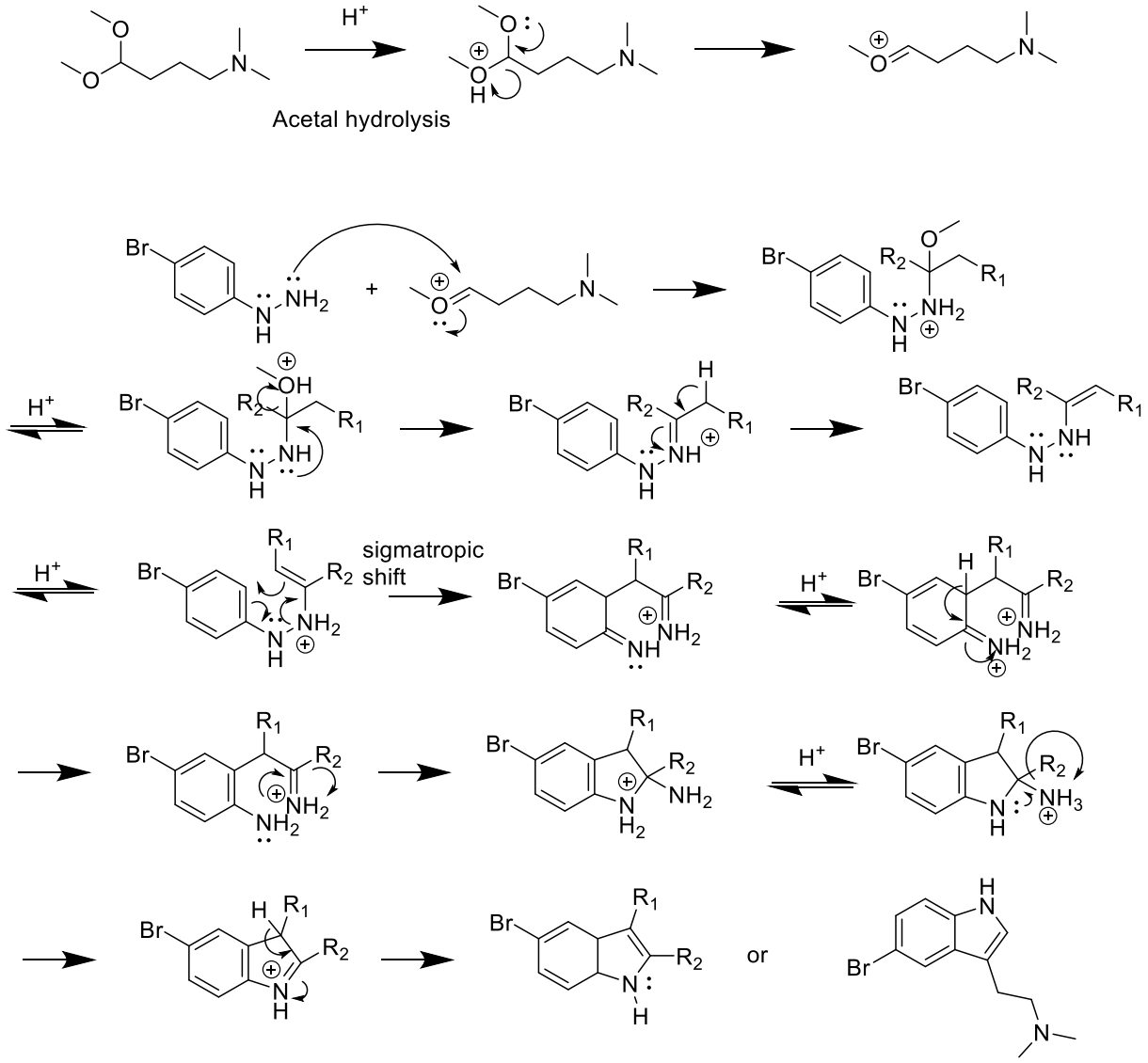

***Figure 2.29**: Synthesis of 5-bromo-DMT following a Fischer Indole reaction mechanism (Valiulin, 2020)*

The reaction conditions for this reaction were followed as described by Chen et al. (1994). 4-Bromophenylhydrazine hydrochloride was added together with the diethyl acetal to a 4% sulphuric acid solution. This was allowed to reflux for 2 hours while being flushed with nitrogen. During the reaction, a pinkish colour shifted to a yellowish colour. The resulting mixture was basified with 30% ammonium hydroxide. This was extracted with DCM, and the organic layer was dried with magnesium sulfate and the solvents evaporated. Next, the residue was dissolved in 9:1 acetone/methanol mixture, and sent over a silica plug. In this way, the starting products were removed. The remaining fraction contained both **24** as its oxidized form **24b**. This resulted in brown oil, with a conversion to **24** and **24b** of 92%.

2.3.2 Suzuki coupling with 5-bromo-DMT

In the subsequent step, a Suzuki coupling using different boronic acids was attempted. For this, a palladium-catalysed coupling reaction using different palladium catalysts and bases was performed, following the Suzuki coupling mechanism.

In a Suzuki coupling or Suzuki Miyaura reaction, organohalides are treated with organoborane compounds and a palladium catalyst. In these reactions, new C-C bonds are formed. Additionally, a base is added to increase the reaction rate. This reaction is both stereo and regiospecific, maintaining the stereochemistry of the reactants in the products. The reactivity of organohalides decreases in the following order: alkenyl halides > aryl halides > alkyl halides. For the halogens, in decreasing order this becomes: iodides > bromides > chlorides. The hybridization of the carbon adjacent to the boron atom in the organoboron species will influence through the steric factor. Sterically hindered compounds react slower than the unhindered alternatives. In general, a B-C(sp^3) carbon will be more sterically hindered than a B-C(sp) carbon. In decreasing order regarding the reactivity, this yields: B-C(sp) > B-C(sp^2) > B-C(sp^3) (Verma et al., 2023).

Similar to the Hirao coupling, a Pd(0) catalyst is required. This catalyst can already exist in the active state or be a Pd(II) catalyst that will be activated in situ with the help of a ligand.

As depicted in Figure 2.30, a sequence of an oxidative addition and trans metallisation allows for a cross-coupling of the components. This type of reaction allows for mild reaction conditions, using relatively environmentally friendly boron reagents and palladium(II) complexes (Lennox et al., 2014).

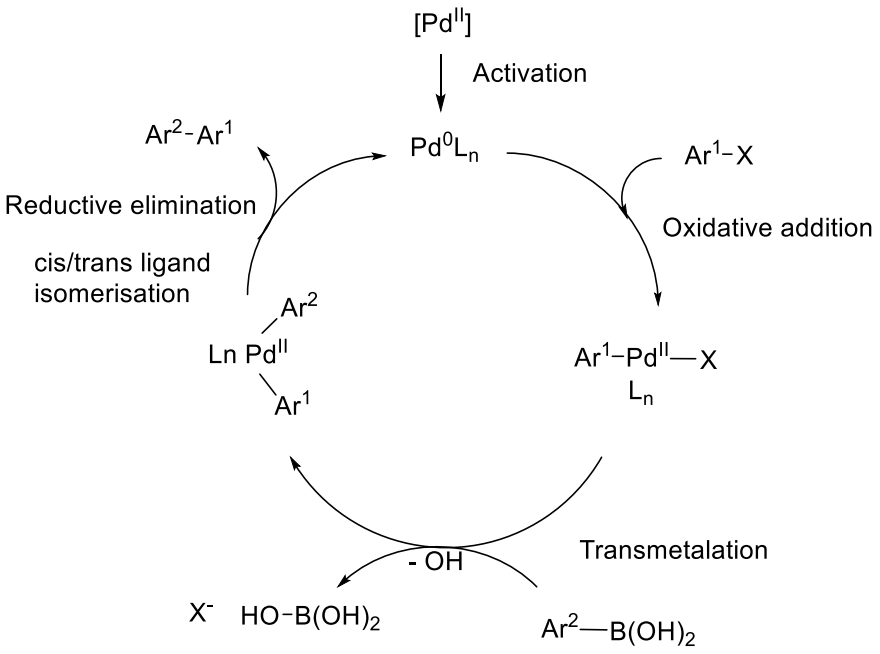

Figure 2.30: *Catalytic cycle of the Suzuki coupling with boronic acids (Lennox et al., 2014)*

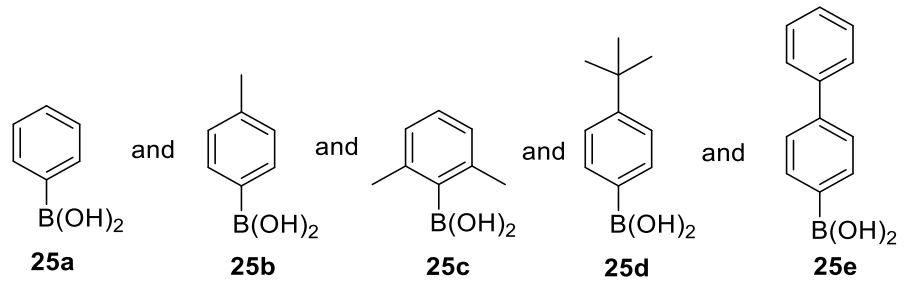

Figure 2.31: *Overview of the different boronic acids*

The different boronic acids used in the coupling reactions were the following: phenylboronic acid **25a**, 4-methylphenylboronic **25b** acid, 2,6-dimethylphenylboronic acid **25c**, 4-tert-butylphenyl boronic acid **25d**, 4-biphenylboronic acid **25e** (Figure 2.31).

A first attempt of this Suzuki coupling was performed with palladium acetate as the catalyst, and potassium hydroxide as the base. This was initially conducted on the simplest boronic acid present in the lab, phenylboronic acid **25a**.

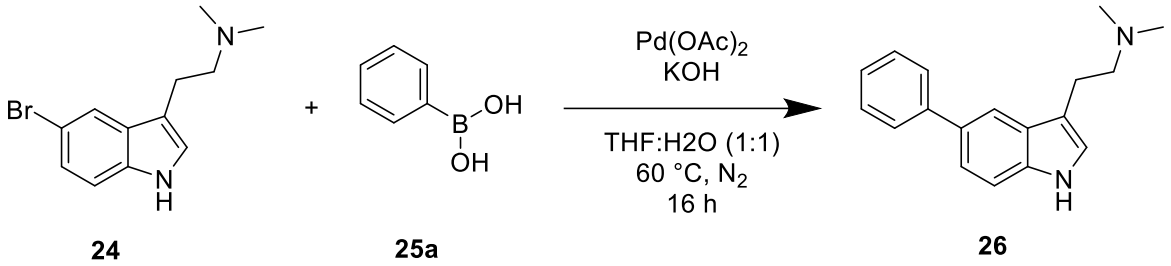

Figure 2.32*: Synthesis of N,N-dimethyl-2-(5-phenyl-1H-indol-3-yl)ethan-1-amine via Suzuki coupling reaction*

An example of a Suzuki coupling using 5-bromo-indole and **25a** was described by Shao et al. (2015). They used $Pd(PPh_3)_4$ as the catalyst, potassium phosphate as the base, and a combination of DME and water as solvents, ensuring all the reagent were dissolved. Because of the absence of DME in the lab, these conditions with solely water as a solvent were tested. However, this resulted in an improper dissolution of the reagents. Therefore, a combination of water and tetrahydrofuran (THF) was used instead. In the first attempt, $Pd(PPh_3)_4$ was replaced by the cheaper $Pd(OAc)_2$ without the addition of additional ligands.

The reaction conditions were as follows: **24** was diluted in THF, while potassium hydroxide, the palladium catalyst, and the boronic acid were first dissolved separately in water. The two mixtures were added together and flushed with nitrogen. The reaction was stirred for 16 hours at 60 °C under nitrogen atmosphere (Figure 2.32). The reaction was stopped, and the residue was diluted with water and extracted with ethyl acetate. Purifications using normal-phase liquid chromatography were attempted but proved unsuccessful. Afterwards, a purification using reversed-phase liquid chromatography using water and methanol as eluents resulted in a successful separation. Compound **26** was isolated as a brown oil with a yield of 64%.

Using similar reaction conditions, the other boronic acids were evaluated as well. However, this proved unsuccessful for the coupling of **25c** and **25d**. In order to tackle this, literature was reviewed for different reaction conditions. Zhou et al. (2016) performed a Suzuki-Miraya coupling using aryl chlorides and boronic acids, evaluating different reaction conditions. Since the reactivity of aryl chlorides is generally lower than those of aryl bromides, these conditions

could be evaluated. The most efficient conditions according to Zhou et al. (2016) appeared to be the use of $[Pd_2(dba)_3]$ as a catalyst, sodium phosphate as the base, and DME as solvent medium. Other conditions, described by Suzuki (2004), reported the use of potassium carbonate, and $Pd(PPh_3)_4$ as a base in reactions with aryl iodides.

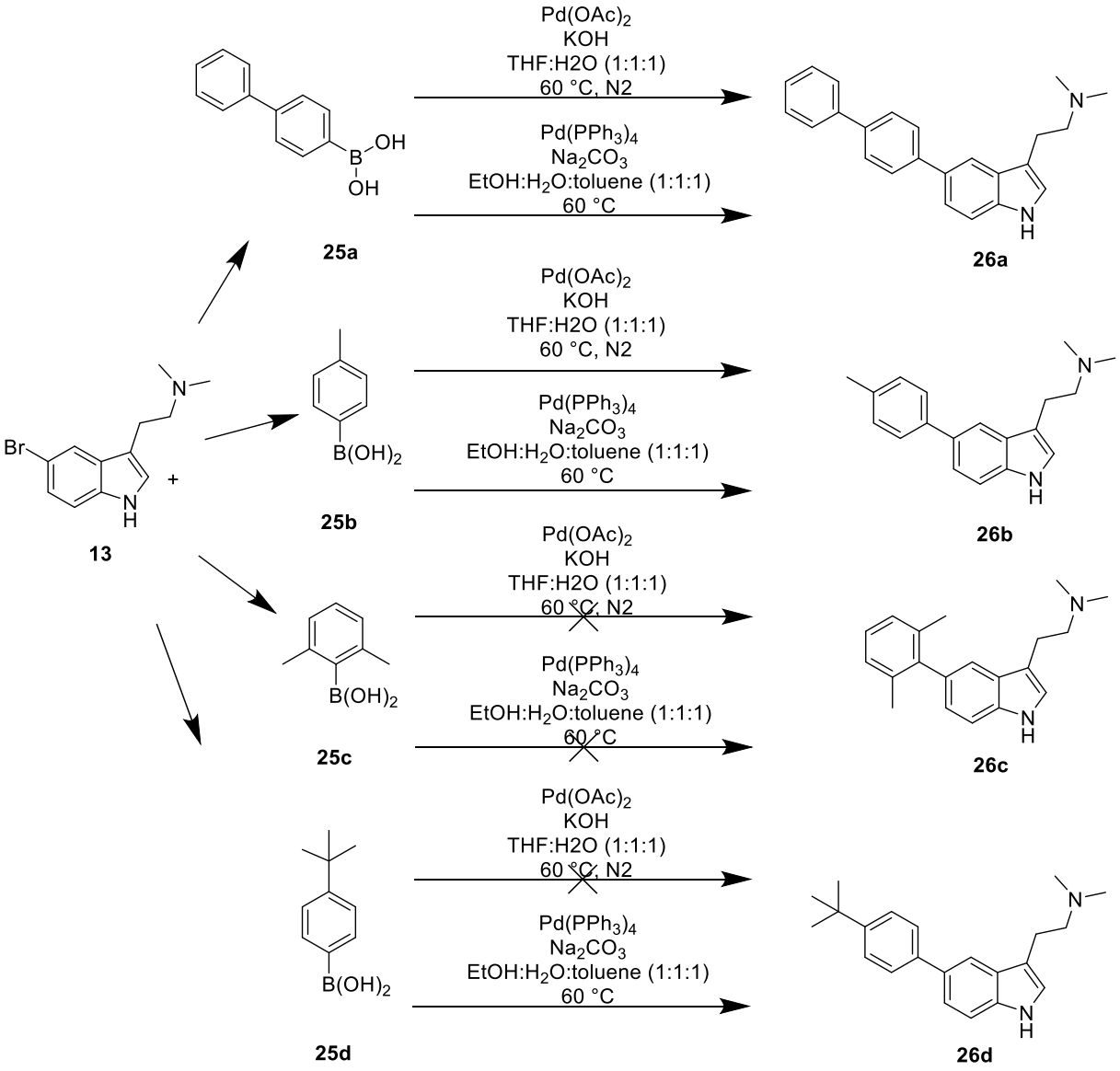

Figure 2.33: *Overview of the different Suzuki coupling with different reaction conditions, tested on different boronic acids*

Reaction conditions using $Pd(PPh_3)_4$ and Na_2CO_3 were tested and proved more successful with the other boronic acids (Figure 2.33). For the solvent mixture, a combination of toluene, water, and ethanol was chosen to dissolve all the compounds. At a temperature of 60 °C, the progress of the reaction was followed up using LC-MS. After 24 hours, the conversions and yields are depicted in table 3-1. However, instead of the desired reaction product, another oxidated form was created. The reagent **24** as well as the desired reaction products (**25a,b** and **d)** were oxidized (Figure 2.34).

Table 3.1: *Overview of reaction progress of the different Suzuki coupling reactions*

Product	Reaction conditions	Yield	Conversion to oxidized product
26a	$Pd(OAc)_2$, KOH, THF:H2O	0%	35%
26a	$Pd(PPh_3)_4$, Na_2CO_3, EtOH:H2O:toluene	0%	39%
26b	$Pd(PPh_3)_4$, Na_2CO_3, EtOH:H2O:toluene	54%	3%
26c	$Pd(OAc)_2$, KOH, THF:H2O	0%	0%
26c	$Pd(PPh_3)_4$, Na_2CO_3, EtOH:H2O:toluene	0%	0%
26d	$Pd(OAc)_2$, KOH, THF:H2O	0%	0%
26d	$Pd(PPh_3)_4$, Na_2CO_3, EtOH:H2O:toluene	0%	11%

To tackle this side product formation, the oxidized compounds were attempted to be reduced (Figure 2.35). Therefore, the residues of the Suzuki reactions were dissolved in a mixture of acetic acid and methanol. Activated zinc dust was used, therefore the zinc dust first needed to be activated. This was performed by stirring the zinc dust in hydrogen chloride with a concentration of 1M. The zinc dust was filtered off and washed with distilled water, ethanol, and anhydrous diethyl ether before it was rigorously dried. In this way, the oxides on the surface of zinc are removed which can be formed upon standing in air. The zinc dust was added in 1.2 equivalents, and allowed to stir for 2 hours at room temperature. The reduction proved successful for the oxidized unreacted form of the reagent **24b**, but remained unsuccessful for the oxidized products (**27,28,29**).

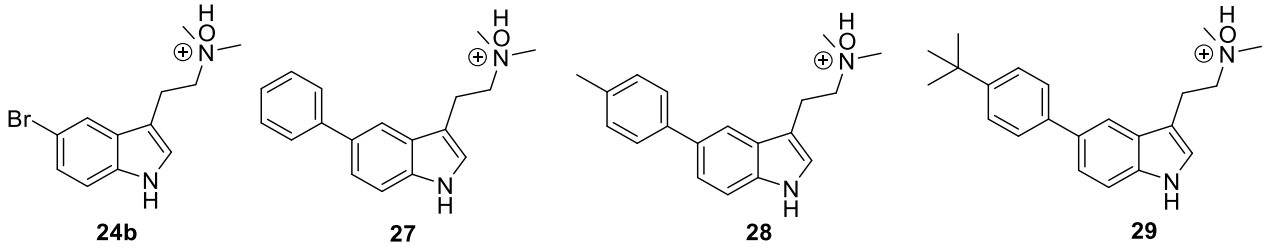

Figure 2.34*: Oxidized compounds*

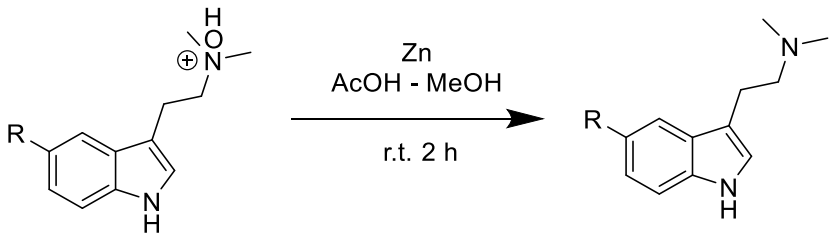

***Figure 2.35**: Reduction of oxidized compounds using activated zinc dust*

Because of progress of other ongoing research at the SynBioc research group, and the difficulties encountered during the synthesis and purification of these compounds, it was opted to combine this strategy with the parallel synthesis of other 5-HT_{2A} agonists, β-carbolines.

2.4 β-carbolines, another group of tryptamine-like compounds

The type of compounds described in this chapter belong to the category of β-carbolines, whereof their base skeleton is depicted in Figure 2.36. These are compounds with a high potential for the treatment of several types of neurological diseases, such as Alzheimer, a chronic neurodegenerative disorder in need of new treatment possibilities. Similar to the Psilocybin analogues, these compounds also bind to the 5-HT receptors. These compounds are heterocyclic amines, derived from tryptophan, which can be found in several plants and animal tissues. They are again resembling human tryptamine-based neurotransmitters like serotonin. Because of this resemblance but also because of the increased rigidity due to the additional ring, they can be synthesized and used as bioactive compounds for targeting several central nervous systems. They interact with a variety of enzymes and are able to inhibit certain brain enzymes.
In current research, their main focus is on the treatment of Alzheimer's disease (Beato et al., 2021).

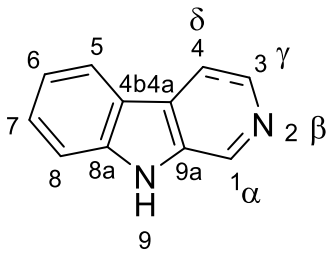

***Figure 2.36**: Carboline alkaloid skeleton (Szabó et al., 2021)*

Many methodologies have already been described in literature to synthesize these sorts of compounds. One of the most important procedures that has been described is the Bischler-Napieralski reaction, in which 3,4-dihydro-β-carbolines are synthesized starting from tryptamine. This is a cyclization type of reaction, requiring harsh conditions and reagents such as $POCl_3$ or P_2O_5 in solvents with high boiling points. Over the last decades, milder reaction conditions have been established for this type of reaction (Abranyi-Balogh et al., 2016). To current date, the Pictet Spengler reaction forms one of the most important synthesis routes. This type of reaction is a condensation reaction, giving rise to tetrahydro-β-carbolines (THBC's), which can be further dehydrogenated to the associated β-carboline alkaloids.

However, due to different issues with polyfunctional aldehydes such as their low yield, the scope of this kind of reaction for more complex derivatives is limited (Pakhare et al., 2015).

This Pictet-Spengler reaction is a condensation type of reaction that was discovered by Pictet and Spengler and forms one of the most important synthesis routes for alkaloid scaffolds. The power of this reaction lies in the ability to construct stereochemical and complex alkaloid molecules. It was in 1911 that Pictet and Spengler discovered that when β-phenylethylamine and formaldehyde were heated with hydrochloric acid, they underwent a cycloaddition reaction. It took 20 years before tryptamine was used as the amine compound. Tatsui was the first in 1928, resulting in the formation of the tetrahydro-β-carboline skeleton. This forms a key structure element for complex synthetic products and natural compounds such as isoquinolines and indole alkaloids. To develop different kinds of these molecules, both the amine compound and the aldehyde (as in the original reaction) can be varied. Over the last few decades, there has been a large progress in the development of highly enantioselective methods for these THBC's by the use of enzymes, which are called the Pictet-Spenglerases. In the biosynthesis of morphine, an enzyme catalysed Pictet-Spengler condensation step is the key in the synthesis route (Stöckigt et al., 2011).

When the Pictet-Spengler reaction is conducted with an amine and an aldehyde, an intermediate **30** is formed. This will then transform into the iminium ion **31**, which will undergo an electrophilic attack, resulting in a tetrahydropyridine moiety **32** (Figure 2.37). This represents the classic Pictet-Spengler reaction (Calcaterra et al., 2020).

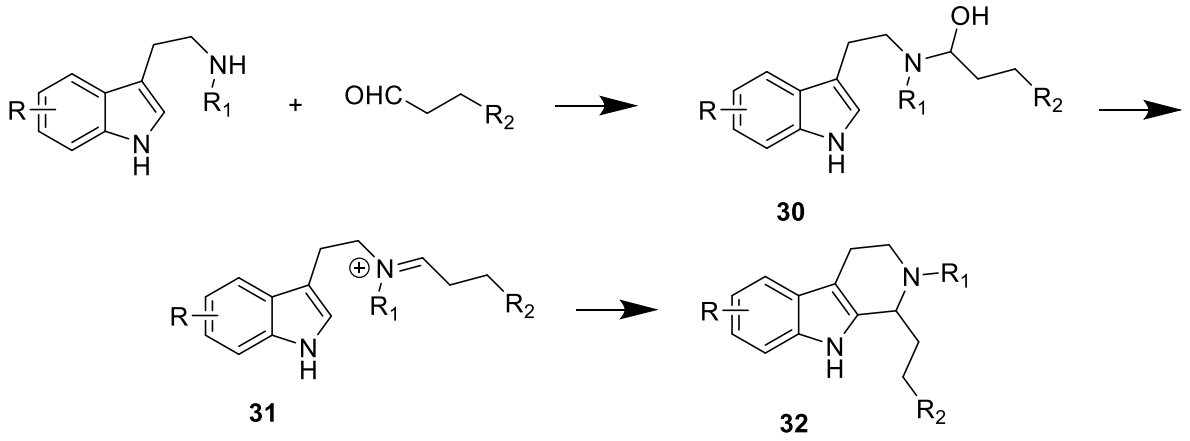

Figure 2.37: *Pictet-Spengler reaction (Calcaterra et al., 2020)*

A modification using a nitril and a tryptamine under hydrogenating conditions already solved a few of the issues. This is the type of reaction that was also evaluated in this dissertation. It should be mentioned, however, that using aldehydes or carboxylic acids represents other forms of the Pictet Spengler type of reaction (Pakhare et al., 2015).

As described by Pakhare et al. (2015), the following reaction conditions were used: a tryptamine derivative was reacted with a nitril, palladium on activated carbon (10%) was used as a catalyst under a hydrogen atmosphere in acetic acid. Subsequently, the formed THBC's were dehydrogenated using potassium permanganate. In the aromatization step, they opted not to use the Pd/C catalyst because of the risk of breakage of the ring during this dehydrogenation step.

The molecules aimed at synthesizing in this master dissertation, were obtained by research at the SynBioc research group. These β-carbolines were clustered in 5 clusters by comparing different characteristics. These 5 clusters are presented below (Figure 2.38).

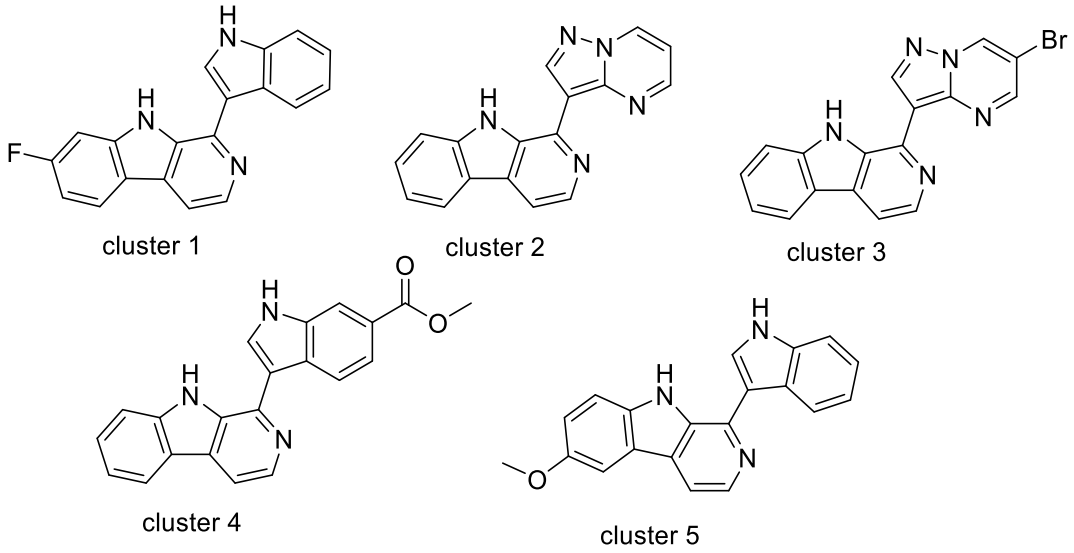

Figure 2.38: *Representation of the 5 clusters of β-carbolines*

For each one of these clusters, one molecule will be attempted to be synthesized. A first step using a Pictet-Spengler reaction, followed by an aromatization step.

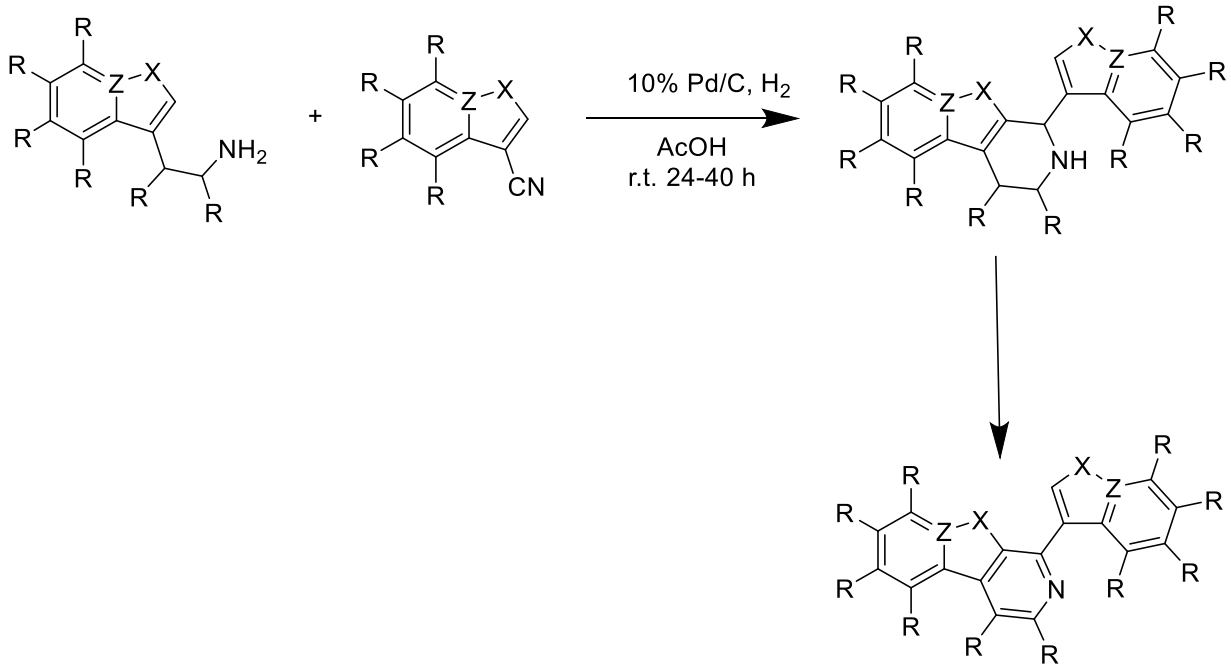

Figure 2.39: *Synthesis of β-carbolines with Pictet Spengler reduction using nitriles, followed by an aromatization step*

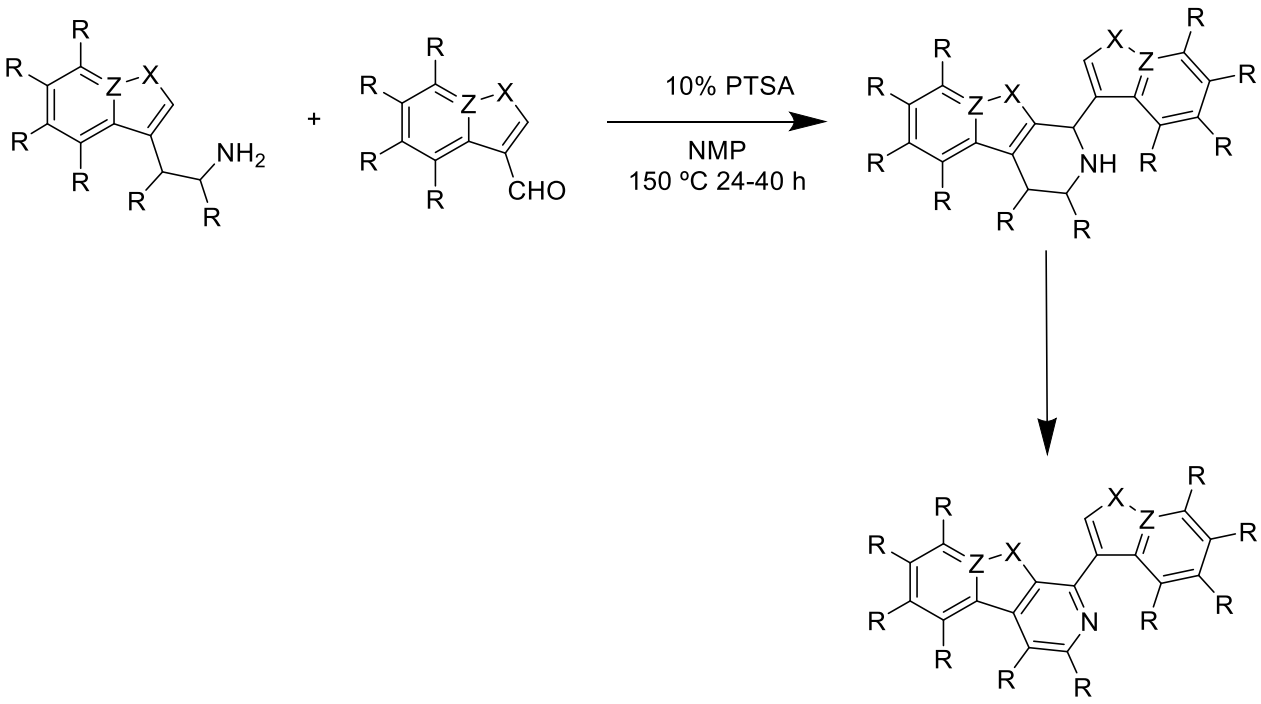

Figure 2.40: *Synthesis of ß-carbolines with Pictet Spengler reduction using aldehydes, followed by an aromatization step*

Because of the time limitation, it was opted to evaluate Pictet-Spengler reactions with amines and nitriles (Figure 2.39). The reaction procedure for this reaction was followed as described by Pakhare et al. (2015). The amine compound, specifically tryptamine, was dissolved in acetic acid, to which the nitril and palladium on activated carbon (Pd/C 10%) were added. This mixture was hydrogenated and stirred at room temperature under a hydrogen balloon atmosphere for 24 to 40 hours. The course of the reaction was followed on LC-MS. After the reaction had run to completion, the catalyst was removed by filtration over celite, and the product purified by chromatography.

2.4.1 Synthesis of tetrahydro-β-carbolines

This first step was performed for the 5 clusters. The reaction conditions were first evaluated for the synthesis of Eudistomin U, the most simple possible β-carboline, starting from tryptamine **33** and 1H-indole-3-carbonitril **34**, resulting in the formation of **35** with a yield of 37% (Figure 2.41).

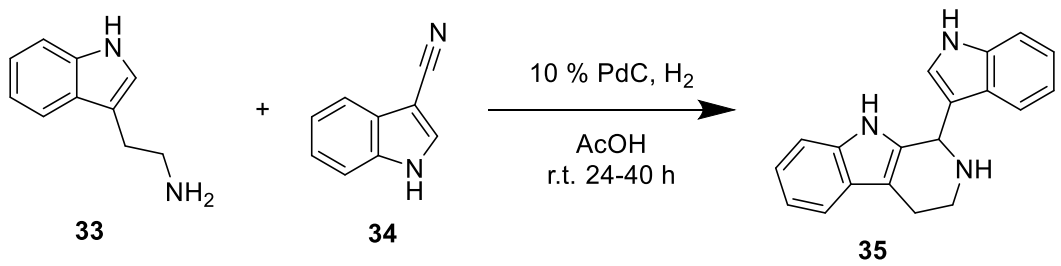

Figure 2.41: *Synthesis of the THBC of Eudistomin U*

The same reaction was performed with the use of a hydrogen generator, where the applied pressure of the hydrogen gas could be adopted. A pressure of 2 bars was tested to determine if this could result in a higher yield. This was however, not the case.

A similar reaction was conducted to yield the THBC's of the five clusters. For cluster 1, the fluorinated tryptamine **36** was reacted with **34**, using similar reaction conditions as described above (Figure 2.42). This was performed both in a flask with a hydrogen balloon creating a hydrogen atmosphere, as with a hydrogen generator, with a pressure of 5 bar. Respectively resulting in a yield for **37** of 11% and 5%.

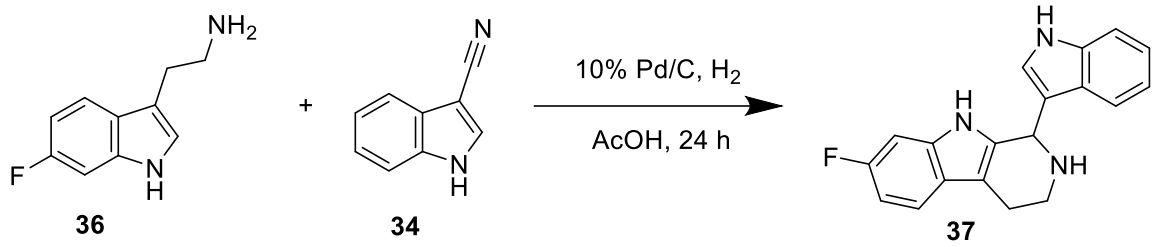

***Figure 2.42**: Synthesis of 7-fluoro-1-(1H-indol-3-yl)-2,3,4,9-tetrahydro-1H-pyrido[3,4-b]indole (cluster 1)*

For cluster 3, this comes down to reacting tryptamine **33** with **38** (Figure 2.43). Again both a hydrogen atmosphere created with a balloon and the use of hydrogen generator at 5 bars were evaluated. However, both setups proved unsuccessful and resulted in a conversion of 0%.

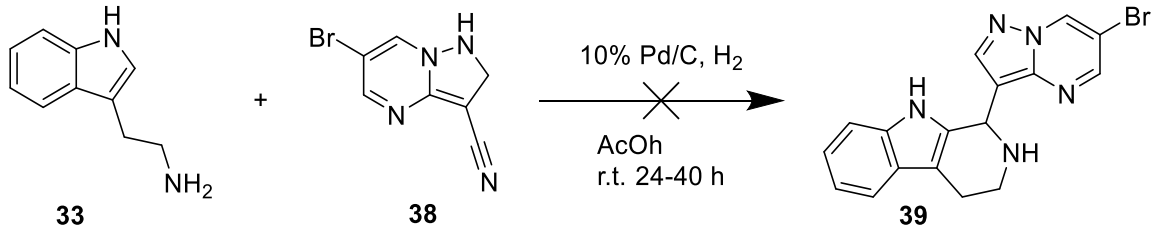

***Figure 2.43**: Synthesis of 1-(6-bromopyrazolo[1,5-a]pyrimidin-3-yl)-2,3,4,9-tetrahydro-1H-pyrido[3,4-b]indole (cluster 3)*

Similarly, for cluster 4, tryptamine **33** was reacted with the carboxylate **40,** resulting in **41** with a yield of 16% and 5%, using the hydrogenator at 2 bar and the hydrogen balloon, respectively (Figure 2.44).

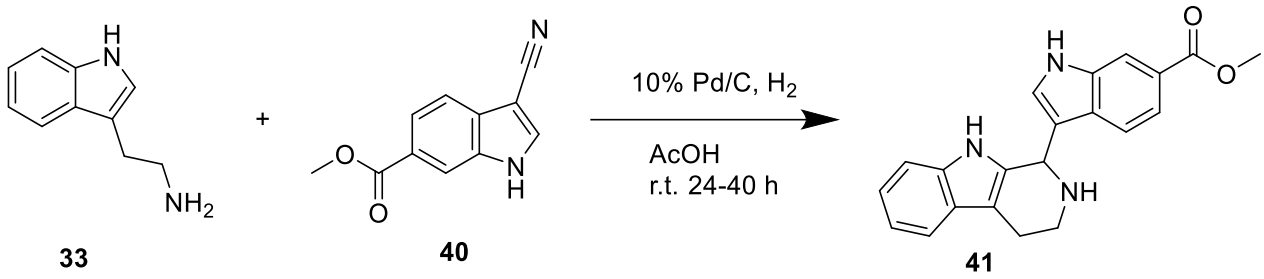

***Figure 2.44**: Synthesis of methyl 3-(2,3,4,9-tetrahydro-1H-pyrido[3,4-b]indol-1-yl)-1H-indole-6-carboxylate (cluster 4)*

Finally, the same was performed for cluster 5, where the methoxy substituted tryptamine **42** was reacted with **34**, resulting in **43** with a yield of 75% using a balloon to create a hydrogen atmosphere (Figure 2.45). This reaction resulted in the highest yield. In order to purify **43**, it was opted to perform a normal-phase liquid chromatography using DCM and methanol as

eluents in a ratio of 95:5, yielding the pure tetrahydro-β-carboline **43** with an isolated yield of 35%. This according to Santhanam et al. (2020).

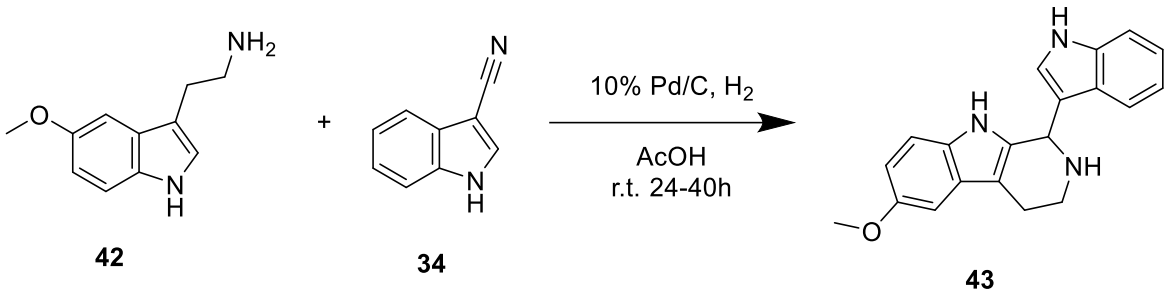

***Figure 2.45**: Synthesis of 1-(1H-indol-3-yl)-6-methoxy-2,3,4,9-tetrahydro-1H-pyrido[3,4-b]indole (cluster 5)*

Similar purification conditions were also tested to purify **37** and **41,** but the attempts remained unsuccessful, neither did a reversed phase-chromatography.

Due to the failure of chromatographic purification of **37** and **41**, efforts were made to achieve a higher conversion by increasing the reaction temperature. This was done in the hope that potentially a crystallization step could be performed, leading to a successful separation. At an elevated temperature of 50 °C using similar reaction conditions as depicted in Figure 2.43 and Figure 2.45, a conversion and yield for **37** and **41** were 18% and 4% and 40% and 11%, respectively.

2.4.2 Dehydrogenation of tetrahydro-β-carbolines to the β-carbolines

The next step for the synthesis of these β-carbolines, consists out of an aromatization of the THBC's. Initially, the reaction conditions described by Pakhare et al. (2015) were evaluated, using palladium on activated carbon at elevated temperatures. This was tested on the tetrahydro-β-carboline derivative **44** (cluster 5). Therefore, **44** was added to toluene, and the mixture was allowed to reflux for 24 to 30 hours (Figure 2.46). However, **44** dissolved very poorly in the toluene and only a partly dehydrogenation of 6% took place.

Another approach for this step, also described by Pakhare et al. (2015), involved using potassium permanganate. Therefore, **44** was dissolved in acetone and 4 equivalents of potassium permanganate were added. This was stirred at room temperature (Figure 2.46). The reaction was monitored on LC-MS. After 4 hours, a partly dehydrogenation of 17% took place.

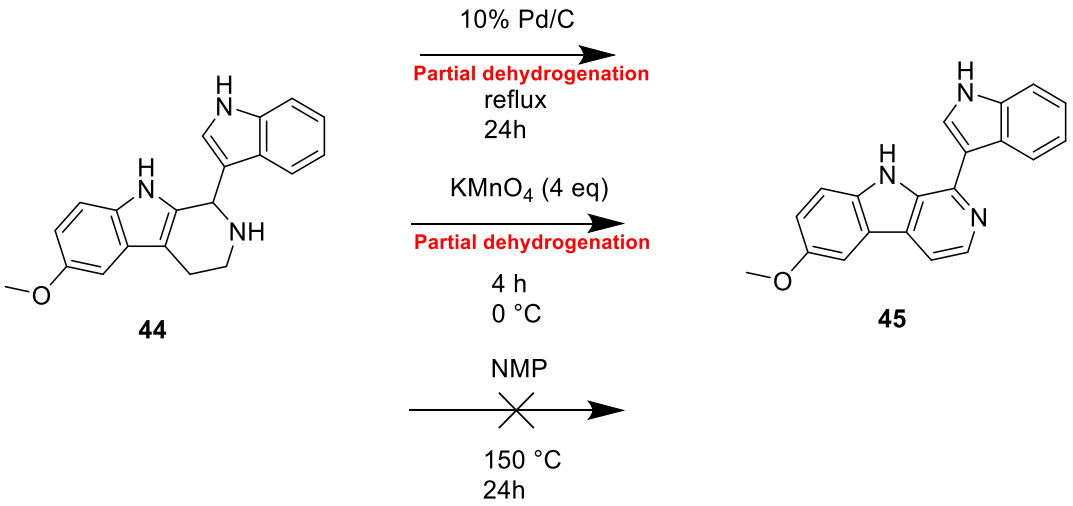

Figure 2.46: *Aromatization of 1-(1H-indol-3-yl)-6-methoxy-2,3,4,9-tetrahydro-1H-pyrido[3,4-b]indole*

Again, another setup for this aromatization was evaluated. Stöckigt et al. (2011) performed an aromatization of THBC's using of N-methylpyrrolidon (NMP) at elevated temperatures. These conditions were also evaluated (figure 2.47). The reaction was monitored on LC-MS, but this did not result in an increase of (partial) dehydrogenation.

3. Conclusion and future perspectives

3.1 Summary and conclusion

During the course of this dissertation, the target molecules were shifted several times. Initially, the primary aim was to synthesize psilocybin analogues with an additional nitrogen atom in the indole ring and a phosphonate group at the 5-position. In this way, the labile P-O link in psilocybin is replaced by a more stable P-C bound, making the molecule less susceptible to the degradation of human enzymes. This choice of the 5-position was made because of the results of previous master's dissertations at the Synbioc Research group, demonstrating an enhanced activity at the receptors responsible for the depressive/antidepressive behaviour. Two types of analogues were targeted: one with a nitrogen at position 7 in the indole ring (7-azaindole core) and one indazole analogue. The alkylations occurred at the N-1 position instead of the C-3 position, giving rise to difficulties from the beginning. However, in further literature review it appeared that substitutions at this N-1 position, even though these were initially undesired, could provide a basis for other compounds with potentially even superior therapeutic effects. In this way, developing analogues with alkylations at the N-1 position, such as the iso-DMT analogues, might form an interesting topic for further research.

The initial pathway was eventually replaced by another one, representing a shortcut of the first. The first step in this pathway employs the borrowing hydrogen strategy, that was able to successfully facilitate the alkylation at the initially targeted C-3 position. Depending on the reaction type and conditions applied, 7-azaindole and indazole will behave in a different way compared to indoles. In this second pathway, the substituted azaindole rings encountered difficulties with phosphonylation. Even when the reaction sequence was reversed, the synthesis of the targeted compounds remained unsuccessful.

Due to these challenges with the 7-azaindole derivatives, the strategy was altered to synthesizing psilocybin analogues without the additional nitrogen in the indole ring. By a Fischer indole synthesis, 5-bromo-DMT was synthesized. This was followed by a Suzuki coupling with boronic acids, which encountered issues with oxidation of the desired products. Attempts at reductions remained to a large extent unsuccessful. At the same time, developments in other research at the Synbioc Research group led to a refocus on newly acquired knowledge. Using computational methods, five clusters of β-carbolines were identified. Synthesizing the molecules from the five clusters varied significantly from the methods that had been used earlier in this dissertation. A Pictet-Spengler reaction was successful for compounds from three clusters, with one of the compounds being successfully purified. However, the aromatization of the THBCs has not yet been successful.

To conclude, reactions with azaindoles or indazoles will lead to different outcomes compared to those with indoles due to their different reactivities. Concerning the synthesis of β-carbolines, the initial steps regarding the synthesis of THBC's are promising, but further research is necessary to come to a successful aromatization of these compounds to their corresponding β-carbolines.

3. 2 Future perspectives

Because of the rising prevalence of depression and the increase of age-related neurological diseases, major depressive disorder and other neurological disorders are becoming

increasingly problematic. Different kinds of natural molecules such as psilocybin and β-carbolines have promising therapeutic potential for these type of disorders.

For a precise targeting of the receptors and their specific interactions, it's important to use computational methods, such as docking studies. Potentially powerful therapeutic compounds can be developed by synergies of different scientific disciplines. This has been demonstrated by the development of the five β-carboline clusters. It is up to further research to develop appropriate aromatization methods for the conversion of the tetrahydro-β-carbolines into their corresponding β-carbolines. Once these compounds have been synthesized, they can be subjected to further biological testing.

4. Material and methods

During the synthesis procedures, there has been made use of commercially available solvents and reagents, purchased from Sigma-Aldrich®, Acros Organics®, Apollo scientific® and TCI®. The demineralized water was obtained by using an Aquadem ion exchanger 22DF type on tap water.

1. Automatic Flash Column chromatography

In automatic flash chromatography, different compounds can be separated and purified because of their differing affinities towards the mobile and stationary phase. There are 2 types of chromatography used here, the normal-phase chromatography and reversed-phase chromatography. In the normal- and reversed-phase chromatography, the stationary phase consists out of silica or C-18 contained in a cartridge. For different weights of the samples, different cartridge sizes are used. The compounds are detected based on their UV absorption, which can be determined by the LC-MS.

A Büchi Pure C-815 flash chromatography system was used to perform normal-phase automatic flash chromatography. This NP Flash system includes a UV detector (200 – 400 nm) that can monitor four wavelengths simultaneously as well as an evaporative light scattering detector (ELSD). The ELSD can monitor compounds that are non-volatile that do not absorb UV, enabling the detector to detect the non UV-absorbing compounds and offering the addition of using a mobile phase that absorbs light at the same wavelength as the compound of interest.

A Reveleris flash chromatography system is used to perform the reversed-phase automatic flash chromatography. In this Reveleris system, there is also a UV-detector built in (200 – 400 nm) that can monitor two wavelengths simultaneously. Additionally, for compounds being non UV active, evaporative light scattering (ELSD) can also be detected, also by a built in ELSD detector.

2. Dry Solvents

An MBraun SPS-800 solvent purification system was used generating dry solvents. In this dissertation, the system was used for dry toluene and THF. The solvents were contained in Pure-Pac containers of 17 L, pressurized with nitrogen gas and eventually passed through 2 filtration and drying columns. These columns have an internal volume of 4.8 L and consist out of stainless steel (1.4301/ US 304) with molecular sieves, tuned to the solvent passing the tube. After the purification and drying, the solvents are collected in glass recipients under inert atmosphere, created by membrane pumps of the type MPC 301 Zp.

3. Liquid chromatography coupled with Mass Spectrometry

In a Liquid Chromatography–Mass Spectrometry system (LC-MS), mixtures can be separated and products can be identified on both UV and MS. It allows for the follow-up of reactions, measurement of m/z, determination of the purity of a sample, measurement of concentrations of compounds, preparation of samples for direct inlet MS and HRMS, or as an alternative to a TLC-analysis. In this system, there is a reversed set up, meaning a polar mobile phase and an apolar stationary phase. The apparatus is equipped with 4 polar solvents: water, acetonitrile, methanol and isopropanol. An Agilent 1200 Series HPLC with a Supelco Ascentic

Express C18 column (3 cm x 4.6 mm, 2.7 µm fused-core particles, 90 Å), a Phenomemnex guard column (SecurityGuard Standard) and a UV-DAD detector was used. This system is coupled to an Agilent 1100 Series MS with electrospray ionization (70 eV) with a single quadrupole detector. A combination of water and acetonitrile (30% to 100% in water) was the mainly used mobile phase, but other gradient and mixtures are also possible.

4. Mass Spectrometry

As described above.

5. Nuclear Magnetic Resonance Spectrometry (NMR)

A Bruker Avance III HD Nanobay spectrometer, equipped with z 1H/BB z-gradient probe (BBO, 5 mm), was used to obtain the ^{1}H-NMR and ^{13}C-NMR spectra. The spectra were obtained at 400 MHz for the ^{1}H-NMR and 100.6 MHz for the ^{13}C-NMR. For dissolving the samples, deuterated solvents were used ($CDCL_3$, MeOD) with tetramethylsilane (TMS) as the internal standard. For assigning the signals, 2 dimensional spectra were also generated, at night or during the weekend because of time management. All spectra were processed using TOPSPIN 3.2. The spectra were acquired through the standard sequences available in the Bruker pulse program library. Other types of spectra could be achieved by custom settings.

6. Infrared Spectroscopy (IR)

A Shimadzu IRAFFINITY-1S Fourier Transform Infrared Spectrophotometer with a signal-to-noise ratio (S/N) of 30 000:1 was used to obtain the infrared spectra from neat samples. A (FTIR)Quest ATR (Attenuated Total Reflectance) accessory with diamond crystal pucks was also contained in the spectrophotometer.

7. Thin layer Chromatography (TLC)

Suitable solvent mixtures in combination with silica plates with a glass back (Merck Silicagel 60 F254, precoats, 25 mm thickness) were used for this type of chromatography. The compounds in this dissertation could be visualized at an UV irradiation of 254 or 365 nm. This type of chromatography was used to follow up on reactions and to find appropriate solvent mixtures for column chromatography.

8. Hydrogen generator

In the hydrogen generator, hydrogen gas is provided up to 5 bar. The pressure is indicated in barg (pressure in excess of atmospheric pressure). To ensure suitable hydrogen conditions, the machine is first flushed three times with hydrogen.

5. Safety

Before starting this dissertation, students have been informed about several risks and hazards linked to working in a lab environment. Before getting into practice, a safety test had to be passed before access to the lab was granted. Three documents concerning the safety had to be signed, this included the internal guidelines of the research group, a document describing safe handling of different classes of compounds, and the wellbeing and environmental guidelines of Ghent university.
All practices in the lab were performed wearing the appropriate protective clothing, such as a lab coat and glasses. Hair was tight up, and long trousers with closed shoes were mandatory. When work was performed with hazardous substances, protective gloves were worn. Because of the toxic nature of certain reagents and products, reactions took place in hoods to provide as much protection as possible. In what follows, the risks and hazards of the most hazardous reagents that were used in this dissertation will be described.

1,1'-Bis(diphenylphosphino)ferrocene (Dppf) - yellow-orange powder that causes skin and serious eye irritation.

2,6-Dimethylphenylboronic acid - white crystalline powder that is harmful when swallowed, causes skin and serious eye irritation, and may cause respiratory irritation.

4-bromophenylhydrazine hydrochloride - beige/white powder that causes severe skin burns and eye damage.

4-Biphenylboronic acid - white powder that is harmful if swallowed, causes skin irritation and serious eye irritation, and may cause respiratory irritation.

4-tert-Butylphenylboronic acid - white/off-white crystalline powder, causing serious eye and skin irritation and may cause respiratory irritation.

5-bromo-1H-indazole - white crystalline powder that may cause respiratory irritation, is toxic if swallowed, causes serious eye irritation and skin irritation.

5-bromo-1H-pyrrolo[2,3-b]pyridine-3-carbaldehyde - white/yellow solid that causes skin and serious eye irritation.

5-Bromo-N,N-dimethyltryptamine - crystalline solid causing skin and serious eye irritation and may cause respiratory irritation.

5-bromo-7-azaindole - white/yellow crystalline powder that can cause serious eye damage/irritation, is corrosive to the skin and causes acute oral toxicity.

Acetonitrile - colourless liquid that is highly flammable, harmful if swallowed or inhaled and causes serious eye irritation.

Ammonium hydroxide (NH_4OH) - colourless aqueous solution, that may be corrosive to metals, causes skin burns and eye damage, may cause respiratory irritation and is very toxic to aquatic life.

Caesium carbonate (Cs_2CO_3) - white crystalline solid causing serious eye damage and may cause damage to organs at prolonged or repeated exposure.

Celite - grey/white powder with a small particle size, with specific organ toxicity (lungs) through prolonged or repeated exposure when inhaled.

Diethyl ether - clear, colourless extremely flammable liquid that is harmful when swallowed and may cause dizziness.

Diethyl phosphite - colourless liquid that may cause an allergic skin reaction and causes serious eye damage.

Dimethylethanolamine - colourless flammable liquid that is harmful when swallowed, causes severe skin burns and eye damage, is toxic if inhaled and is harmful to aquatic life.

Dimethyl sulphide - colourless flammable liquid that causes serious eye damage/irritation.

Dimethylamine - colourless gas that causes severe skin burns and eye damage, may cause respiratory irritation and is harmful when swallowed or inhaled.

Formaldehyde - gas contained in a colourless liquid that is acutely toxic when inhaled, swallowed or when it comes into contact with the skin, and causes damage to the eye. It's a flammable liquid.

Glacial acetic acid - colourless liquid that causes severe skin burns and eye damage.

Hydrochloric acid (HCl) - colourless liquid that is highly corrosive, causes severe skin burns, and eye damage.

Indole-3-carbonitrile - off-white powder that is harmful when swallowed, causes skin and eye irritation, and may cause respiratory irritation.

Methanol - colourless liquid that is highly flammable, causing acute toxicity if swallowed or inhaled.

NaOMe - white powder that causes severe skin burns and eye damage, is toxic if swallowed or when it comes into contact with skin or when inhaled.

Nitromethane - colourless oily flammable liquid that is suspected of causing cancer and the fertility or the unborn child.

N,N-Dimethylformamide (DMF) - flammable colourless liquid that causes serious eye irritation and is harmful when in contact with the skin or when inhaled.

Pentamethylcyclopentadienyliridium(III) chloride, dimer ($[Cp^*IrCl_2]_2$) - orange/red coloured powder that causes skin and serious eye irritation.

Phenylboronic acid - white powder that is harmful when swallowed.

$Pd(OAc)_2$ - red-brown solid crystals, causes serious eye damage and may cause an allergic skin reaction, and is very toxic to the aquatic environment.

$POCl_3$ - colourless liquid that may be corrosive to metals, is harmful if swallowed, causes severe skin burns and eye damage, is fatal if inhaled, and causes damage to organs at prolonged or repeated exposure.

Potassium carbonate (K_2CO_3) - white solid that causes skin and eye irritation.

Potassium hydroxide (KOH) - white solid that may be corrosive to metals, is harmful when swallowed, causes severe skin burns and eye damage, and can cause respiratory irritation.

Silica - white powder that may cause damage to the lungs through prolonged or repeated exposure when inhaled because of its small particle size.

Sodium Carbonate (Na_2CO_3) - white hygroscopic solid causing serious eye irritation.

Sulphuric acid - used in solution as a colourless liquid, may be corrosive to metals, causes severe skin burns and eye damage, may cause cancer when inhaled and it is harmful to aquatic life.

Tetrahydrofuran (THF) - clear colourless highly flammable liquid, causes acute oral toxicity and serious eye irritation, is carcinogen and has a specific target organ toxicity.

Tetrakis(trifenylfosfine)palladium(0) ($Pd(pph_3)_4$) - yellow/brown powder that is harmful when swallowed.

Tripotassium phosphate (K_3PO_4) - white powder that causes serious eye damage and may cause respiratory irritation.

Toluene - clear, colourless highly flammable liquid that may be fatal if swallowed, causes skin irritation and may cause dizziness, may cause damage to the organs, and is harmful to aquatic life.

Tryptamine - pale white to yellow needles, that are harmful when swallowed, cause serious eye damage and may cause an allergic skin reaction.

Zinc acetate dihydrate ($Zn(OAc)_2.2H_2O$) - white crystals that are harmful when swallowed and cause serious eye damage.

Zinc dust - grey dust that is hazardous to the aquatic environment.

6. Experimental section

1-(5-bromo-1H-pyrrolo[2,3-b]pyridin-1-yl)-N,N-dimethylmethanamine

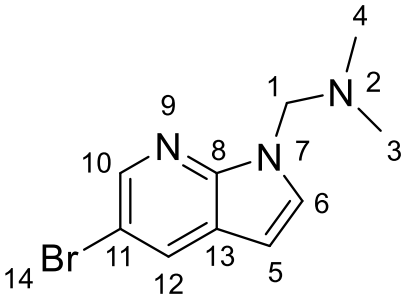

^{1}H-NMR (400 MHz, MeOD): δ = 8.33 (1H, d, $J_{H\text{-}H}$ = 2.2 Hz, $C^{10}\underline{H}$), 8.02 (1H, d, $J_{H\text{-}H}$ = 2.1 Hz, $C^{12}\underline{H}$), 7.30 (1H, d, , $J_{H\text{-}H}$ = 3.6 Hz, $C^{6}\underline{H}$), 6.43 (1H, d, , $J_{H\text{-}H}$ = 3.5 Hz, $C^{5}\underline{H}$), 5.02 (2H, s, $C^{1}\underline{H}_2$), 2.33 (6H, s, $C^{4,3}\underline{H}_3$); **^{13}C-NMR** (100.6 MHz, MeOD): δ = 146.77 (1C, C^{8}), 143.50 (1C, C^{10}), 130.70 (1C, C^{6}), 130.21 (1C, C^{12}), 121.84 (1C, C^{13}), 111.84 (1C, C^{11}), 199.55 (1C, C^{5}), 65.98 (1C, C^{1}), 42.35 (2C, $C^{3,4}$); **MS** (70 eV): m/z % 254.1 ($[M+H]^+$, 100), 256.0 ($[M+H]^+$, 97), 257.0 ($[M+H]^+$, 16)

5-bromo-7-azaindole (300 mg, 1.52 mmol, 1 eq.) was dissolved in a 10 mL flask with acetonitrile and glacial acetic acid in a ratio of 3:1. Subsequently formaldehyde (53 mg, 1.78 mmol, 1.17 eq.) and dimethylamine (91 mg, 2.03 mmol, 1.33 eq.) were added to the flask. This was allowed to stir for 2 hours at room temperature. The acetonitrile was evaporated and the residue was basified using potassium hydroxide. This mixture was extracted twice using ethyl acetate. The organic fraction was dried with magnesium sulphate and the solvents were evaporated. The mixture was purified using normal phase liquid chromatography, with chloroform and acetone as eluents with a gradient going from 100:0 to 0:100. The product remained as a white powder with an isolated yield of 12%.

1-(5-bromo-1H-pyrrolo[2,3-b]pyridin-1-yl)-N,N,N-trimethylmethanaminium

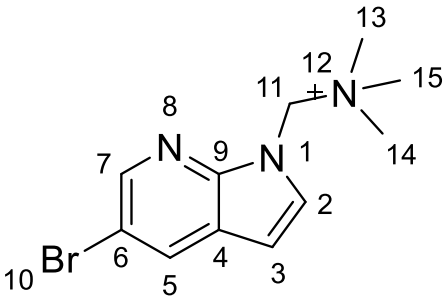

^{1}H-NMR (400 MHz, $CDCl_3$): δ = 8.44 (1H, d, , $J_{H\text{-}H}$ = 2.1 Hz, $C^{7}\underline{H}$), 8.27 (1H, d $J_{H\text{-}H}$ = 2.1 Hz, $C^{5}\underline{H}$), 7.72 (1H, d, $J_{H\text{-}H}$ = 3.8 Hz, $C^{2}\underline{H}$), 6.77 (1H, d, $J_{H\text{-}H}$ = 3.8 Hz, $C^{3}\underline{H}$), 5.82 (2H, s, $C^{11}\underline{H}_2$), 3.24 (9H, s, $C^{13,14,15}\underline{H}_3$); **^{13}C-NMR** (100.6 MHz, $CDCl_3$): δ = 147.07 (1C, C^{9}), 144.26 (1C, C^{7}), 131.77 (1C, C^{5}), 131.23 (1C, C^{2}), 122.79 (1C, C^{4}), 113.51 (1C, C^{6}), 103.45 (1C, C^{3}), 70.32 (1C, C^{11}), 50.72 (3C, $C^{13,14,15}$); **MS** (70 eV): m/z % 270.1 ($[M+H]^+$, 100), 268.1 ($[M+H]^+$, 100), 271.1 ($[M+H]^+$, 16)

In a flask 1-(5-bromo-1H-pyrrolo[2,3-b]pyridin-1-yl)-N,N-dimethylmethanamine (399 mg, 1.57 mmol, 1eq.) was dissolved in 3.4 mL methanol. Next natrium methoxide (116 mg, 2.15 mmol, 1.37 eq.) and dimethyl sulphate were added (396 mg, 3.14 mmol, 2 eq.) along with 6.8 mL nitromethane. The mixture was stirred at room temperature for one and a half hour. The solvents were evaporated and the residue was extracted with sodium bicarbonate and dichloromethane. The residue was subjected to reversed-phase liquid chromatography with acetonitrile and water as eluents. This resulted in an isolated yield of 35% as a white/yellow powder.

5-bromo-1H-indazole-1-carbaldehyde

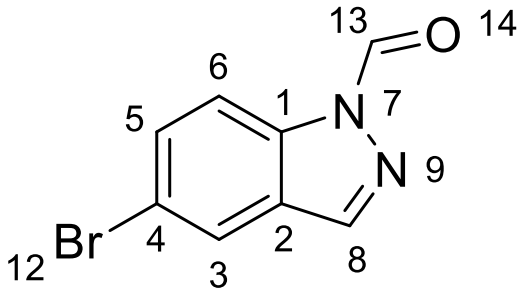

^{1}H-NMR (400 MHz, $CDCl_3$): δ = 9.42 (1H, s, $C^{13}\underline{H}$), 8.28 (1H, d, $J_{H\text{-}H}$ = 8.7 Hz, $C^{3}\underline{H}$), 8.21 (1H, s, $C^{8}\underline{H}$), 7.93 (1H, d, $J_{H\text{-}H}$ = 1.5 Hz, $C^{6}\underline{H}$), 7.70 (1H, d x d, $J_{H\text{-}H}$ = 8.8 Hz, $J_{H\text{-}H}$ = 1.8 Hz, $C^{5}\underline{H}$); **MS** (70 eV): m/z % 224.8 ($[M+H]^+$, 100), 226.9 ($[M+H]^+$,100)

5-Bromo-1H-indazole (300 mg, 1.53 mmol, 1 eq.) was dissolved in 0.25 mL DMF. The Vilsmeier reagent was made with made 1 mL DMF, where $POCL_3$ (256 mg, 1.67 mmol, 1.1 eq.) was added dropwise over 15 minutes at a temperature of 0 °C. The reaction mixture with 5-Bromo-1H-indazole was subsequently added dropwise to the prepared Vilsmeier reagent. This was allowed to stir for 16 hours at room temperature. The colour of the reaction mixture changed from white to yellow. After 16 hours, the mixture was poured over crushed ice. Potassium hydroxide was added and a white/yellow precipitate arose. This precipitate was filtered off and recrystalized in hot ethanol. The product remained as yellow crystals with an isolated yield of 31%.

2-(5-bromo-1H-pyrrolo[2,3-b]pyridin-3-yl)-N,N-dimethylethan-1-amine

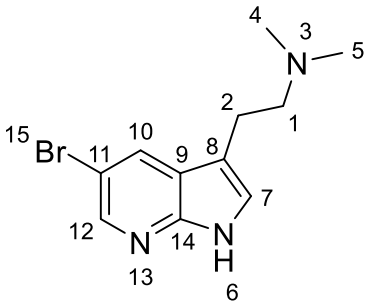

^{1}H-NMR (400 MHz, CDCl3): δ = 9.50 (1H, s, $N\underline{H}$), 8.31 (1H, d, $J_{H\text{-}H}$ = 1.9 Hz, $C^{12}\underline{H}$), 8.03 (1H, d, $J_{H\text{-}H}$ = 1.9 Hz, $C^{10}\underline{H}$), 7.16 (1H, s, $C^{7}H$), 2.88 (2H, t, $J_{H\text{-}H}$ = 8.0 Hz, $C^{2}\underline{H_2}$), 2.60 (2H, t, $J_{H\text{-}H}$ = 8.2 Hz, $C^{1}\underline{H_2}$), 2.33 (6H, s, $C^{4,5}\underline{H_3}$); **^{13}C-NMR** (100.6 MHz, CDCl3): δ = 147.12 (1C, C^{14}), 143.41 (1C, C^{12}), 129.39 (1C, C^{10}), 123.48 (1C, C^{7}), 121.76 (1C, C^{9}), 112.97 (1C, C^{11}), 111.22 (1C, C^{8}), 60.00 (1C, C^{1}), 23.76 (1C, C^{2}), 45.49 (2C, $C^{4,5}$); **IR (cm^{-1}):** 3144, 2931, 989, 1465, 1406, 754; **MS** (70 eV): m/z % 270.0 ($[M+H]^+$, 97), 268.1 ($[M+H]^+$, 97), 269.0 ($[M+H]^+$, 15), 271.0 ($[M+H]^+$, 17)

5-Bromo-7-azaindole (100 mg, 0.51 mmol, 1 eq.), Cs_2CO_3 (182 mg, 0.56 mmol, 1.1 eq.), pentamethylcyclopenta-dienyliridium(II) chloride, dimer (10 mg, 0.013 mmol, 0.025 eq.), and 2-dimethylamino-ethanol (136 mg, 1.53 mmol, 3 eq.) were added to a flame dried GC-MS vial. The mixture was flushed with nitrogen and stirred at 120 °C for 48 hours. This residue was dissolved in an ethyl acetate/methanol mixture with a ratio of 9 to 1 and this was filtered through a silica plug. The product was purified with a reversed-phase liquid chromatography using water and methanol as eluents. The product was isolated as a brown/beige solid with a yield of 85%.

diethyl (1H-pyrrolo[2,3-b]pyridin-5-yl)phosphonate

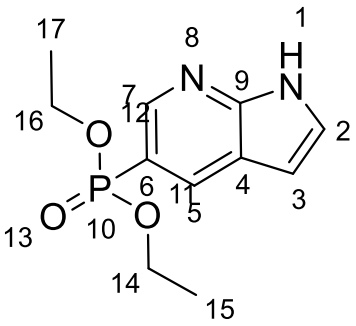

^{1}H-NMR (400 MHz, MeOD): δ = 12.02 (1H, s, NH), 8.78 (1H, d, J_{H-H}= 6.2 Hz, $C^{7}H$), 8.45 (1H, d x d, J_{H-H}=13.8 Hz and J_{H-H}= 1.5 Hz, $C^{5}H$), 7.51 (1H, s, $C^{3}H$), 6.62 (1H, d, J_{H-H} = 2.4 Hz, $C^{2}H$), 4.09-4.27 (4H, m, $C^{14,16}H_2$), 1.36 (6H, t, J_{H-H}= 7.1 Hz, $C^{15,17}H_3$); **^{13}C-NMR** (100.6 MHz, MeOD): δ = 150.27 (1C, C^{9}), 145.35 (1C, C^{7}), 133.38 (1C, C^{5}), 127.02 (1C, C^{2}), 120.01 (1C, C^{4}), 116.25 (1C, C^{6}), 101.62 (1C, C^{3}), 62.23 (2C, $C^{14,16}$), 16.35 (2C, $C^{15,17}$); **IR (cm^{-1}):** 1620, 1340, 989, 827, 692; **MS** (70 eV): m/z % 255.1 ([M+H]$^{+}$, 100), 256.1 ([M+H]$^{+}$, 20)

5-Bromo-7-azaindole (100 mg, 0.51 mmol, 1 eq.), $Pd(OAc)_2$ (11 mg, 0.051 mmol, 0.1 eq.), DPPF (28 mg, 0.051 mmol, 0.1 eq.) and K_2CO_3 (140 mg, 1.02 mmol, 2 eq.) were added to a 10 mL flask. This flask was flushed with nitrogen, while 3.8 mL dry toluene was added. The bottle of diethyl phosphite was first flushed with nitrogen and then diethyl phosphite (140 mg, 1.02 mmol, 2 eq.) was added to the flask. This was flushed with nitrogen for another 5 minutes. The reaction was stirred at 90 °C for 16 hours. The solvents were evaporated and the residue was dissolved in ethyl acetate and sent over a silica plug. This residue was subjected to reversed-phase liquid chromatography using acetonitrile and water as eluents. The product was isolated as a transparent oil with a yield of 63%.

N,N-dimethyl-2-(5-phenyl-1H-indol-3-yl)ethan-1-amine

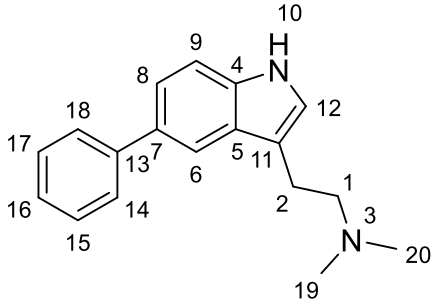

^{1}H-NMR (400 MHz, $CDCl_3$): δ = 8.16 (1H, NH), 7.80 (1H, s, $C^{8}H$), 7.66 (2H, d, J_{H-H} = 7.9 Hz, $C^{14,18}H$), 7.38-7.48 (4H, m, $C^{6,9,15,17}H$), 7.31 (1H, t, J_{H-H} = 7.4 Hz, $C^{16}H$), 7.04 (1H, s, $C^{12}H$), 2.99 (2H, t, J_{H-H} = 7.71 Hz, $C^{2}H_2$), 2.67 (2H, t, J_{H-H} = 8.87 Hz, $C^{1}H_2$), 2.35 (6H, s, $C^{19,20}H_3$); **^{13}C-NMR** (100.6 MHz, $CDCl_3$): δ = 142.67 (1C, C^{7}), 135.83 (1C, C^{13}), 132.91 (1C, C^{4}), 128.65 (2C, $C^{15,17}$), 127.43 (2C, $C^{14,18}$), 126.30 (1C, C^{16}), 124.75 (1C, C^{5}), 122.17 (1C, C^{12}), 121.87 (1C, C^{6}), 117.37 (1C, C^{8}), 112.53 (1C, C^{11}), 111.33 (1C, C^{9}), 60.33 (1C, C^{1}), 45.48 (2C, $C^{19,20}$), 23.63 (1C, C^{2}); **IR (cm^{-1})** 2941, 2857, 2778, 1599, 1460, 1036, 795, 754, 698; **MS** (70 eV): m/z % 265.2 ([M+H]$^{+}$, 100), 266.2 ([M+H]$^{+}$, 22)

The observed [M+H]$^{+}$ values are in accordance with literature (Wu et al., 2002).

5-bromo-dimethyltryptamine (176 mg, 0.66 mmol, 1eq.) was dissolved in 2 mL THF. In 2 mL water, phenylboronic acid (96 mg, 0.79 mmol, 1.2 eq.), palladium acetate (7.4 mg, 0.033 mmol, 0.05 eq.), and potassium hydroxide (74 mg, 1.32 mmol, 2 eq.) were dissolved. The two mixtures were added together and the reaction mixture was flushed with nitrogen. The flask was sealed off, and a nitrogen balloon was placed on the flask. The reaction was stirred at 60 °C for 16 hours. The reaction mixture was allowed to cool to room temperature, afterwards diluted with water and extracted with ethyl acetate. The organic phase was dried with magnesium sulfate and the solvents evaporated. The residue was subjected to reversed-phase chromatography using water and methanol as eluents. This resulted in an isolated yield of 64% as a brown oil.

1-(1H-indol-3-yl)-6-methoxy-2,3,4,9-tetrahydro-1H-pyrido[3,4-b]indole

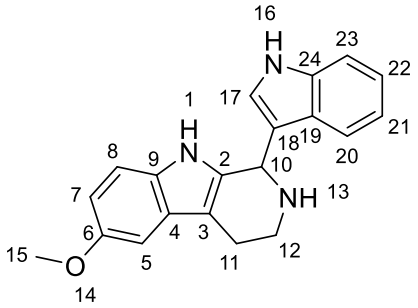

^{1}H-NMR (400 MHz, $CDCl_3$): δ = 8.17 (1H, s, $N^{16}\underline{H}$), 7.51 (1H, s, $N^{1}\underline{H}$), 7.40 (2H, T, J_{H-H} = 8.0 Hz, $C^{20,23}\underline{H}$), 7.16-7.22 (2H, m, $C^{17,22}\underline{H}$), 7.00-7.09 (3H, m, $C^{5,8,21}\underline{H}$), 6.77 (1H, d x d, J_{H-H} = 8.8 Hz, J_{H-H} = 2.5 Hz, $C^{7}\underline{H}$), 5.53 (1H, s, $C^{10}\underline{H}$), 3.88 (3H, s, $C^{15}\underline{H}_3$), 3.21 (2H, m, $C^{12}\underline{H}_2$), 2.88 (2H, m, $C^{11}\underline{H}_2$); **^{13}C-NMR (**100.6 MHz, $CDCl_3$): δ = 154.15 (1C, C^{6}), 148.96 (1C, C^{24}), 132.57 (1C, C^{2}), 128.05 (1C, C^{9}), 126.43 (1C, C^{4}), 122.51 (2C, $C^{17,22}$), 120.16 (1C, C^{21}), 119.26 (1C, C^{20}), 111.32 (1C, C^{18}), 111.82 (1C, C^{7}), 111.21 (2C, $C^{23,8}$), 109.25 (1C, C^{3}), 100.62 (1C, C^{5}), 55.96, (1C, C^{10}), 50.48 (1C, C^{15}), 43.35 (1C, C^{12}), 22.69 (1C, C^{11}); **MS** (70 eV): m/z % 318.2 ($[M+H]^+$, 100), 319.2 ($[M+H]^+$, 30), 320.2 ($[M+H]^+$, 10)

This is in accordance with literature (Sas et al., 2016)

2-(5-methoxy-1H-indol-3-yl)ethan-1-amine (190 mg, 1mmol, 1eq.) was dissolved in 10 mL glacial acetic acid along with 1H-indole-3-carbonitril (213 mg, 1.5 mmol, 1.5 eq.) and 10% palladium on activated carbon (22 mg, 0.2 mmol, 0.2 eq.). This was hydrogenated under balloon pressure for 48 hours at room temperature. The catalyst was removed by filtering the mixture over celite and washing it with dichloromethane. The resulting reaction mixture was basified with aqueous ammonia and extracted with dichloromethane. The organic phase was dried with magnesium sulfate and the solvents evaporated. The residue was purified using normal-phase chromatography using dichloromethane and methanol (95:5) as eluents. After purification, the product remained as a yellow liquid with an isolated yield of 35%.

7. Bibliography

Abranyi-Balogh, P., Földesi, T., Grün, A., Volk, B., Keglevich, G., & Milen, M. (2016). Synthetic study on the T3P®-promoted one-pot preparation of 1-substituted-3, 4-dihydro-β-carbolines by the reaction of tryptamine with carboxylic acids. Tetrahedron Letters, 57(18), 1953-1957.

Agrawal, D. C., & Dhanasekaran, M. (Eds.). (2023). Mushrooms with Therapeutic Potentials: Recent Advances in Research and Development.

Albujuq, N. R., Meana, J. J., Diez-Alarcia, R., Muneta-Arrate, I., Naqvi, A., Althumayri, K., & Alsehli, M. (2023). Design, Synthesis, Molecular Docking, and Biological Evaluation of Novel Pimavanserin-Based Analogues as Potential Serotonin 5-HT2A Receptor Inverse Agonists. Journal of Medicinal Chemistry, 66(13), 9057-9075.

Alzweiri, M., Alsegiani, A. S., Karaj, E., Almarghalani, D. A., Tabaza, Y., Shah, Z. A., & Tillekeratne, L. V. (2021). The structural simplification of lysergic acid as a natural lead for synthesizing novel anti-Alzheimer agents. Bioorganic & medicinal chemistry letters, 47, 128205.

Asghar, S., Mushtaq, N., Khan, A., Akhtar, S., Munawar, R., Ansari, S., & Saify, Z. S. (2022). Tryptamine Analogs as Antidepressant and Anxiolytic Agents: Synthesis and In Vivo Evaluation. Pharmaceutical Chemistry Journal, 56(7), 918-924.

Bartolucci, S., Mari, M., Bedini, A., Piersanti, G., & Spadoni, G. (2015). Iridium-catalyzed direct synthesis of tryptamine derivatives from indoles: exploiting N-protected β-amino alcohols as alkylating agents. *The Journal of Organic Chemistry*, *80*(6), 3217-3222.

Bartolucci, S., Mari, M., Di Gregorio, G., & Piersanti, G. (2016). Observations concerning the synthesis of tryptamine homologues and branched tryptamine derivatives via the borrowing hydrogen process: synthesis of psilocin, bufotenin, and serotonin. Tetrahedron, 72(18), 2233-2238.

Beato, A., Gori, A., Boucherle, B., Peuchmaur, M., & Haudecoeur, R. (2021). β-Carboline as a privileged scaffold for multitarget strategies in Alzheimer's disease therapy. Journal of Medicinal Chemistry, 64(3), 1392-1422.

Beck, A. T., Ward, C. H., Mendelson, M., Mock, J., & ERBAUGH, J. (1961). An inventory for measuring depression. Archives of general psychiatry, 4(6), 561-571.

Brnardic, E. J. (1998). Synthesis of aza-tryptophan derivatives.

Calcaterra, A., Mangiardi, L., Delle Monache, G., Quaglio, D., Balducci, S., Berardozzi, S., ... & Ghirga, F. (2020). The pictet-spengler reaction updates its habits. Molecules, 25(2), 414.

Cameron, L. P., Benetatos, J., Lewis, V., Bonniwell, E. M., Jaster, A. M., Moliner, R., ... & Aguilar-Valles, A. (2023). Beyond the 5-HT2A Receptor: Classic and Nonclassic Targets in Psychedelic Drug Action. Journal of Neuroscience, 43(45), 7472-7482.

Cameron, L. P., Patel, S. D., Vargas, M. V., Barragan, E. V., Saeger, H. N., Warren, H. T., ... & Olson, D. E. (2023). 5-HT2ARs mediate therapeutic behavioral effects of psychedelic tryptamines. ACS Chemical Neuroscience, 14(3), 351-358.

Cao, D., Yu, J., Wang, H., Luo, Z., Liu, X., He, L., ... & Wang, S. (2022). Structure-based discovery of nonhallucinogenic psychedelic analogs. Science, 375(6579), 403-411.

Chen, C. Y., Senanayake, C. H., Bill, T. J., Larsen, R. D., Verhoeven, T. R., & Reider, P. J. (1994). Improved Fischer indole reaction for the preparation of N, N-dimethyltryptamines: Synthesis of L-695,894, a potent 5-HT1D receptor agonist. The Journal of Organic Chemistry, 59(13), 3738-3741.

Córdova, A. (2004). The direct catalytic asymmetric Mannich reaction. Accounts of chemical research, 37(2), 102-112.

de Teresa, M. G. (2022). Selling the Priceless Mushroom: A History of Psilocybin Mushroom Trade in the Sierra Mazateca (Oaxaca). Journal of Illicit Economies and Development, 4(2).

Dodd, S., Norman, T. R., Eyre, H., Stahl, S. M., Phillips, A., Carvalho, A. F., & Berk, M. (2022). Psilocybin in Neuropsychiatry: a review of its pharmacology, safety and efficacy. *CNS spectrums*, 1-36.

Dunlap, L. E., Azinfar, A., Ly, C., Cameron, L. P., Viswanathan, J., Tombari, R. J., ... & Olson, D. E. (2020). Identification of psychoplastogenic N, N-dimethylaminoisotryptamine (isoDMT) analogues through structure–activity relationship studies. *Journal of medicinal chemistry*, *63*(3), 1142-1155..

Fricke, J., Kargbo, R., Regestein, L., Lenz, C., Peschel, G., Rosenbaum, M. A., ... & Hoffmeister, D. (2020). Scalable hybrid synthetic/biocatalytic route to psilocybin. Chemistry–A European Journal, 26(37), 8281-8285.

Fricke, J., Sherwood, A. M., Halberstadt, A. L., Kargbo, R. B., & Hoffmeister, D. (2021). Chemoenzymatic synthesis of 5-methylpsilocybin: A tryptamine with potential psychedelic activity. Journal of natural products, 84(4), 1403-1408.

Glatfelter, G. C., Pottie, E., Partilla, J. S., Sherwood, A. M., Kaylo, K., Pham, D. N., ... & Baumann, M. H. (2022). Structure–Activity Relationships for Psilocybin, Baeocystin, Aeruginascin, and Related Analogues to Produce Pharmacological Effects in Mice. *ACS Pharmacology & Translational Science*, *5*(11), 1181-1196.

Grieco, S. F., Castrén, E., Knudsen, G. M., Kwan, A. C., Olson, D. E., Zuo, Y., ... & Xu, X. (2022). Psychedelics and neural plasticity: therapeutic implications. Journal of Neuroscience, 42(45), 8439-8449.

Gukasyan, N., Davis, A. K., Barrett, F. S., Cosimano, M. P., Sepeda, N. D., Johnson, M. W., & Griffiths, R. R. (2022). Efficacy and safety of psilocybin-assisted treatment for major depressive disorder: Prospective 12-month follow-up. Journal of Psychopharmacology, 36(2), 151-158.

Heilman, J. (2023). The History, Legalization and Potentials of Psilocybin-Assisted Psychotherapy. Journal of Scientific Exploration, 36(4), 623-640.

Henyecz, R., & Keglevich, G. (2019). New developments on the Hirao reactions, especially from “green” point of view. Current Organic Synthesis, 16(4), 523-545.

Hofmann, A., Frey, A., Ott, H., Zilka, P., & Troxler, F. (1958). Elucidation of the structure and the synthesis of psilocybin. Experientia, 14(11), 397-399.

Holze, F., Becker, A. M., Kolaczynska, K. E., Duthaler, U., & Liechti, M. E. (2023). Pharmacokinetics and pharmacodynamics of oral psilocybin administration in healthy participants. Clinical Pharmacology & Therapeutics, 113(4), 822-831.

Immadisetty, K., Geffert, L. M., Surratt, C. K., & Madura, J. D. (2013). New design strategies for antidepressant drugs. Expert opinion on drug discovery, 8(11), 1399-1414.

Kannaboina, P., Mondal, K., Laha, J. K., & Das, P. (2020). Recent advances in the global ring functionalization of 7-azaindoles. Chemical Communications, 56(79), 11749-11762.

Lennox, A. J., & Lloyd-Jones, G. C. (2014). Selection of boron reagents for Suzuki–Miyaura coupling. Chemical Society Reviews, 43(1), 412-443.

Meyer, M., & Slot, J. (2023). The Evolution and Ecology of Psilocybin in Nature. Fungal Genetics and Biology, 103812.

Nakagawasai, O., Arai, Y., Satoh, S. E., Satoh, N., Neda, M., Hozumi, M., ... & Tadano, T. (2004). Monoamine Oxidase and Head-Twitch Response in Mice: Mechanisms of α-Methylated Substrate Derivatives. Neurotoxicology, 25(1-2), 223-232.

Nichols, D. E. (2020). Psilocybin: From ancient magic to modern medicine. The Journal of antibiotics, 73(10), 679-686.

Nichols, D. E., & Frescas, S. (1999). Improvements to the synthesis of psilocybin and a facile method for preparing the O-acetyl prodrug of psilocin. Synthesis, 1999(06), 935-938.

Otte, C., Gold, S. M., Penninx, B. W., Pariante, C. M., Etkin, A., Fava, M., ... & Schatzberg, A. F. (2016). Major depressive disorder. Nature reviews Disease primers, 2(1), 1-20.

Pakhare, D. S., & Kusurkar, R. S. (2015). Synthesis of tetrahydro-β-carbolines, β-carbolines, and natural products,(±)-harmicine, eudistomin U and canthine by reductive Pictet Spengler cyclization. Tetrahedron Letters, 56(44), 6012-6015.

Popowycz, F., Routier, S., Joseph, B., & Mérour, J. Y. (2007). Synthesis and reactivity of 7-azaindole (1H-pyrrolo [2, 3-b] pyridine). Tetrahedron, 63(5), 1031-1064.

Raison, C. L., Sanacora, G., Woolley, J., Heinzerling, K., Dunlop, B. W., Brown, R. T., ... & Griffiths, R. R. (2023). Single-dose psilocybin treatment for major depressive disorder: A randomized clinical trial. JAMA, 330(9), 843-853.

Reed-Berendt, B. G., Latham, D. E., Dambatta, M. B., & Morrill, L. C. (2021). Borrowing hydrogen for organic synthesis. ACS Central Science, 7(4), 570-585.

Rucker, J. J., Marwood, L., Ajantaival, R. L. J., Bird, C., Eriksson, H., Harrison, J., ... & Young, A. H. (2022). The effects of psilocybin on cognitive and emotional functions in healthy participants: Results from a phase 1, randomised, placebo-controlled trial involving simultaneous psilocybin administration and preparation. Journal of Psychopharmacology, 36(1), 114-125.

Sandoval, O. (2023). Potential Antidepressant Efficacy of Psilocybin and Related Tryptamines (Doctoral dissertation, Miami University).

Santhanam, S., Ramu, A., Baburaj, B., & Kalpatu Kuppusamy, B. (2020). Application of metal free aromatization to total synthesis of perlolyrin, flazin, eudistomin U and harmane. Journal of Heterocyclic Chemistry, 57(5), 2121-2127.

Sas, J., Szatmári, I., & Fulop, F. (2016). One-pot α-arylation of β-carboline with indole and naphthol derivatives. Current Organic Synthesis, 13(4), 611-616.

Schwan, A. L. (2004). Palladium catalyzed cross-coupling reactions for phosphorus–carbon bond formation. Chemical Society Reviews, 33(4), 218-224.

Serreau, R., Amirouche, A., Benyamina, A., & Berteina-Raboin, S. (2022). A Review of Synthetic Access to Therapeutic Compounds Extracted from Psilocybe. Pharmaceuticals, 16(1), 40.

Shao, C., Shi, G., Zhang, Y., Pan, S., & Guan, X. (2015). Palladium-Catalyzed C–H Ethoxycarbonyldifluoromethylation of Electron-Rich Heteroarenes. Organic letters, 17(11), 2652-2655.

Sherwood, A. M., Halberstadt, A. L., Klein, A. K., McCorvy, J. D., Kaylo, K. W., Kargbo, R. B., & Meisenheimer, P. (2020). Synthesis and biological evaluation of tryptamines found in hallucinogenic mushrooms: norbaeocystin, baeocystin, norpsilocin, and aeruginascin. Journal of natural products, 83(2), 461-467.

Shirota, O., Hakamata, W., & Goda, Y. (2003). Concise large-scale synthesis of psilocin and psilocybin, principal hallucinogenic constituents of “magic mushroom”. Journal of natural products, 66(6), 885-887.

Smith, J. B., Lee, A. K., & Jackson, J. (2020). The claustrum. Current Biology, 30(23), R1401-R1406.

Stöckigt, J., Antonchick, A. P., Wu, F., & Waldmann, H. (2011). The Pictet–Spengler reaction in nature and in organic chemistry. Angewandte Chemie International Edition, 50(37), 8538-8564.

Strauss, D., Ghosh, S., Murray, Z., & Gryzenhout, M. (2022). Psilocybin containing mushrooms: a rapidly developing biotechnology industry in the psychiatry, biomedical and nutraceutical fields. *3 Biotech*, *12*(12), 339.

Suzuki, A. (2004). Organoborane coupling reactions (Suzuki coupling). Proceedings of the Japan Academy, Series B, 80(8), 359-371.

Szabó, T., Volk, B., & Milen, M. (2021). Recent advances in the synthesis of β-carboline alkaloids. Molecules, 26(3), 663.

Tatsui, G. J. (1928). Preparation of 1-methyl-1, 2, 3, 4-tetrahydro-β-carboline. J. Pharm. Soc. Jpn, 48, 92.

Tylš, F., Páleníček, T., & Horáček, J. (2014). Psilocybin–summary of knowledge and new perspectives. European Neuropsychopharmacology, 24(3), 342-356.

Valiulin, R. (2020). Organic Chemistry: 100 Must-Know Mechanisms. Berlin, Boston: De Gruyter.

Van Court, R. C., Wiseman, M. S., Meyer, K. W., Ballhorn, D. J., Amses, K. R., Slot, J. C., ... & Uehling, J. K. (2022). Diversity, biology, and history of psilocybin-containing fungi: suggestions for research and technological development. Fungal Biology, 126(4), 308-319.

van Elk, M., & Yaden, D. B. (2022). Pharmacological, neural, and psychological mechanisms underlying psychedelics: A critical review. Neuroscience & Biobehavioral Reviews, 104793.

Vargas, A. S., Luís, Â., Barroso, M., Gallardo, E., & Pereira, L. (2020). Psilocybin as a new approach to treat depression and anxiety in the context of life-threatening diseases—a systematic review and meta-analysis of clinical trials. Biomedicines, 8(9), 331.

Verma, D. K., Dewangan, Y., & Verma, C. (2023). Handbook of Organic Name Reactions: Reagents, Mechanism and Applications. Elsevier.

von Rotz, R., Schindowski, E. M., Jungwirth, J., Schuldt, A., Rieser, N. M., Zahoranszky, K., ... & Vollenweider, F. X. (2023). Single-dose psilocybin-assisted therapy in major depressive disorder: A placebo-controlled, double-blind, randomised clinical trial. EClinicalMedicine, 56.

Wager, T. T., Hou, X., Verhoest, P. R., & Villalobos, A. (2016). Central nervous system multiparameter optimization desirability: application in drug discovery. ACS chemical neuroscience, 7(6), 767-775.

Wu, T. Y., & Schultz, P. G. (2002). A versatile linkage strategy for solid-phase synthesis of N, N-dimethyltryptamines and β-carbolines. Organic Letters, 4(23), 4033-4036.

Yakhontov, L. N. (1968). The chemistry of azaindoles [pyrrolo [2, 3] pyridines]. Russian Chemical Reviews, 37(7), 551.

Yang, L., Lin, J., Kang, L., Zhou, W., & Ma, D. Y. (2018). Lewis Acid-Catalyzed Reductive Amination of Aldehydes and Ketones with N, N-Dimethylformamide as Dimethylamino Source, Reductant and Solvent. Advanced Synthesis & Catalysis, 360(3), 485-490.

Yin, Y. N., & Gao, T. M. (2023). Non-hallucinogenic Psychedelic Analog Design: A Promising Direction for Depression Treatment. Neuroscience Bulletin, 39(1), 170-172.